Behind the surface: X ray Microtomography for Cutural Heritage

Federico Bernardini[1-2]

(1) Dipartimento di Studi Umanistici, Università Ca' Foscari, Venezia, Italy;
(2) Multidisciplinary Laboratory, The “Abdus Salam” International Centre for Theoretical Physics, Trieste, Italy;

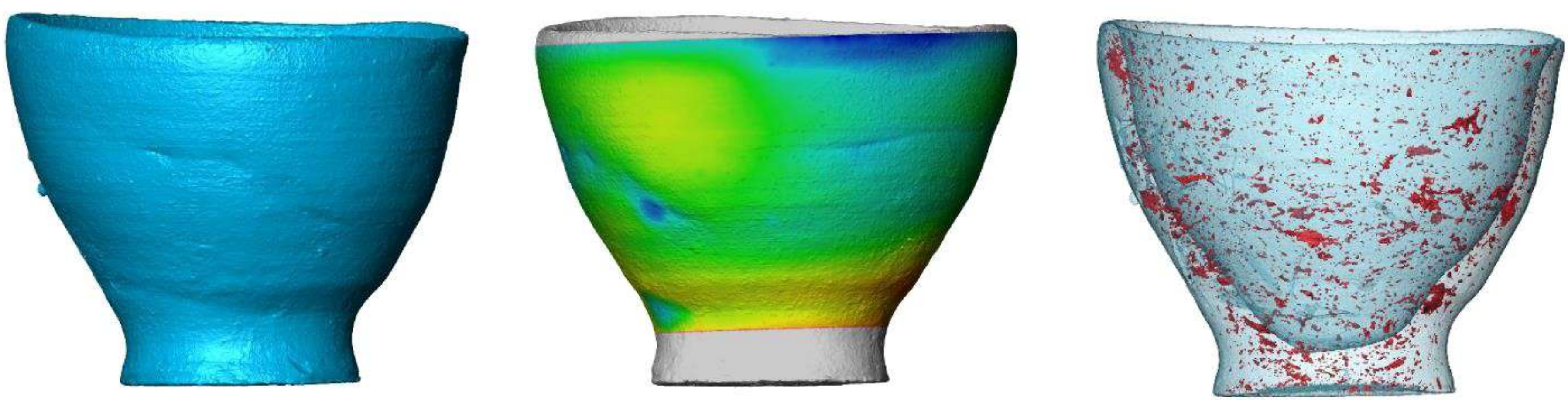

1st Mesoamerican Workshop on Reconfigurable X-ray and Scientific Instrumentation for Cultural Heritage" (16 - 20 June 2025)

1895 discovery of X rays by Wilhelm Röntgen

In the same year Röntgen also discovered possible medical use of X rays when he made a picture of his wife's hand: the first radiograph of a human body part using x rays

Radiography was **first used in paleoanthropology** to image some Neanderthal and Upper Paleolithic human remains from Belgium (La Naulette, Goyet), Croatia (Krapina), Germany (Mauer), and Moravia (Pøedmostí) (Walkhof, 1902; Gorjanovic-Kramberger, 1906; Schoetensack, 1908).

1906

D. Gorjanovic-Kramberger used radiographs to analyze internal features of fossil hominids. He started describing a frontal bone and teeth of the Krapina Neanderthals and little later came up with a description of a new diagnostic feature by using x-rays.

Computed Axial Tomography

1973
The introduction of **Computed Tomography** (Hounsfield, 1973) ultimately opened a new dimension for anthropology.

X-ray computed microtomography (microCT), evolved from clinical CT scanning in the **late 1980s** (Feldkamp et al., 1989), is a relatively new important tool for the non-destructive microstructural analysis of different types of hard materials

The cone-beam mCT station at ICTP

The **mCT** has been designed by **ICTP** and **Elettra Sincrotrone Trieste**.

This mCT system has been specifically designed for the investigation of large objects (with dimensions up to 20 cm and a weight up to 15 kg) at 40-50 micron resolution. Smaller objects can be also studied with spatial resolution of the order of 5-10 micron. **The system complements the instruments operated by Elettra, the synchrotron set-up at the SYRMEP beamline and the TomoLab station(s)**

Main Components

- **Tube**: X-rays are produced by a Hamamatsu microfocus X-ray source (150 kV max. voltage, 500 µA max. current, 5 µm min. focal spot size).

- **Detector**: is a Hamamatsu flat panel sensor coupled to a fiber optic plate under the GOS scintillator. It is a large-area device with small pixel size (50x50 µm) and high efficiency in the radiation conversion.

- **Sample positioning system**: Aerotech high-performance mechanical components with two linear translation axes and rotation stage.

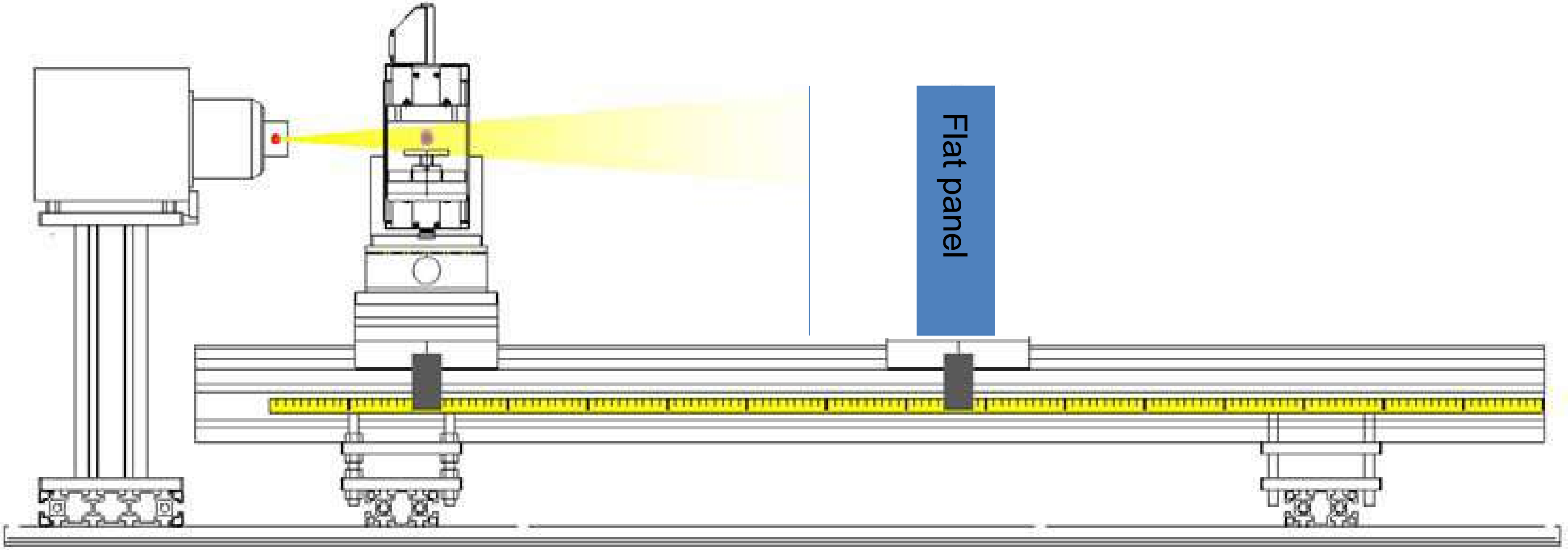

The source-detector system and the sample manipulator are mounted on a flexible mechanical set-up

Desktop mCT station

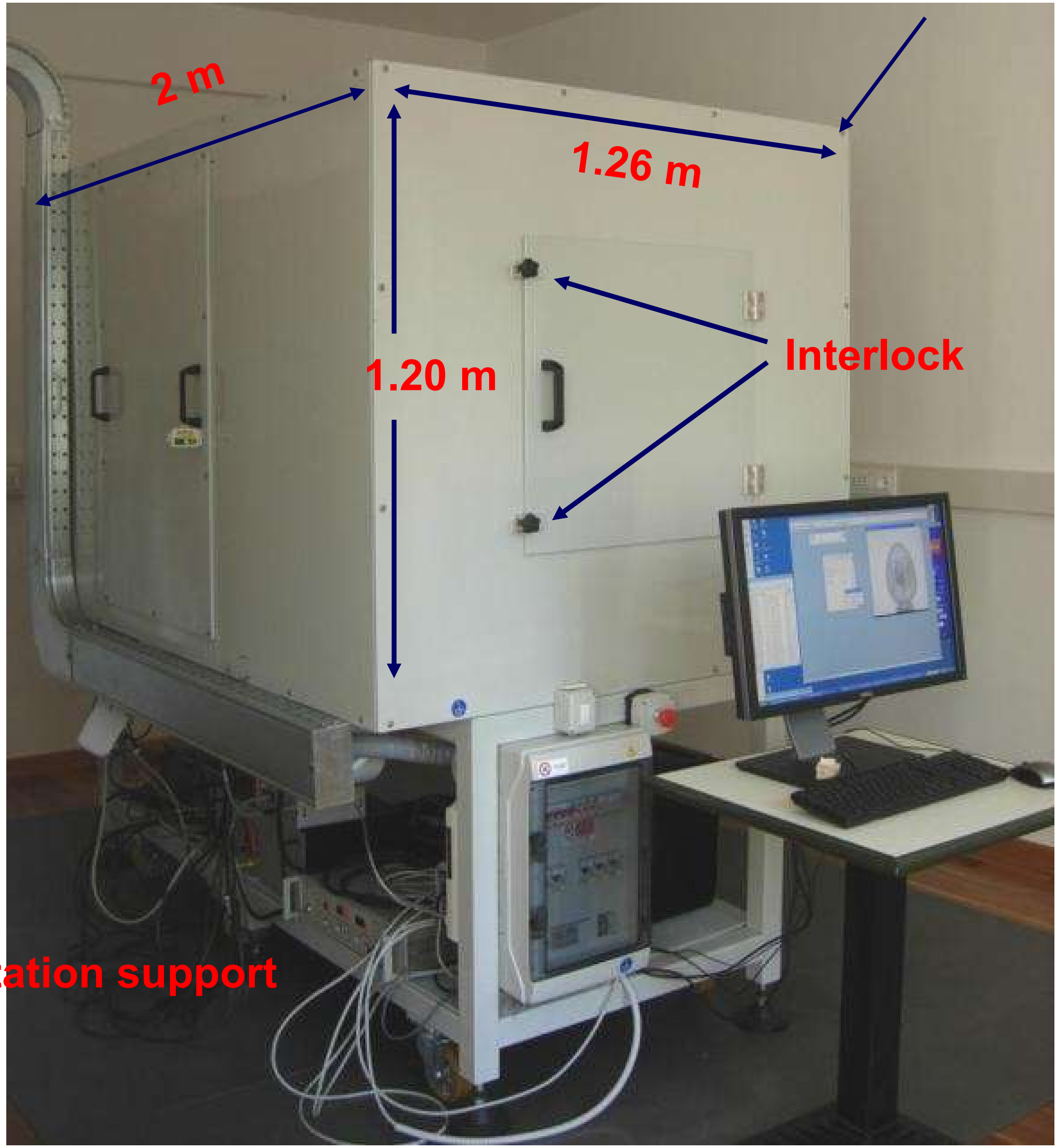

Inside the facility

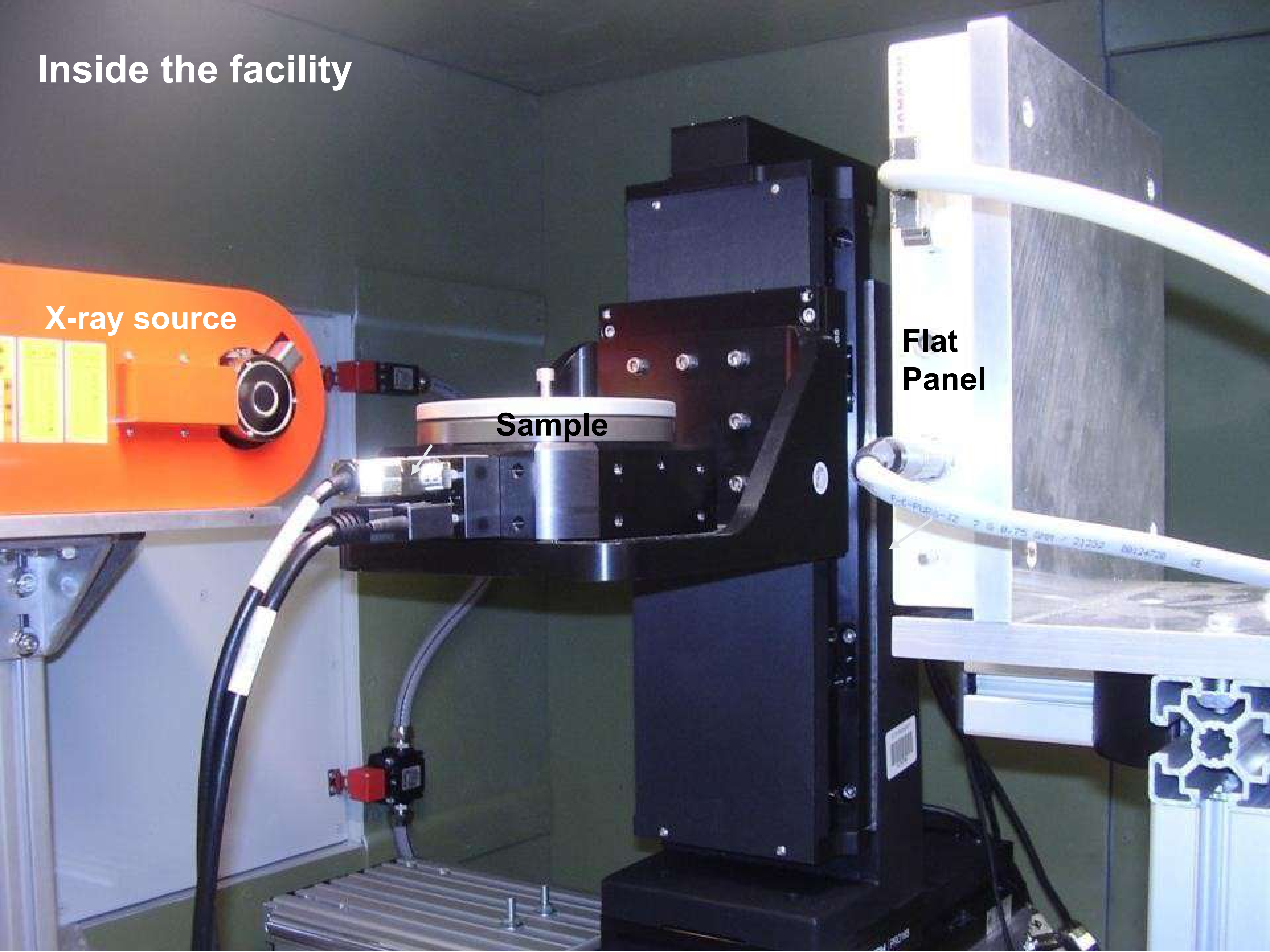

General principles

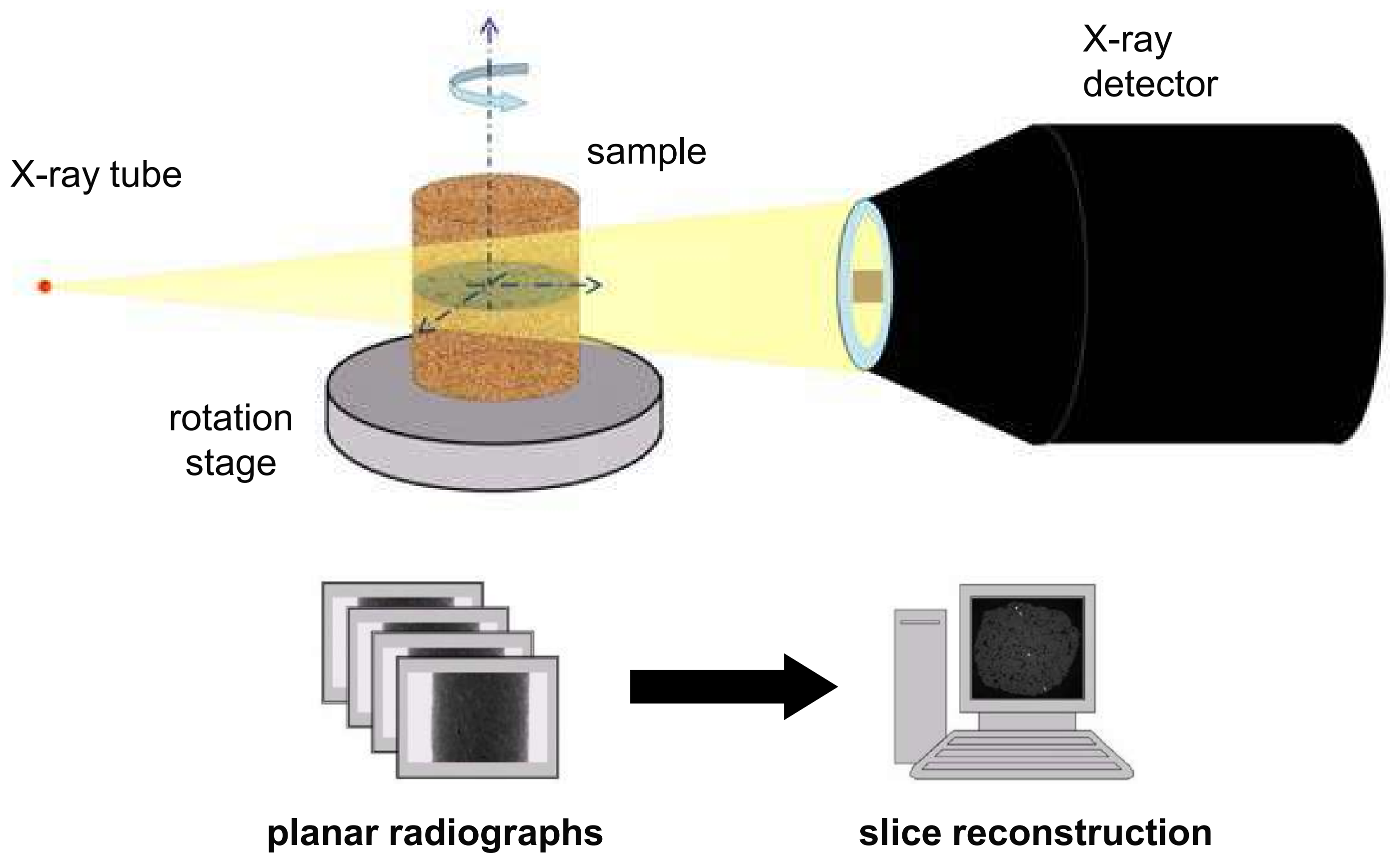

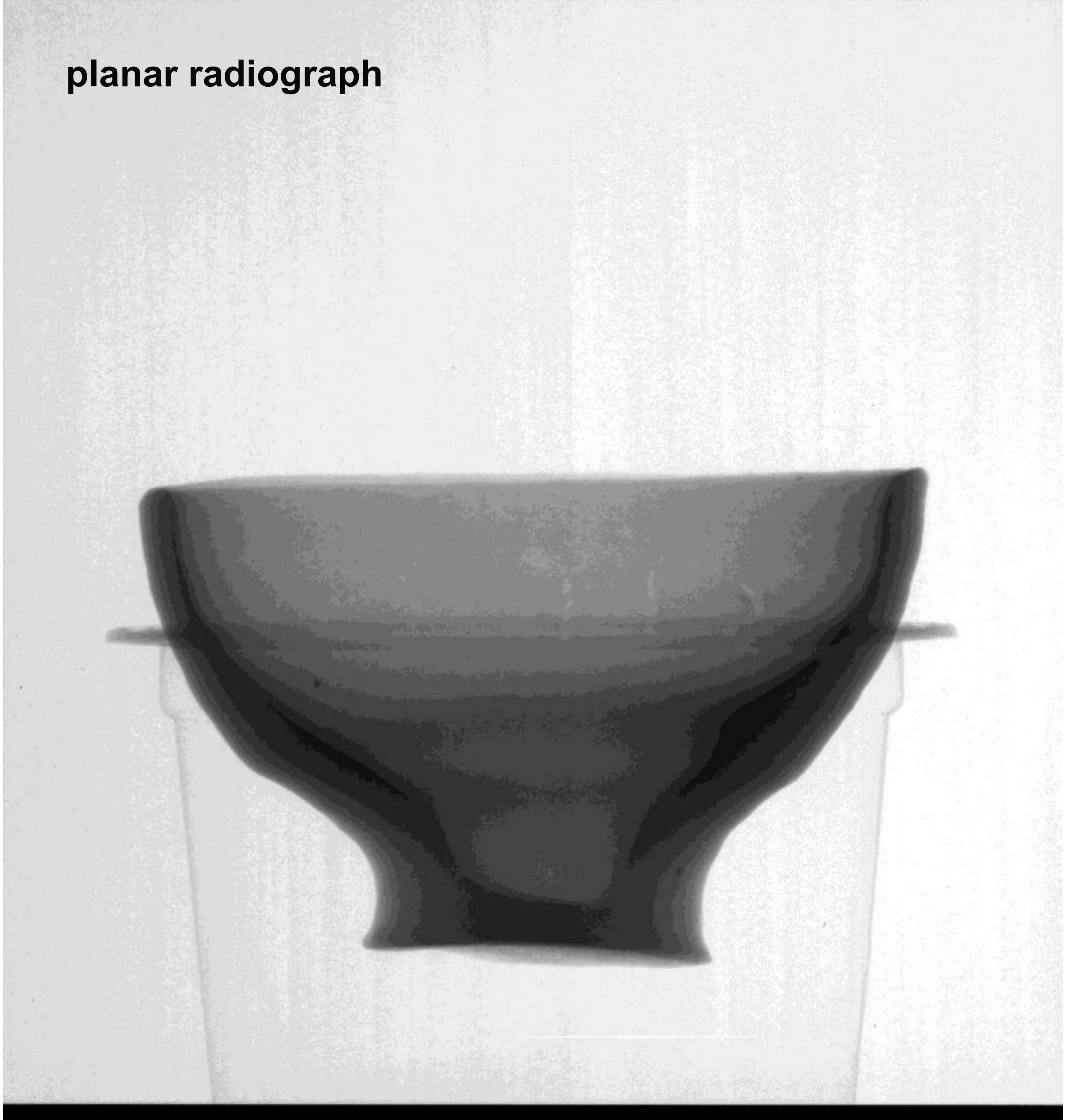

planar radiograph

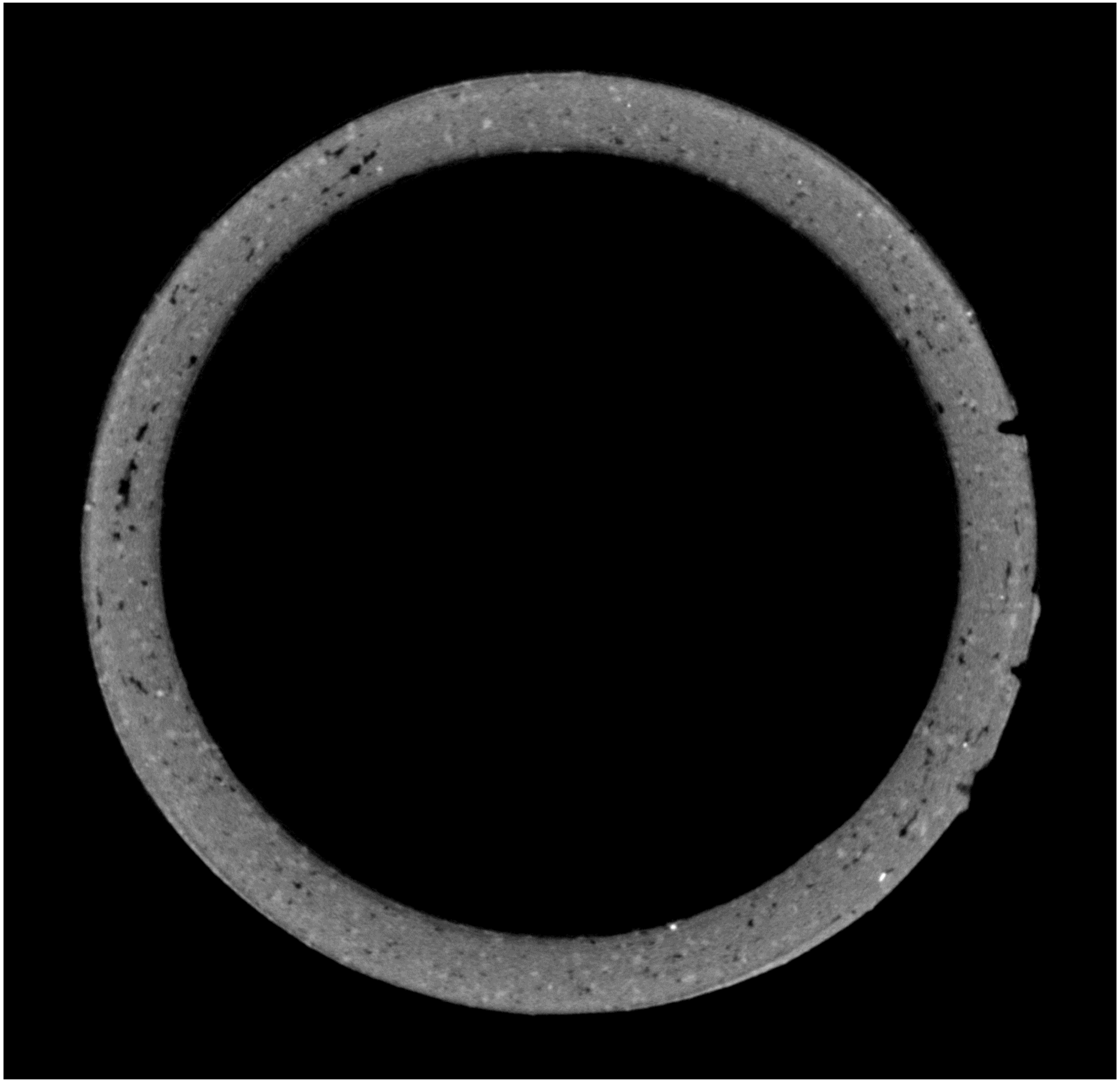

slice

Non-destructive capability to investigate the inner structure of precious human remains and ancient artefacts that could not be damaged through traditional sampling procedures.

If microCT is often not comparable to two-dimensional (2D) analysis of specimen sections, in terms of resolution and direct identification of sample components, it gives non-invasive access to three-dimensional **(3D) information**.

1 Paleontology

PLOS | ONE

RESEARCH ARTICLE

A Reappraisal of the Purported Gastric Pellet with Pterosaurian Bones from the Upper Triassic of Italy

Borja Holgado[1,2]*, Fabio Marco Dalla Vecchia[1], Josep Fortuny[1], Federico Bernardini[3,4], Claudio Tuniz[3,4,5]

1 Mesozoic Research Group, Institut Català de Paleontologia 'Miquel Crusafont' (ICP), C/ Escola Industrial 23, E-08201 Sabadell, Catalonia, Spain, **2** Department of Geology, Universitat de València, C/ Doctor Moliner 50, E-46100 Burjassot, Valencia, Spain, **3** Centro Fermi, Museo Storico della Fisica e Centro di Studi e Ricerche "Enrico Fermi", Piazza del Viminale 1, 00184 Rome, Italy, **4** The 'Abdus Salam' International Centre for Theoretical Physics (ICTP), Multidisciplinary Laboratory, via Beirut 31, I-34014 Trieste, Italy, **5** Centre for Archaeological Science, School of Earth and Environmental Sciences, University of Wollongong, Wollongong, New South Wales 2522, Australia

* bortx.holgado@gmail.com

CrossMark
click for updates

Citation: Holgado B, Dalla Vecchia FM, Fortuny J, Bernardini F, Tuniz C (2015) A Reappraisal of the Purported Gastric Pellet with Pterosaurian Bones from the Upper Triassic of Italy. PLoS ONE 10(11): e0141275. doi:10.1371/journal.pone.0141275

Editor: Brian Lee Beatty, New York Institute of Technology College of Osteopathic Medicine, UNITED STATES

Received: June 25, 2015

Accepted: October 5, 2015

Published: November 11, 2015

Abstract

A small accumulation of bones from the Norian (Upper Triassic) of the Seazza Brook Valley (Carnic Prealps, Northern Italy) was originally (1989) identified as a gastric pellet made of pterosaur skeletal elements. The specimen has been reported in literature as one of the very few cases of gastric ejecta containing pterosaur bones since then. However, the detailed analysis of the bones preserved in the pellet, their study by X-ray microCT, and the comparison with those of basal pterosaurs do not support a referral to the Pterosauria. Comparison with the osteology of a large sample of Middle-Late Triassic reptiles shows some affinity with the protorosaurians, mainly with *Langobardisaurus pandolfii* that was found in the same formation as the pellet. However, differences with this species suggest that the bones belong to a similar but distinct taxon. The interpretation as a gastric pellet is confirmed.

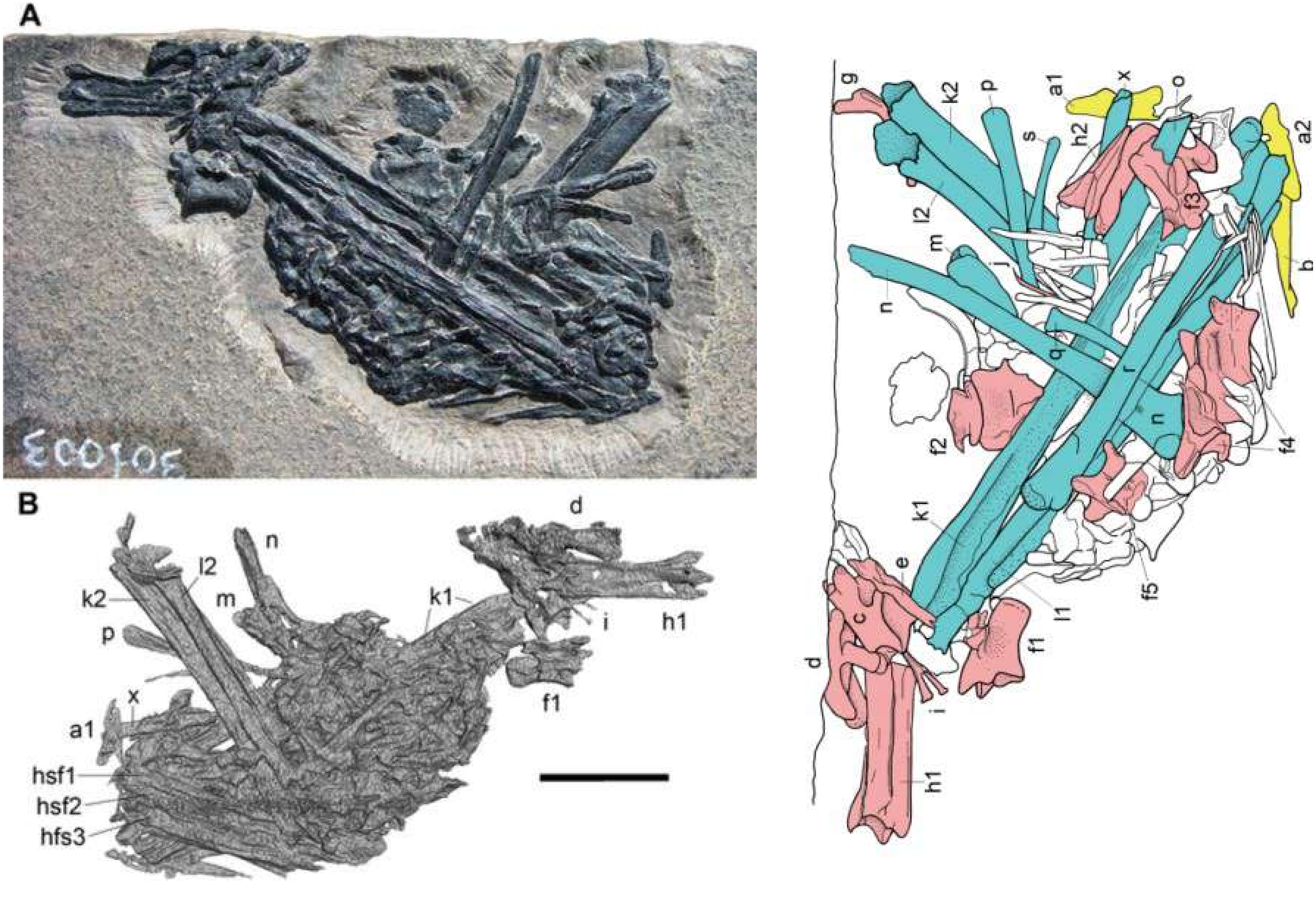

A
E00105
B
d
n
l2
k2
m
k1
p
i
h1
f1
x
a1
hsf1
hsf2
hfs3

Contents lists available at ScienceDirect

Comptes Rendus Palevol

www.sciencedirect.com

General Palaeontology, Systematics and Evolution (Vertebrate Palaeontology)

New remains of *Diplocynodon* (Crocodylia: Diplocynodontidae) from the Early Miocene of the Iberian Peninsula

Nouveaux restes de Diplocynodon *(Crocodylia : Diplocynodontidae) du Miocène inférieur de la péninsule Ibérique*

José Luis Díaz Aráez[a], Massimo Delfino[a,b], Àngel H. Luján[a], Josep Fortuny[a,c], Federico Bernardini[c,d], David M. Alba[a,*]

[a] *Institut Català de Paleontologia Miquel Crusafont, Universitat Autònoma de Barcelona, Edifici (ICTA-ICP), Carrer de les Columnes s/n, Campus de la UAB, 08193 Cerdanyola del Vallès, Barcelona, Spain*

[b] *Dipartimento di Scienze della Terra, Università di Torino, Via Valperga Caluso 35, 10125 Torino, Italy*

[c] *Multidisciplinary Laboratory, the 'Abdus Salam' International Centre for Theoretical Physics, Via Beirut 31, 34151 Trieste, Italy*

[d] *Centro Fermi, Museo Storico della Fisica e Centro di Studi e Ricerche "Enrico Fermi", Piazza del Viminale 1, 00184 Roma, Italy*

ARTICLE INFO

Article history:
Received 27 July 2015
Accepted after revision 9 November 2015
Available online xxx

Handled by Lars van den Hoek Ostende

Keywords:
Fossil crocodiles
Alligatoroidea
Diplocynodon ratelii
Cranial anatomy
Catalonia
Spain

ABSTRACT

We describe crocodylian remains from the Early Miocene (MN4) site of Els Casots (Subirats, Vallès-Penedès Basin, NE of the Iberian Peninsula). Referral to *Diplocynodon* (Alligatoroidea: Diplocynodontidae) is justified by several cranial and postcranial features, including: (1) the subequal and confluent alveoli of the maxilla (fourth and fifth) and dentary (third and fourth); (2) the position of the foramen aëreum on the quadrate; (3) the small and ventrally reflected medial hemicondyle of the quadrate; (4) the distinct dorsoventral step on the frontal; and (5) the bipartite ventral osteoderms. Multiple morphological features are consistent with an attribution to *Diplocynodon ratelii*, previously known from the Early Miocene (MN2) of France, and discount an alternative attribution to other species of the genus, including *Diplocynodon ungeri* from the Middle Miocene (MN5) of Austria. The described material from Els Casots is smaller in size than the French material of *D. ratelii*, possibly reflecting an earlier ontogenetic stage. The described remains constitute the first report of *D. ratelii* and the youngest record of *Diplocynodon* in the Iberian Peninsula, where only *Diplocynodon muelleri* and *Diplocynodon tormis* have been previously reported. The presence of *Diplocynodon* further supports the lacustrine depositional environment previously inferred for Els Casots and also indicates a relatively high temperature.

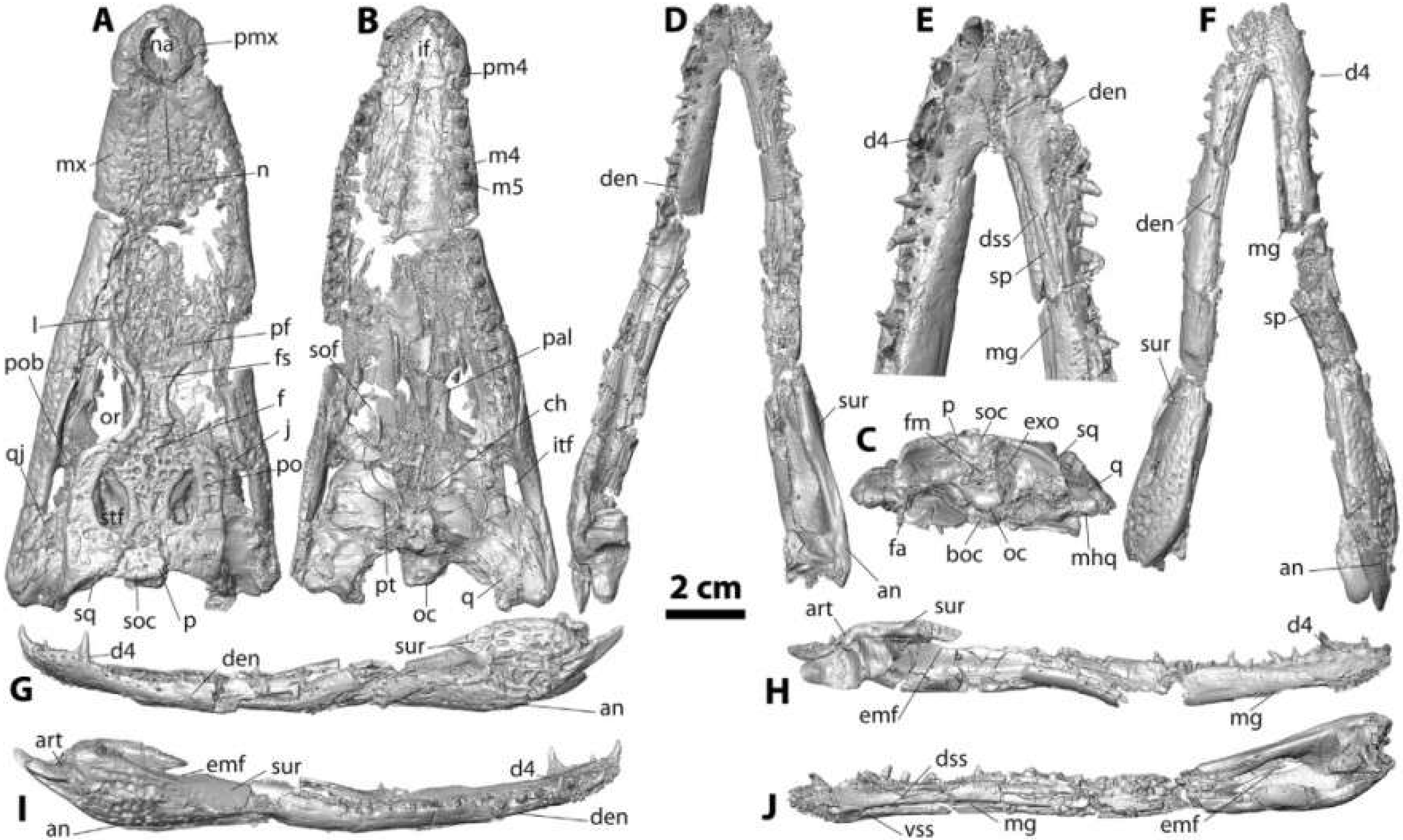

A
B
D
E
F
C
G
H
I
J
na
pmx
mx
n
l
pf
fs
pob
or
f
j
qj
po
stf
sq
soc
p
if
pm4
m4
m5
sof
pal
ch
itf
pt
oc
q
den
sur
an
d4
dss
sp
mg
fm
exo
fa
boc
mhq
2 cm
art
emf
vss

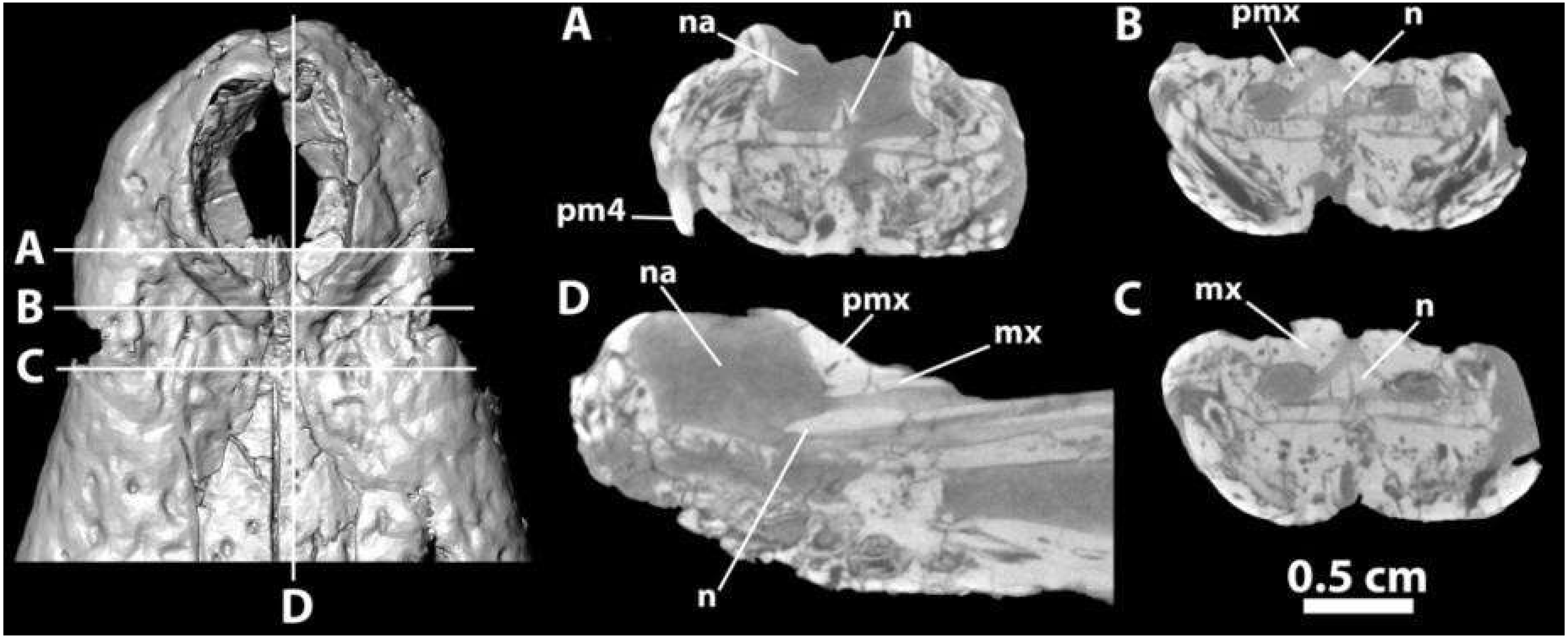

A
B
C
D
A
na
n
pm4
B
pmx
n
D
na
pmx
mx
n
C
mx
n
0.5 cm

ICTP - Centro Fermi - Elettra - MUSE - University of Alberta (Canada) - University of Warsaw (Polland) - University of Bristol (UK) - Flinders University, Adelaide (Australia) - Midwestern University (USA)

LETTER 2018

https://doi.org/10.1038/s41586-018-0093-3

The origin of squamates revealed by a Middle Triassic lizard from the Italian Alps

Tiago R. Simões[1]*, Michael W. Caldwell[1,2], Mateusz Talanda[3], Massimo Bernardi[4,5], Alessandro Palci[6], Oksana Vernygora[1], Federico Bernardini[7,8], Lucia Mancini[9] & Randall L. Nydam[10]

Modern squamates (lizards, snakes and amphisbaenians) are the world's most diverse group of tetrapods along with birds[1] and have a long evolutionary history, with the oldest known fossils dating from the Middle Jurassic period—168 million years ago[2–4]. The evolutionary origin of squamates is contentious because of several issues: (1) a fossil gap of approximately 70 million years exists between the oldest known fossils and their estimated origin[5–7]; (2) limited sampling of squamates in reptile phylogenies; and (3) conflicts between morphological and molecular hypotheses regarding the origin of crown squamates[6,8,9]. Here we shed light on these problems by using high-resolution microfocus X-ray computed tomography data from the articulated fossil reptile *Megachirella wachtleri* (Middle Triassic period, Italian Alps[10]). We also present a phylogenetic dataset, combining fossils and extant taxa, and morphological and molecular data. We analysed this dataset under different optimality criteria to assess diapsid reptile relationships and the origins of squamates. Our results re-shape the diapsid phylogeny and present evidence that *M. wachtleri* is the oldest known stem squamate. *Megachirella* is 75 million years older than the previously known oldest squamate fossils, partially filling the fossil gap in the origin of lizards, and indicates a more gradual acquisition of squamatan features in diapsid evolution than previously thought. For the first time, to our knowledge, morphological and molecular data are in agreement regarding

for the postorbital; a well-developed alar process of the prootic; a well-developed radial condyle on the humerus; an ulnar patella; a secondary curvature of the clavicles; and an expanded epiphysis of the first metacarpal along with the absence of the first distal carpal (suggesting its fusion with the first metacarpal, as observed in modern squamates[12]). Finally, the micro-CT scans indicate that *Megachirella* has features that are absent in all rhynchocephalians (the sister lineage to squamates), including the earliest forms such as *Gephyrosaurus*: the presence of a splenial; the ectopterygoids are directed anteriorly (not laterally as in rhynchocephalians); the presacral pleurocentra lack a notochordal canal; and dorsal (coronoid) expansion of the surangular and dentary bones is absent. The new information presented here, along with our extensive revision of diapsid and early squamate phylogeny, unambiguously resolves the placement of *Megachirella* as the oldest known squamate. As expected for a squamate that is 85 million years (Myr) older than the oldest previously known articulated squamates for which the osteology is well known—*Eichstaettisaurus* and *Ardeosaurus* from the Late Jurassic of Germany[8,13]—*Megachirella* retains numerous plesiomorphic features. These features are observed in other diapsid reptiles, and some are retained in rhynchocephalians, but they are almost entirely lost in crown squamates. These include amphicoelic vertebrae (although present in geckoes and *Huehuecuetzpalli*), a small quadratojugal, gastralia and an entepicondylar foramen in the humerus.

Assessing the phylogenetic position of *Megachirella* and other lepido-

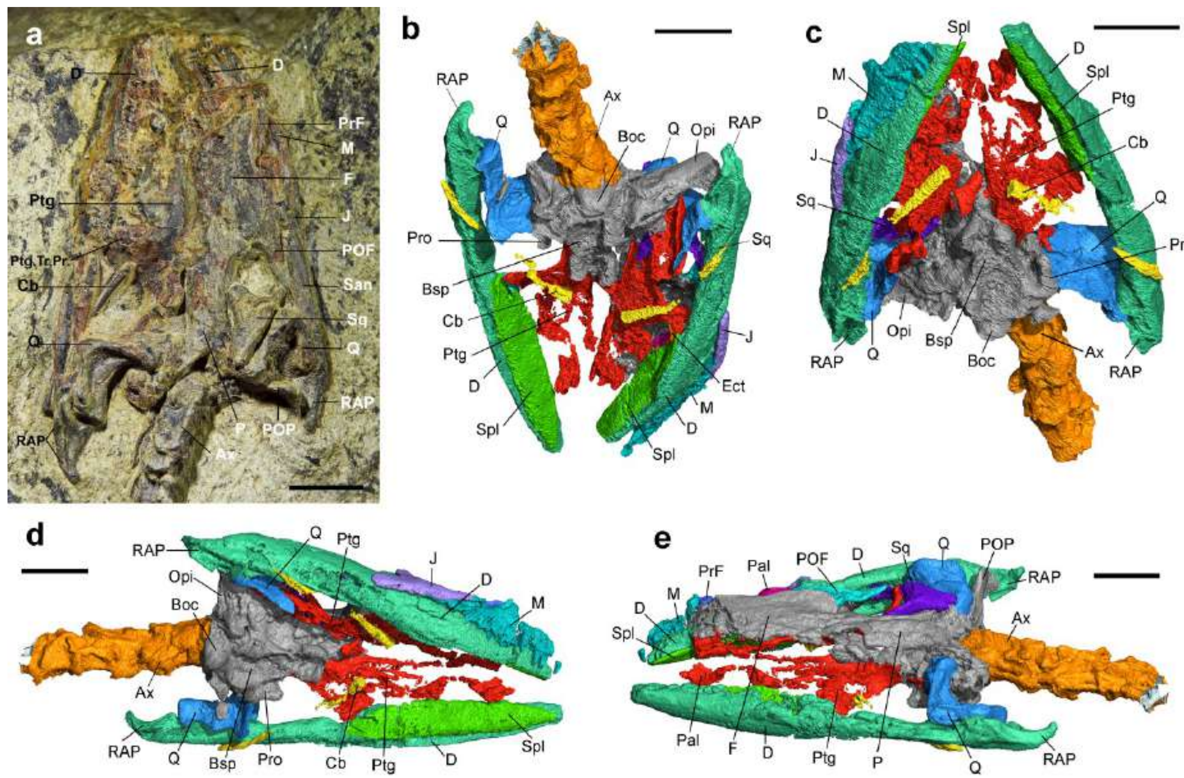
a
D
D
PrF
M
F
J
Ptg
POF
Ptg Tr Pr
Cb
San
Sq
Q
Q
RAP
RAP
P
POP
Ax
b
RAP
Q
Ax
Boc
Q
Opi
RAP
Pro
Sq
Bsp
Cb
Ptg
J
D
Ect
M
Spl
D
Spl
c
Spl
M
D
Spl
D
Ptg
J
Cb
Sq
Q
Pro
RAP
Q
Opi
Bsp
Boc
Ax
RAP
d
RAP
Q
Ptg
J
D
Opi
M
Boc
Ax
RAP
Q
Bsp
Pro
Cb
Ptg
D
Spl
e
PrF
Pal
POF
D
Sq
Q
POP
RAP
M
D
Ax
Spl
Pal
F
D
Ptg
P
Q
RAP

2 Paleoanthropology


Ceprano

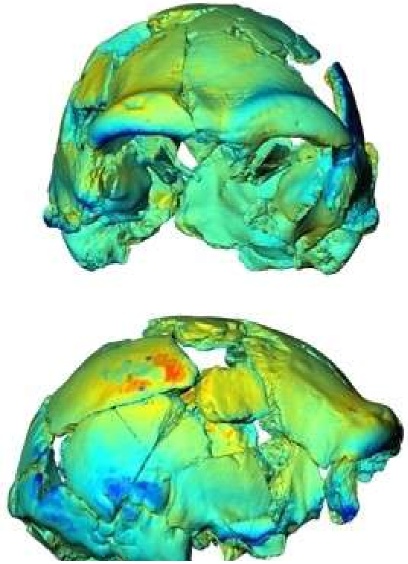

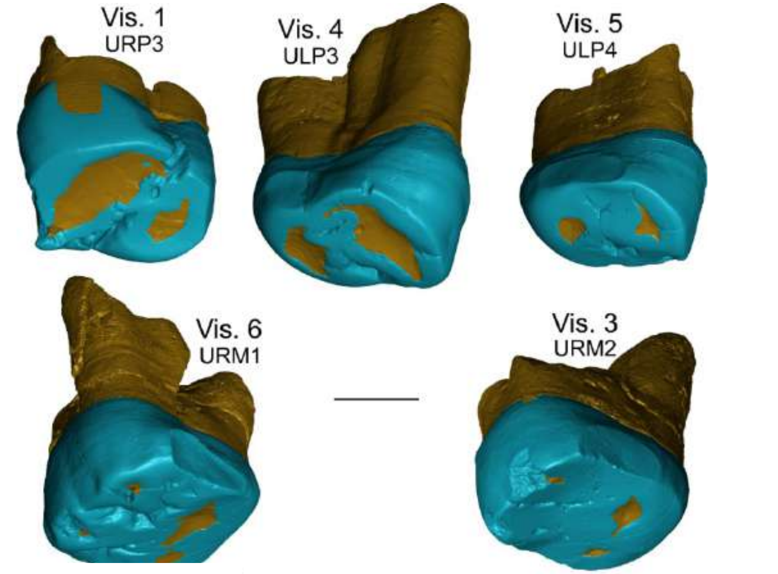


Saccopastore 1


Saccopastore 2

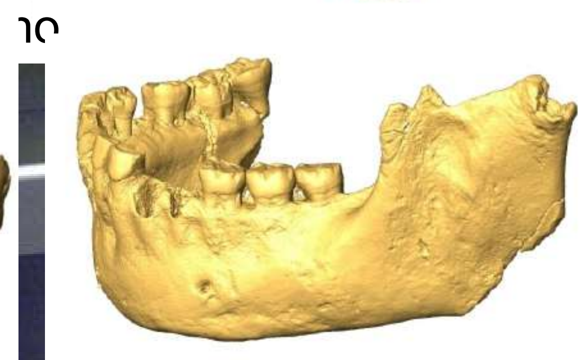
Guattari 3


Archi

Teeth structure and morphology

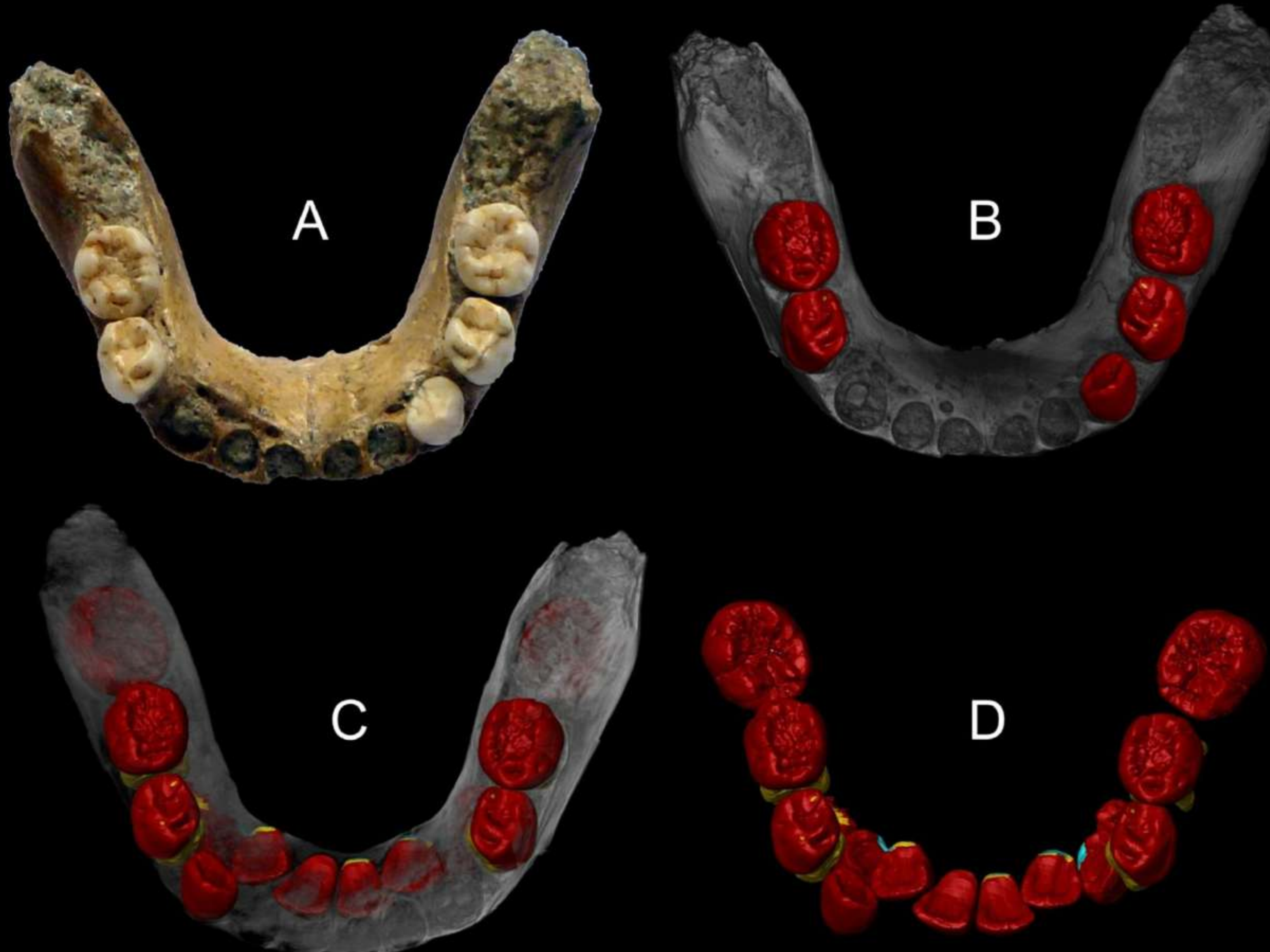

Bernardini F. et al 2013 Microtomographic-based structural analysis of the Neanderthal child mandible from Archi, Southern Italy. *Proceedings of the European Society for Human Evolution* 2: 44.

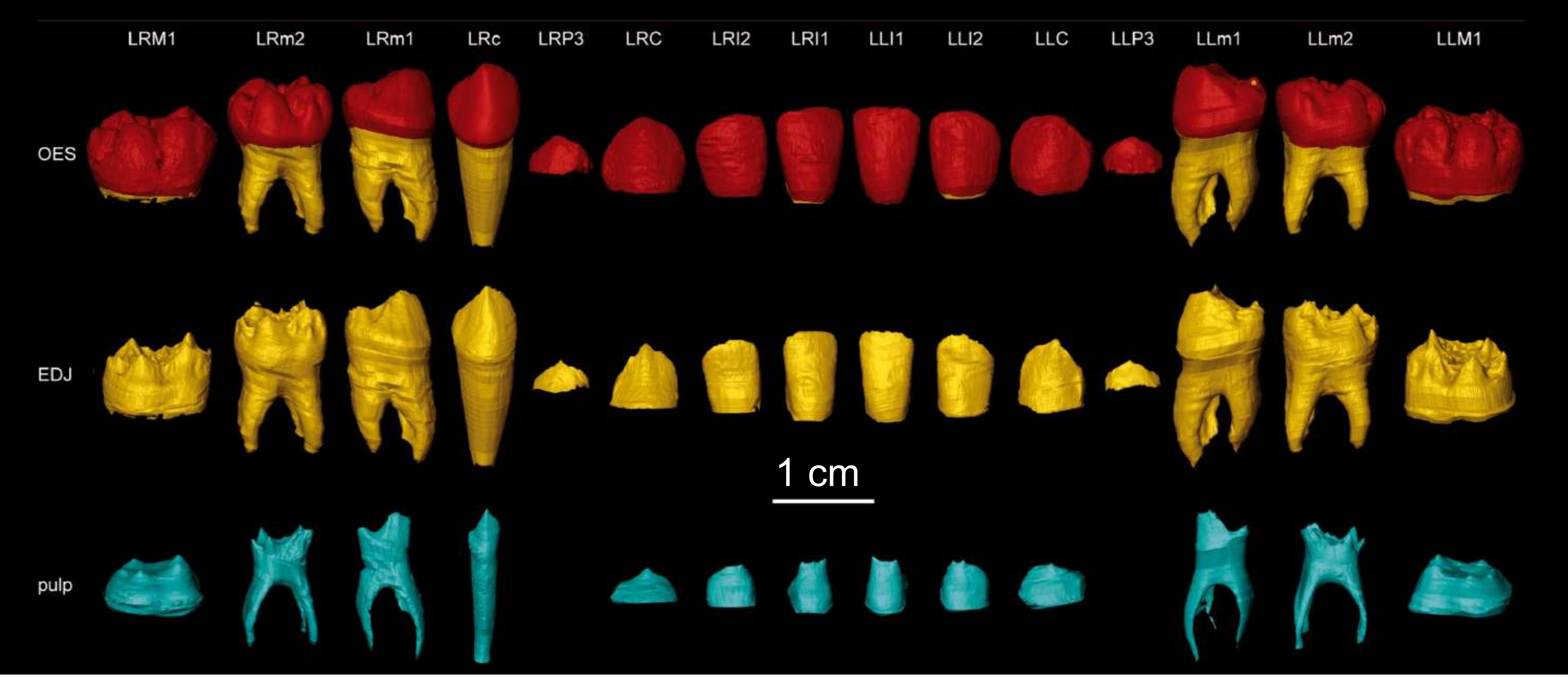
LRM1
LRm2
LRm1
LRc
LRP3
LRC
LRI2
LRI1
LLI1
LLI2
LLC
LLP3
LLm1
LLm2
LLM1
OES
EDJ
pulp
1 cm

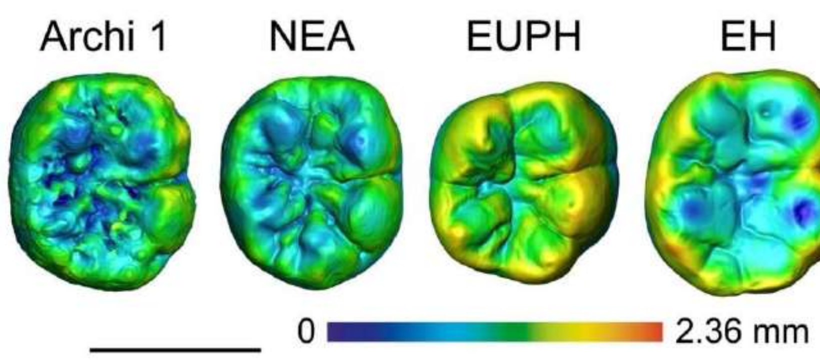
Archi 1
NEA
EUPH
EH
0
2.36 mm

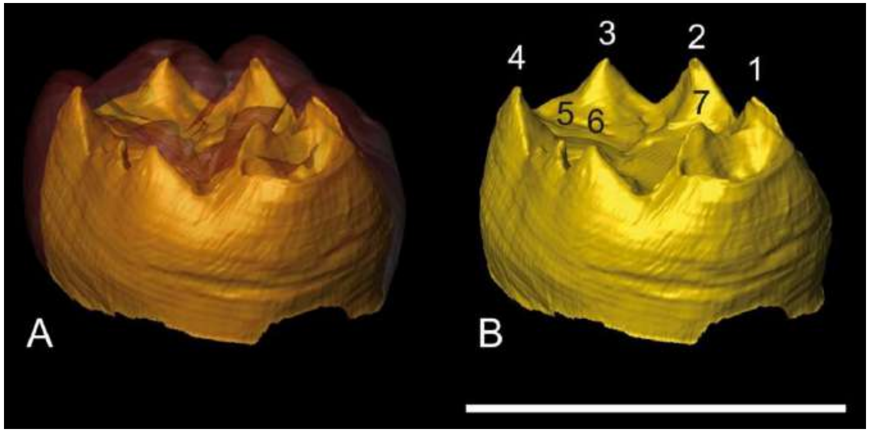
A
B
1
2
3
4
5
6
7

Virtual endocasts of ancient humans

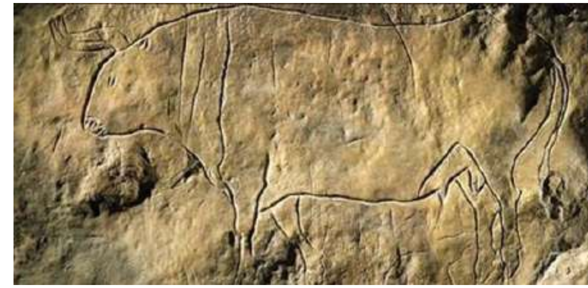

The Romito skull, dated to 17 ky, is part of a Epigravettian burial discovered in the famous Romito cave in Calabria.

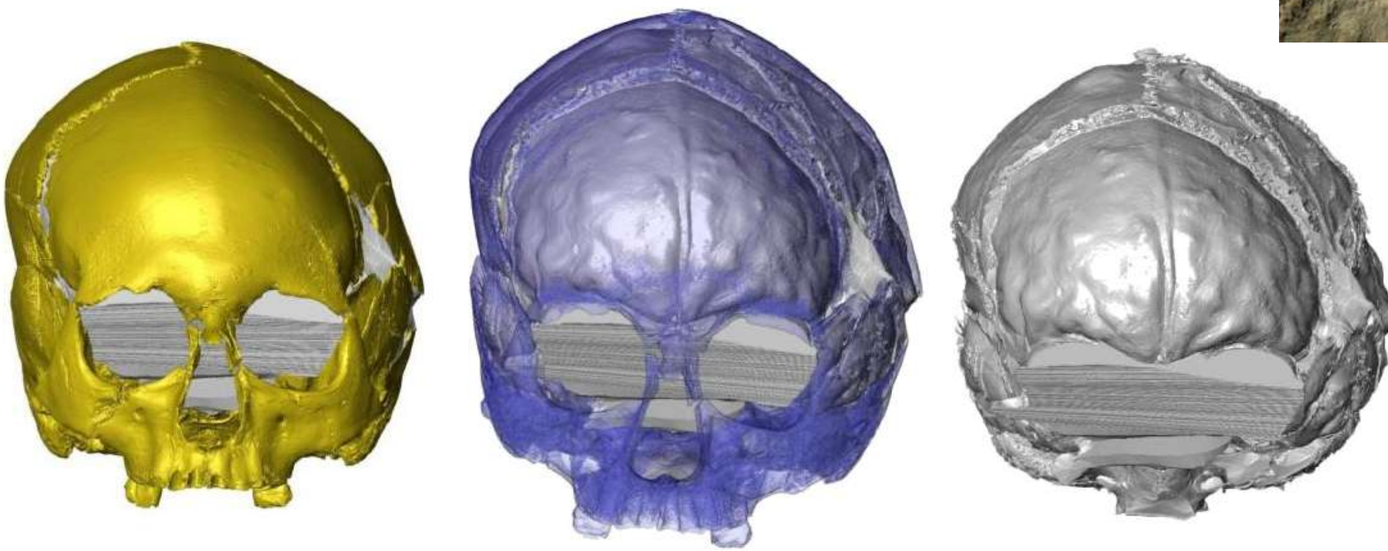

The ancient Bronze Age Mompaderno Skull from Istria, Croatia.

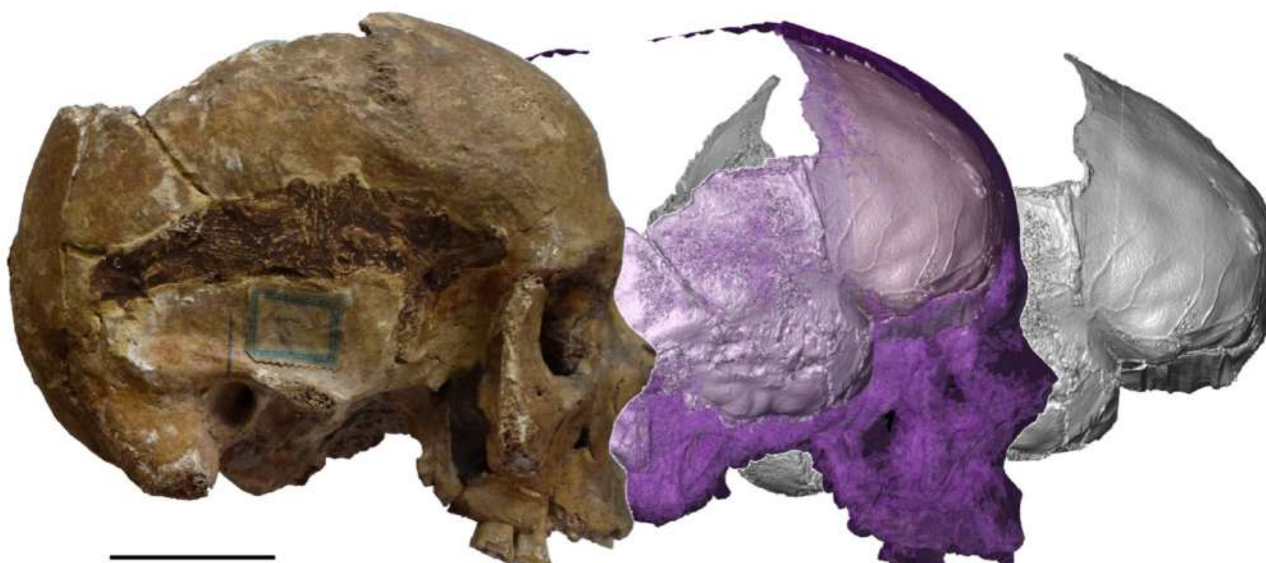

Virtual restoration and retrodeformation of human skulls

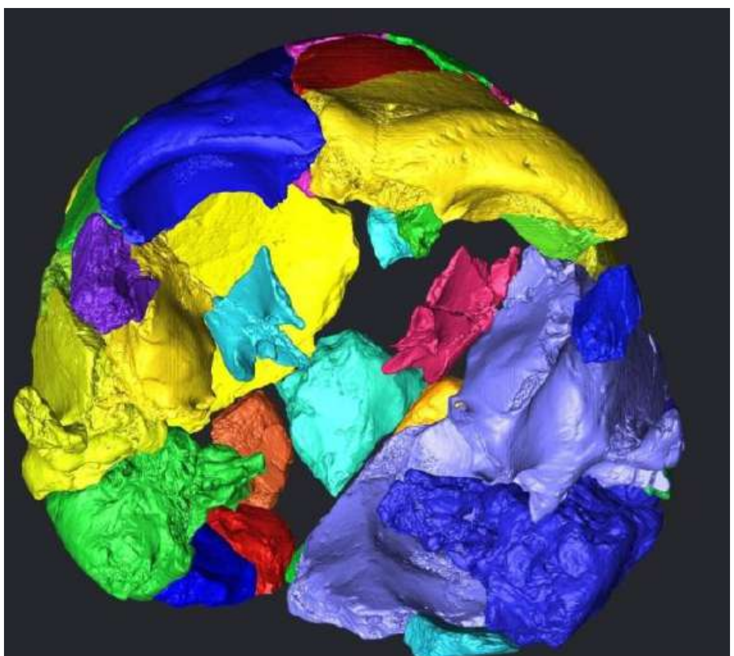

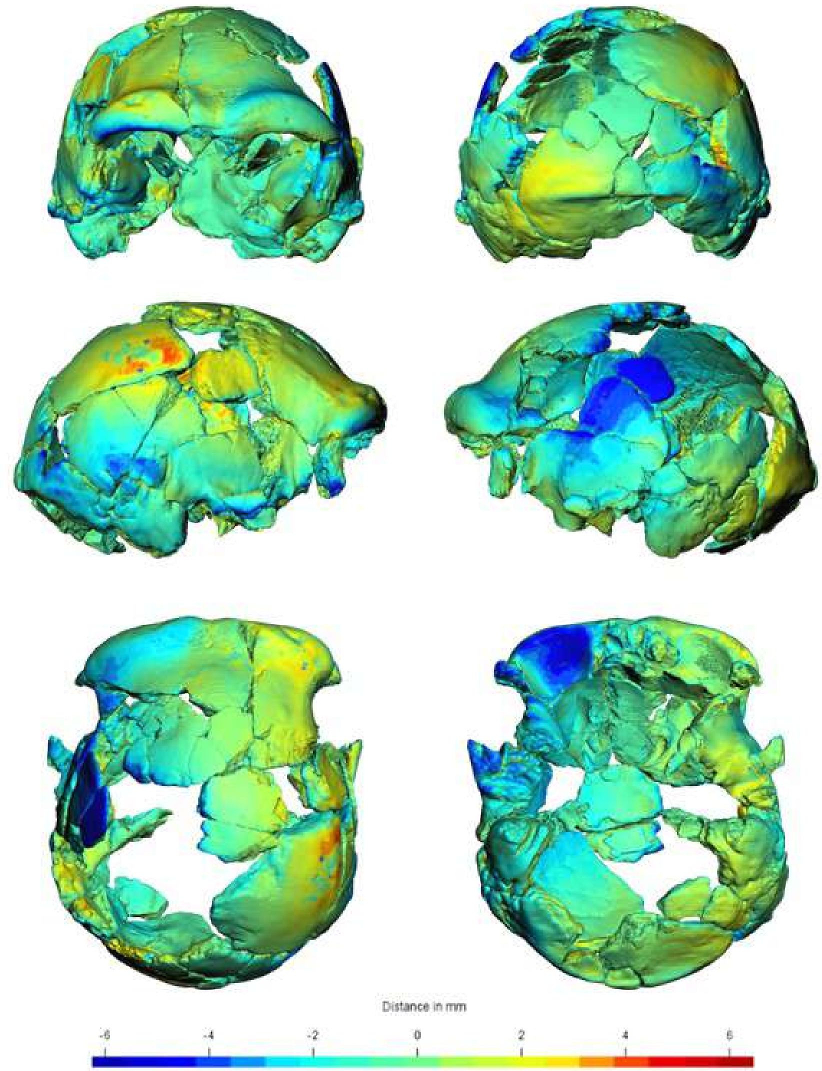

Di Vincenzo F. et al 2017 Digital reconstruction of the Ceprano calvarium (Italy), and implications for its interpretation. *Scientific Reports* 7 doi:10.1038/s41598-017-14437-2.

3 Archaeology

Pottery

Characterization of ancient Ghana clay figurines (about 1ky BP)

collaboration ICTP - Ghana Atomic Energy Commission (GAEC) - National Nuclear Research Institute (NNRI)

Dr. Nuviadenu Christian Kwasi at ICTP lab preparing the samples for microCT analysis

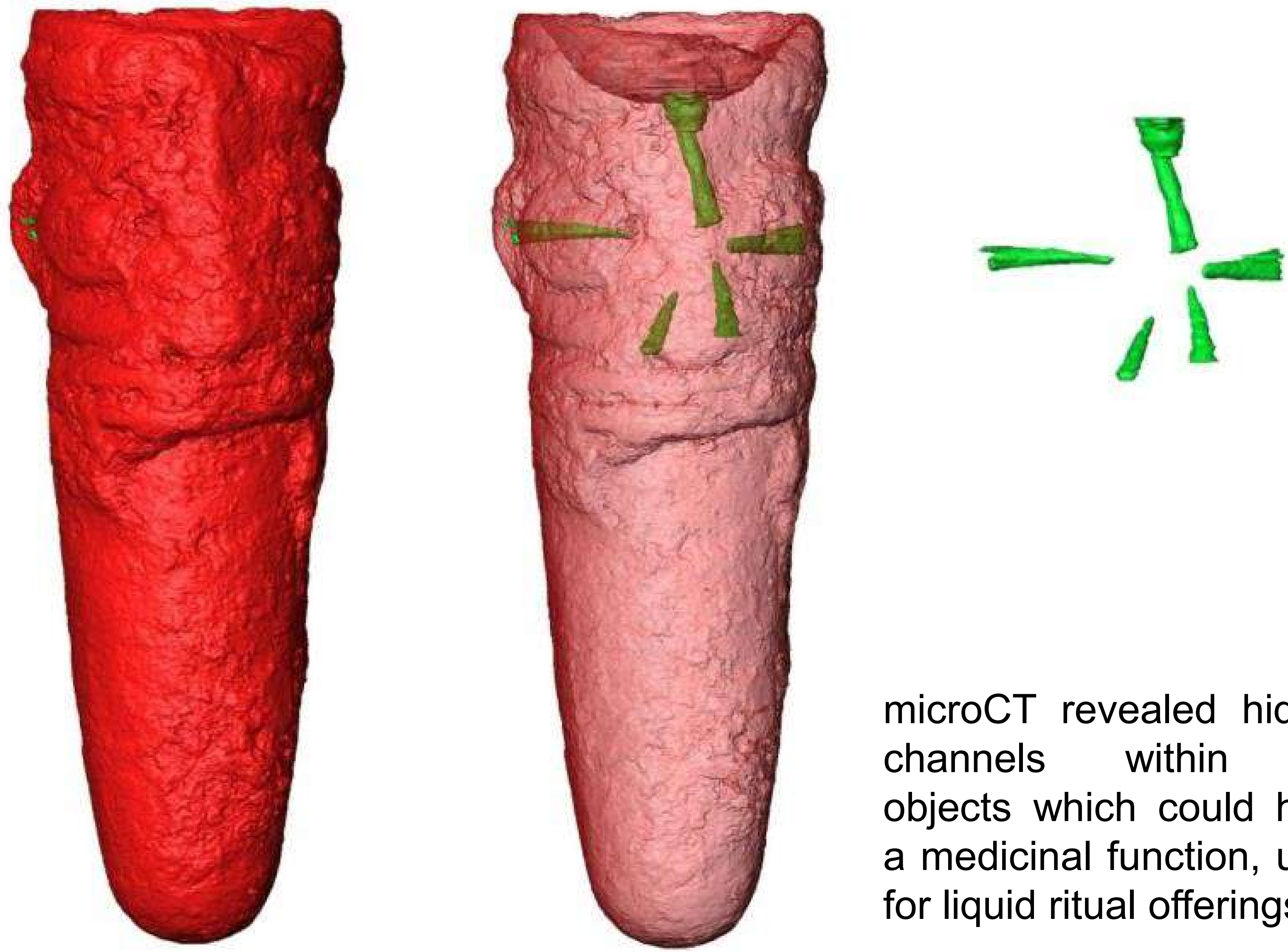

microCT revealed hidden channels within the objects which could have a medicinal function, used for liquid ritual offerings.

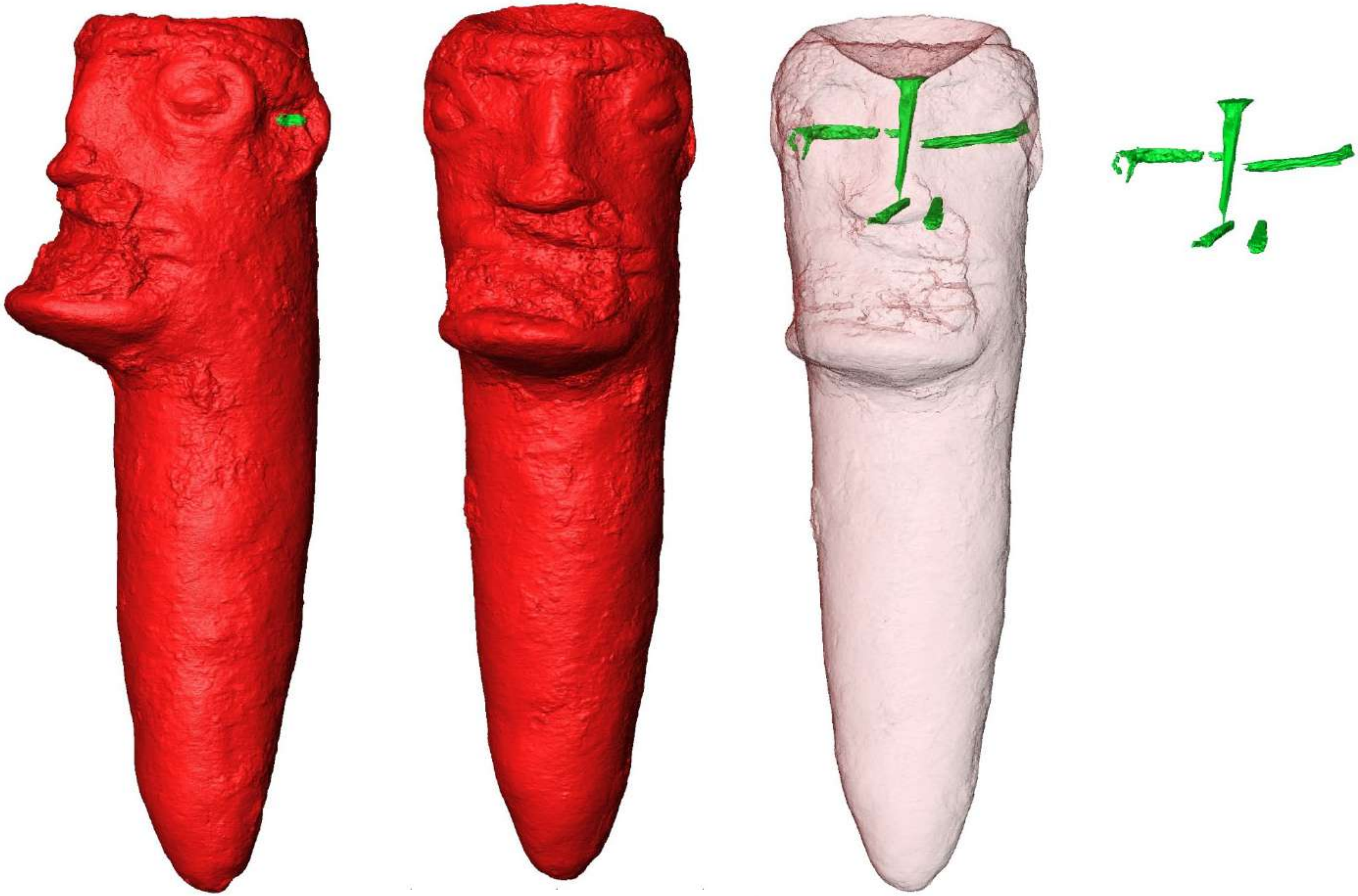

Pottery: forming techniques

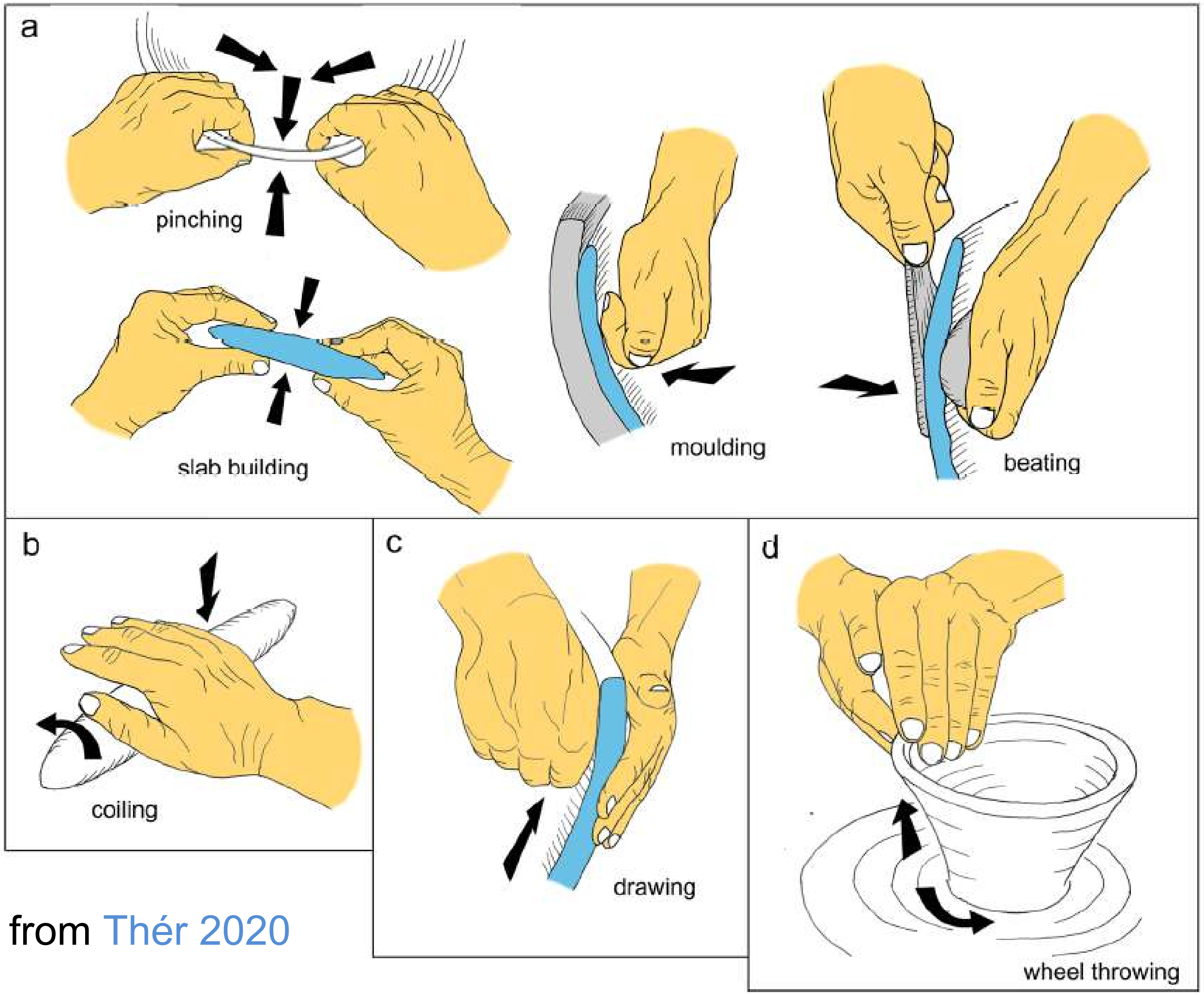

from Thér 2020

Fig. 1 Actions used to model a basic object, considered as a set of physical forces acting on plastic clay during forming. **a** Techniques using pressure or percussion perpendicular to the vessel wall or surface of the shaped segment causing predominantly compressive deformation. **b** Techniques using pressure with a revolving movement of the deformed mass. **c** Techniques using pressure parallel to the wall margins causing a combination of shear and compression deformation. **d** Techniques using pressure parallel to the wall margins in combination with rotation of the formed object causing compressive and shear deformation

Alignment of voids and inclusions according to the forming technique (from Berg 2008)

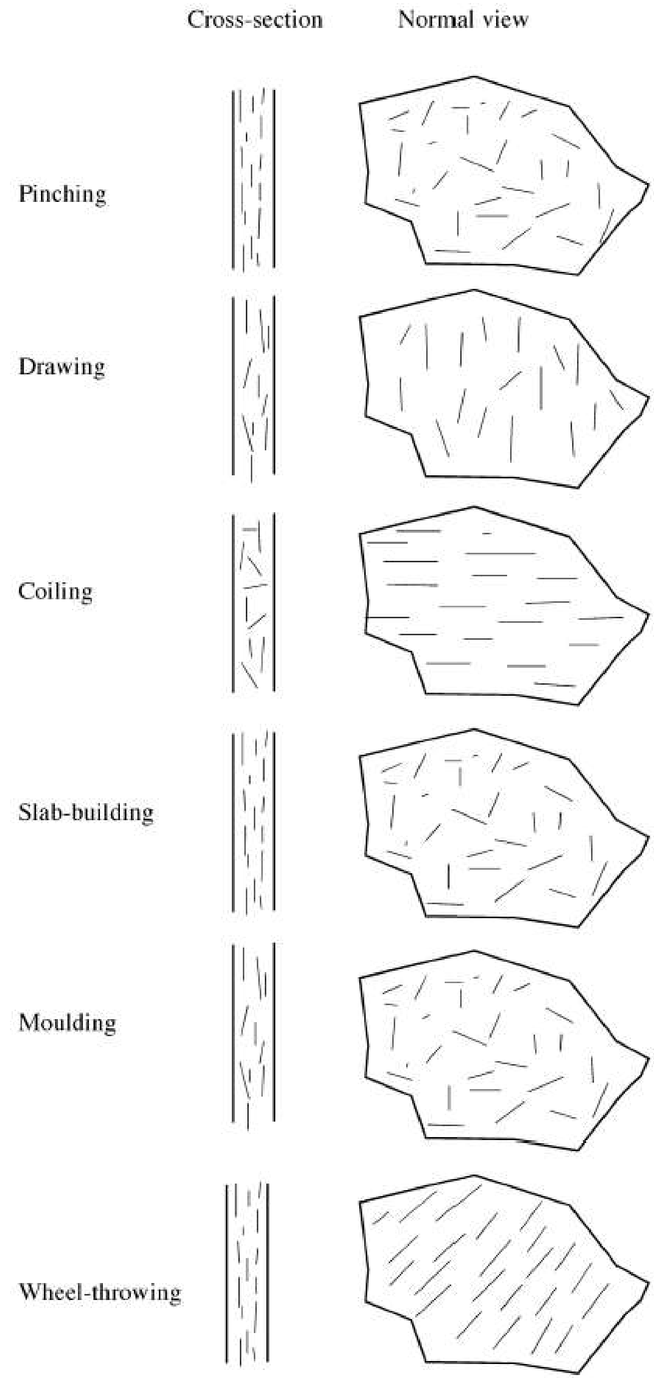

Wheel-made vs. wheel-shaped

“Pottery specialists commonly classify vessels as either wheel-made or handmade vessels based on distinct surface features. However, anthropological case studies have shown that **this binary classification is a modern construct and does not reflect past reality**.

Instead, pottery manufacturing techniques should best be visualised as ranging from completely handmade through combination techniques to completely wheel-made ones.” (from Berg 2008)

Relevant diagnostic attributes of pottery-forming practices

They can be divided into five categories:

(a) surface morphology and topography

Remnants of segmental joints: Copper Age bowls from Italy and Slovenia

Decorated bowls with cross-shaped foots are peculiar Late Copper Age vessels widespread in Central Europe and northern Balkans. They are very common in the Deschmann's pile dwellings, located in the Ljubljansko barje (Central Slovenia), but quite rare in the caves of Trieste Karst (north-eastern Italy).

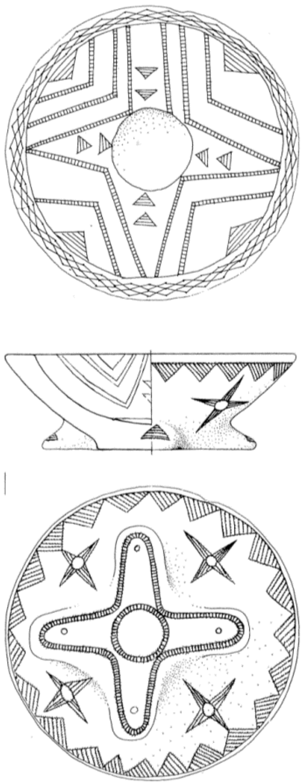

Ciclami Cave
20591 (Trieste)

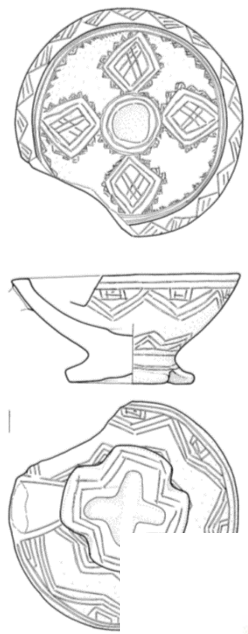

Deschmann's pile dwellings
B1842 (Ljubljana)

Bernardini F. et al. 2019 - X-ray computed microtomography of Late Copper Age decorated bowls with crossshaped foots from central Slovenia and the Trieste Karst (north-eastern Italy): technology and paste characterization, *Archaeological and Anthropological Sciences*

Coiling technique vs Modelling technique

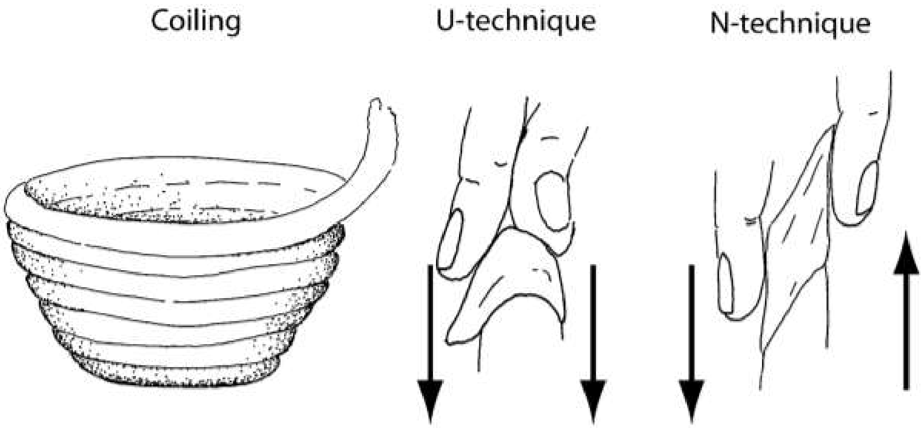

From **Lindahl and Pikirayi 2010**

U-coiling technique N-coiling technique

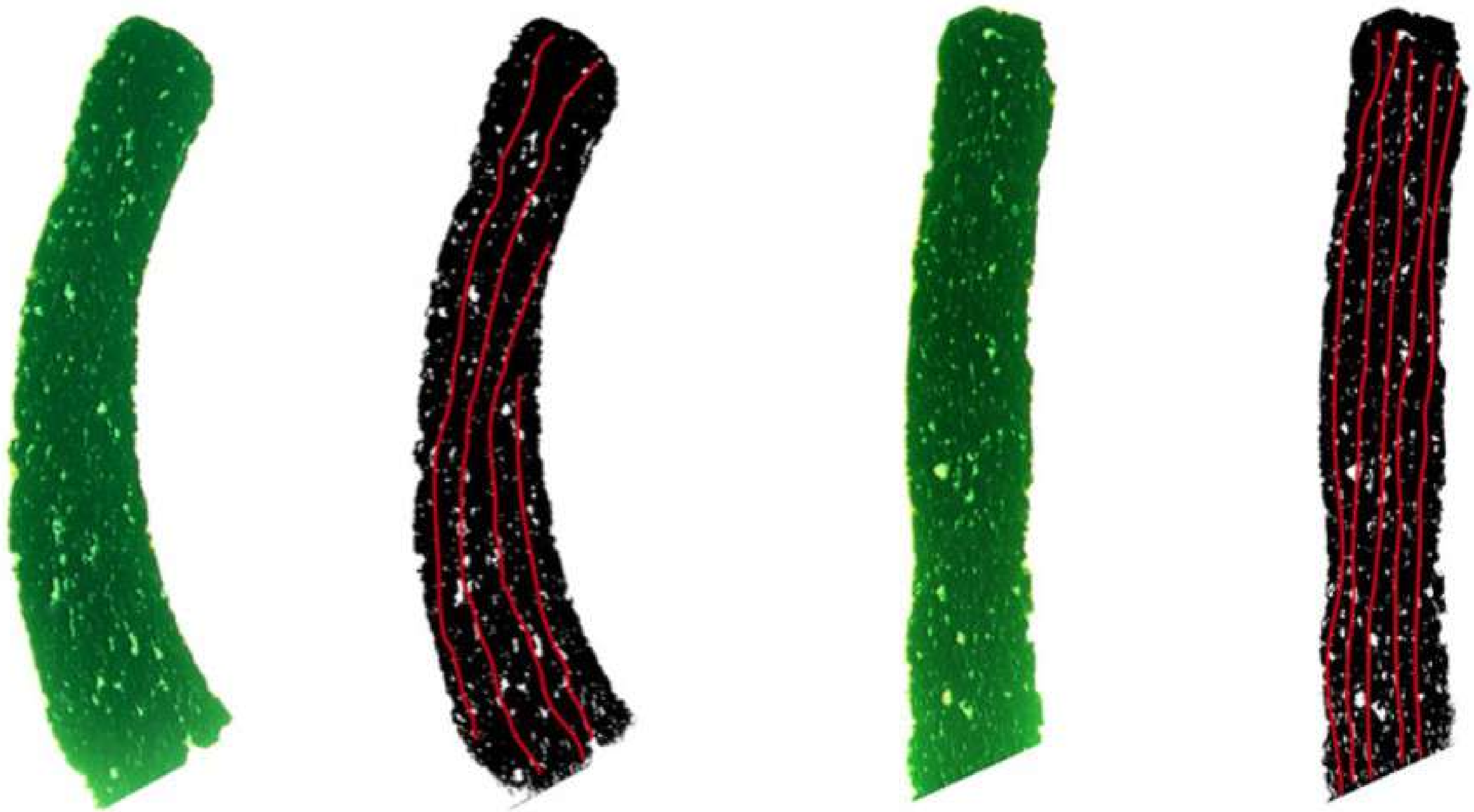

Modelling technique

MicroCT data can be used to produce 3D renderings of external surfaces but they are especially useful to see beyond the appearance.

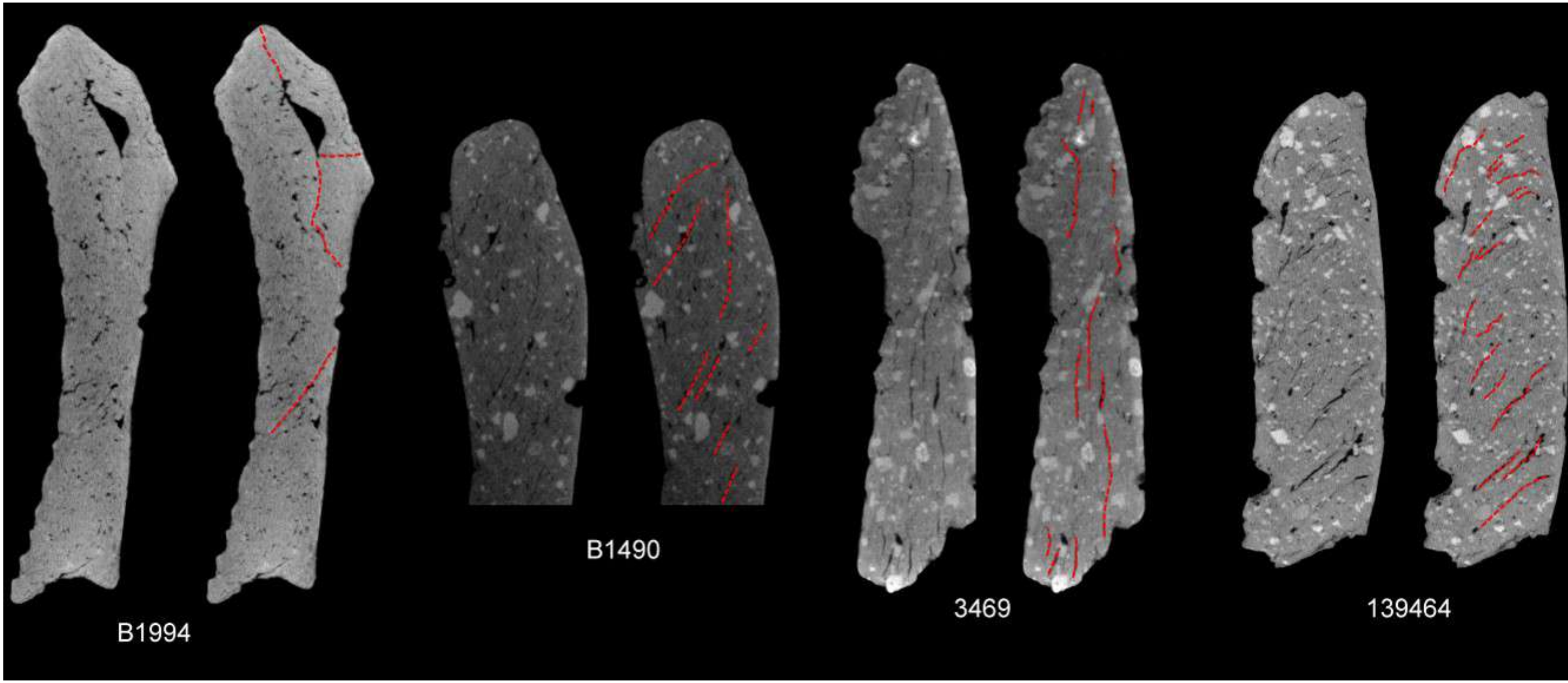

Virtual transversal sections of selected rims of investigated bowls showing technological traces highlighted by dotted red lines.

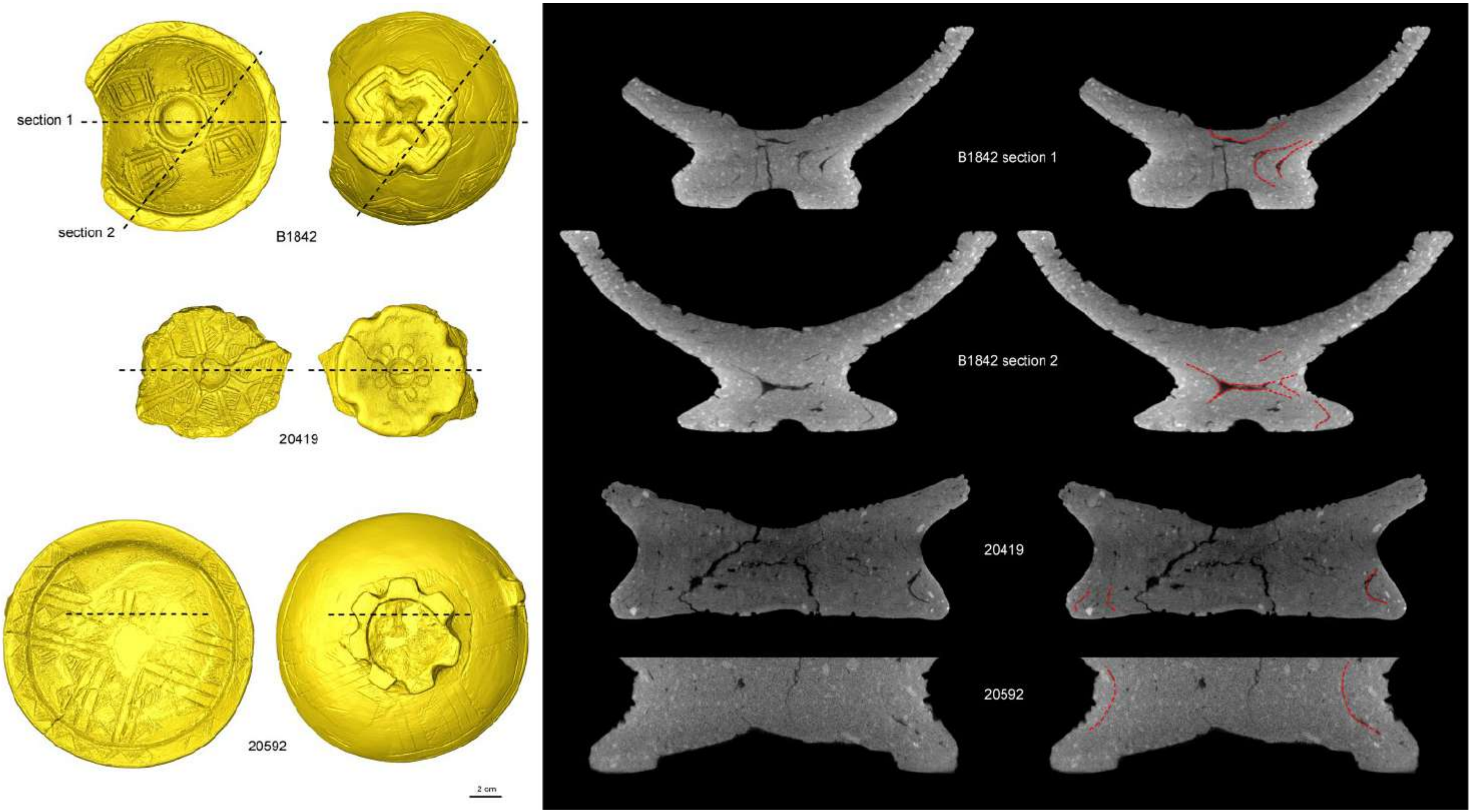

Virtual transversal sections of the base of selected bowls from Slovenia (B1482) and Italy (20419 and 20592) showing technological traces highlighted by dotted red lines.

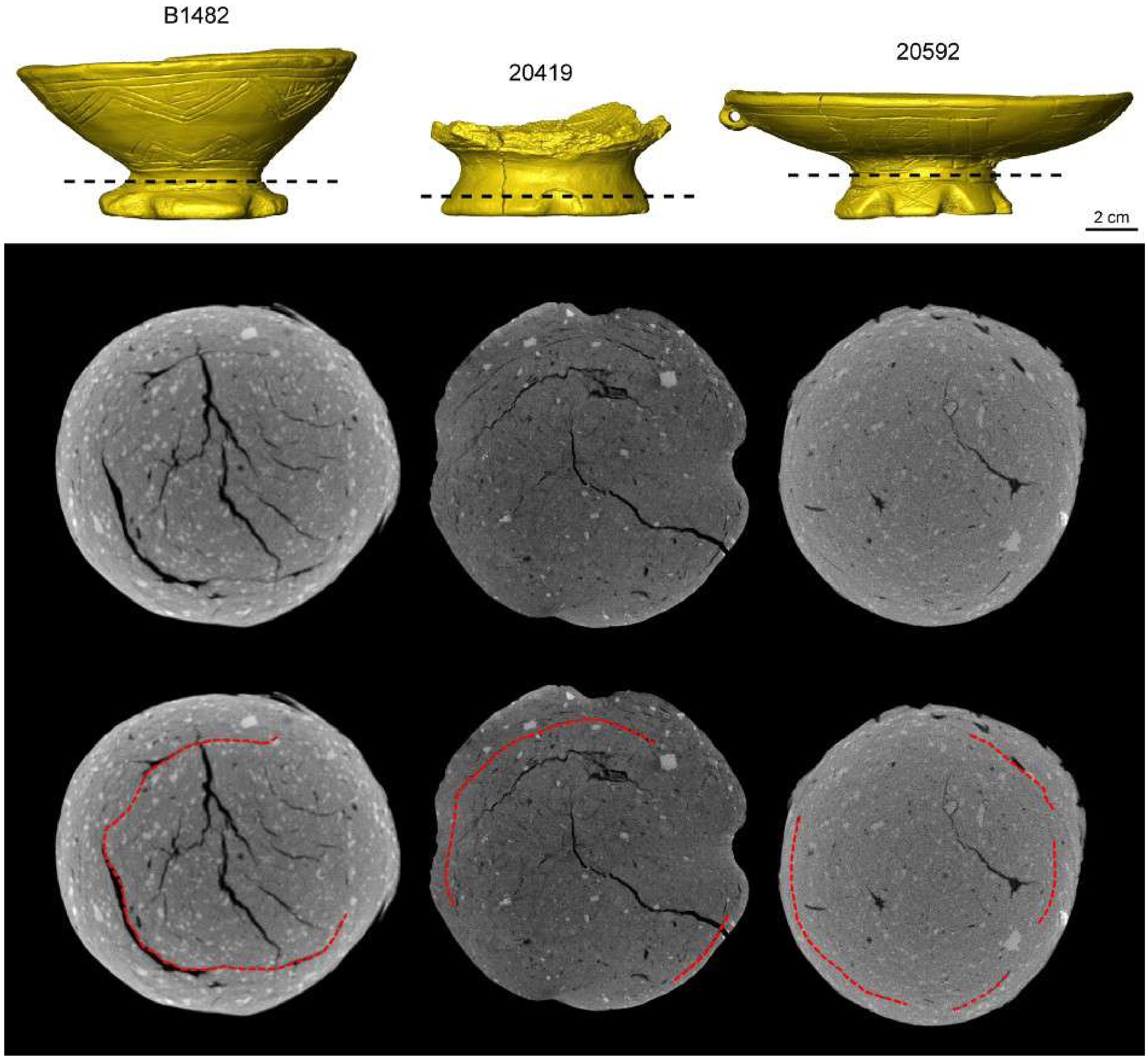
B1482
20419
20592
2 cm

Wall thickness and orientation of voids and inclusions

ELSEVIER

Journal of Archaeological Science

Volume 169, September 2024, 106025

Revealing primary forming techniques in wheel-made ceramics with X-ray microCT

Ilaria Caloi [a], Federico Bernardini [a b]

Show more

Add to Mendeley Share Cite

https://doi.org/10.1016/j.jas.2024.106025 Get rights and content

Highlights

- 3D X-ray microCT analysis on experimental wheel-made pottery vessels.
- 3D and 2D quantification of thickness variation in vessel walls.
- Evaluation of 3D voids orientation and identification of structural joints.
- Integrating macroscopic and microCT data unveils primary forming techniques.

Modern replicas of conical cups reproduced using five different forming techniques on a Minoan-type potter's wheel. Ceramic technology at Phaistos in Middle Minoan IIA (18th cent. BC), Ilaria Caloi, Ca' Foscari University of Venice

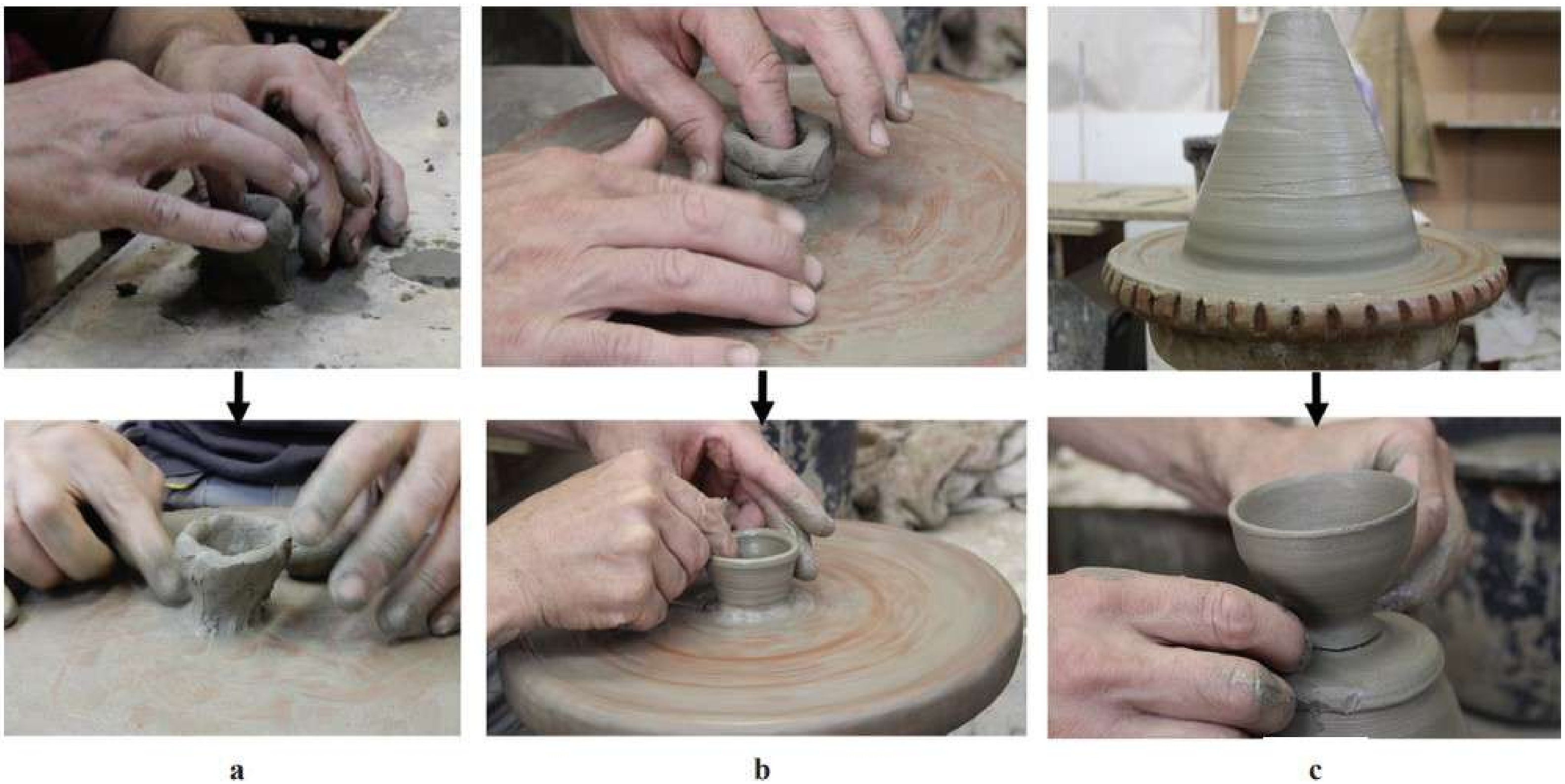

Figure 4. The three forming techniques used by the potter V. Politakis to reproduce MM IIA handleless conical cups from Phaistos: a) pinching and final shaping on the wheel; b) wheel-coiling; c) throwing-off-the-hump. Photographs by author.

(from Caloi 2021)

Replica produced by the wheel throwing technique (throwing-off-the-hump)

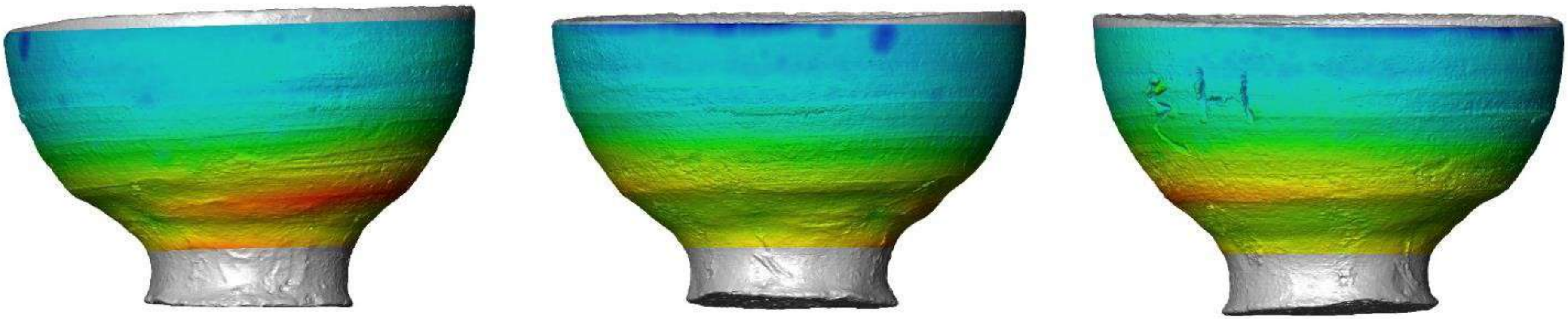

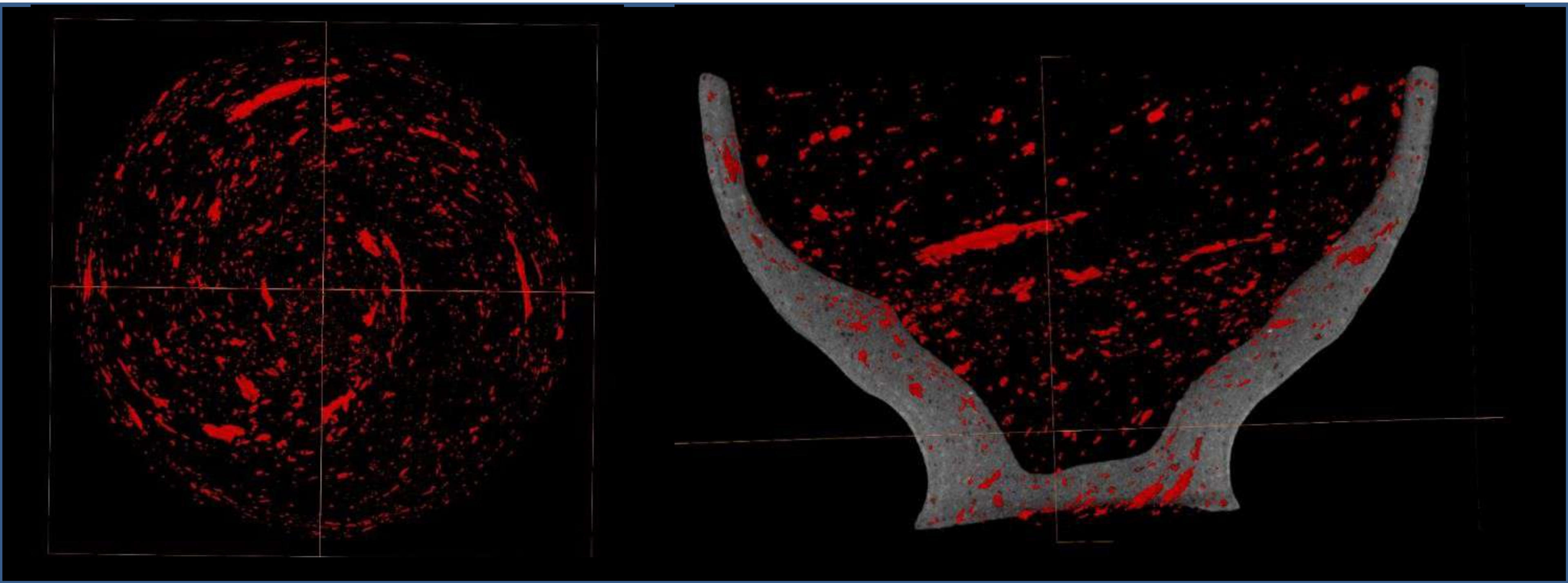

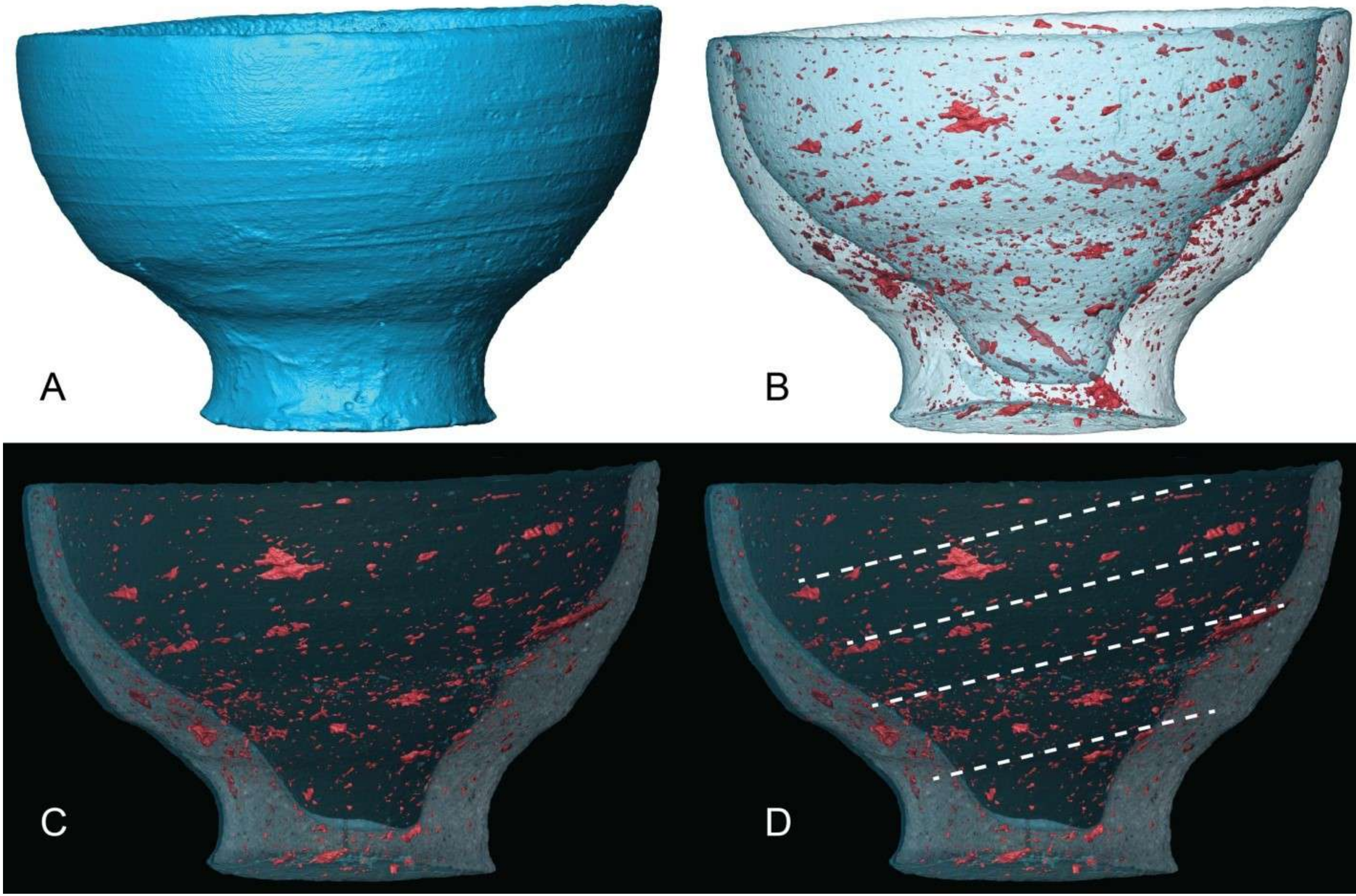
A
B
C
D

Replica produced through the coil-wheeling (produced by coiling and refined on the potter's wheel)

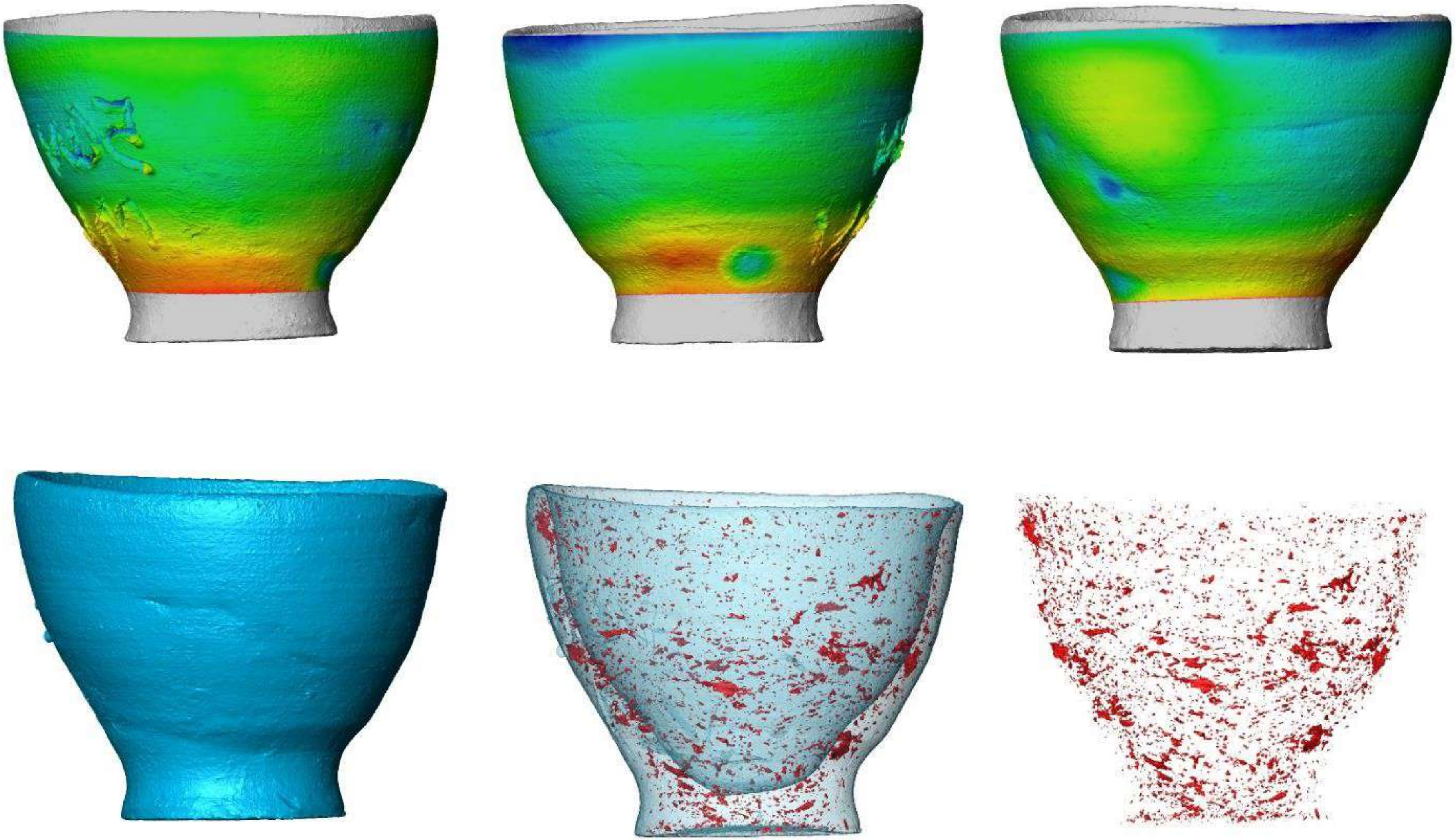

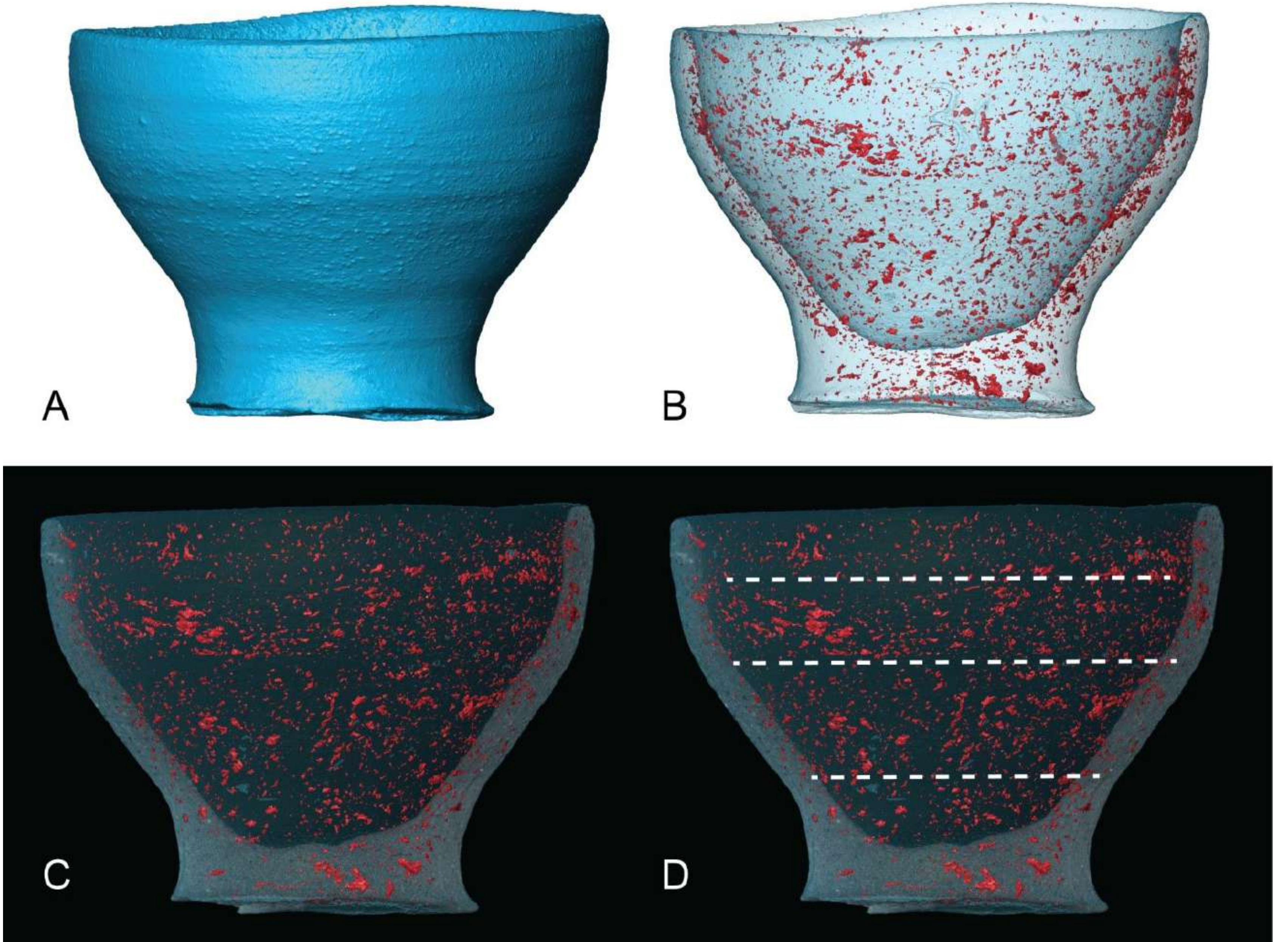
A
B
C
D

From experimental replicas to original vessels: Minoan vessels produced using the weel-throwing technique

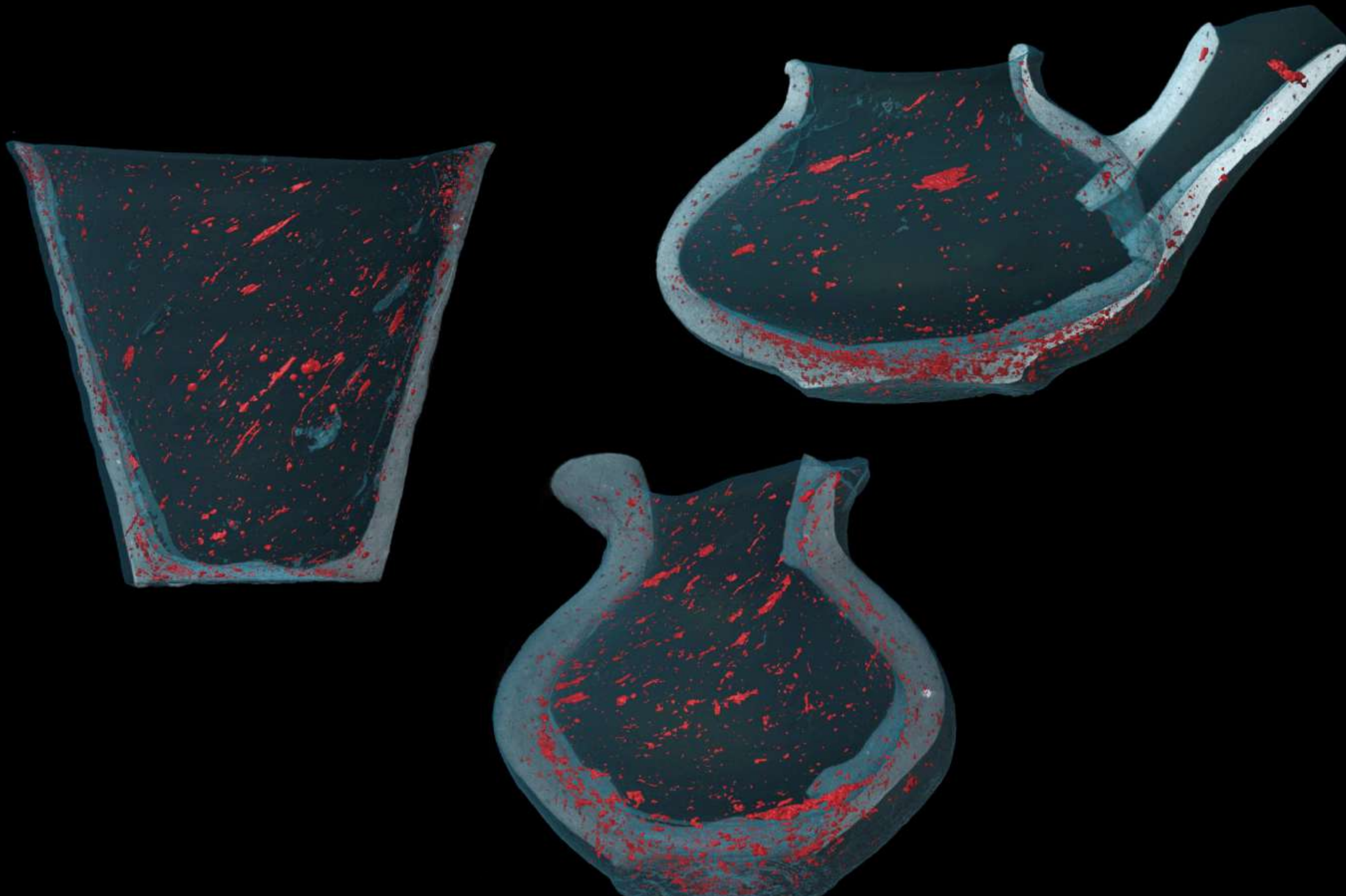

From experimental replicas to original vessels: Minoan vessel produced using the slab-building technique

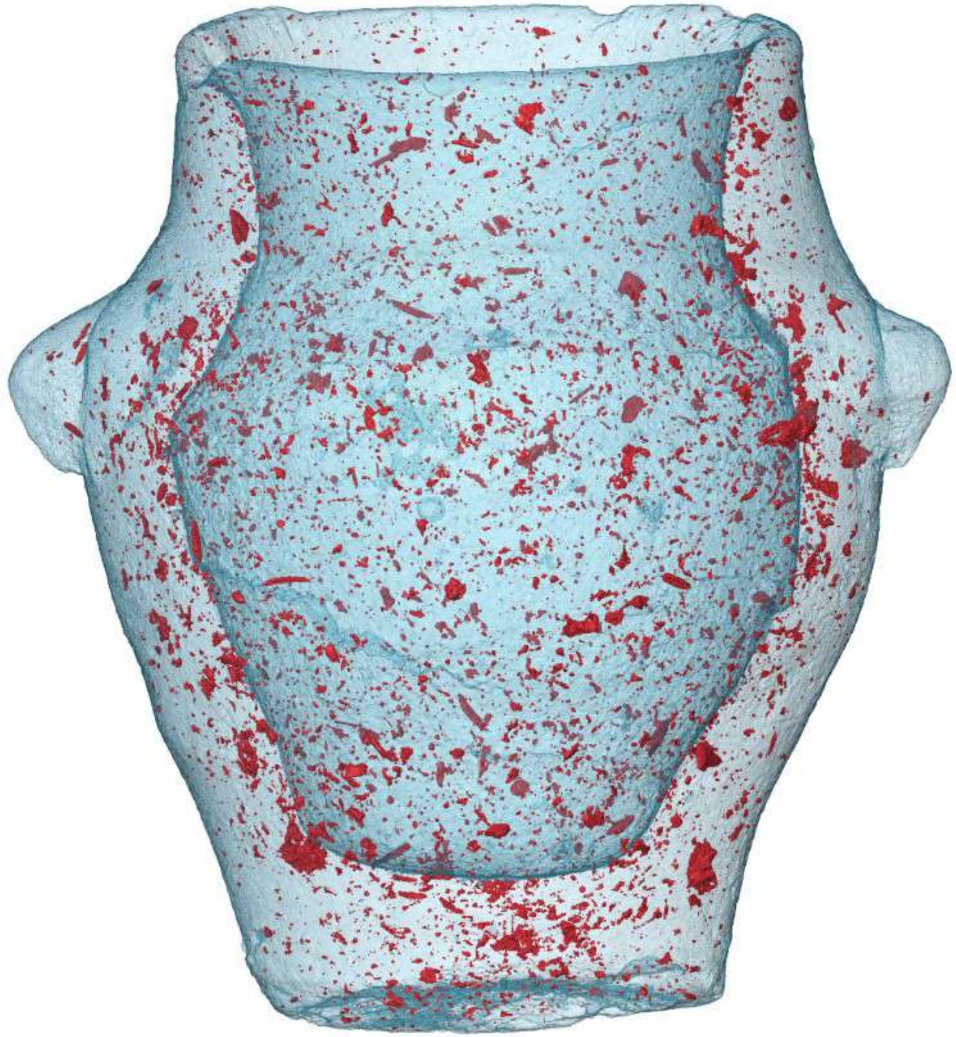

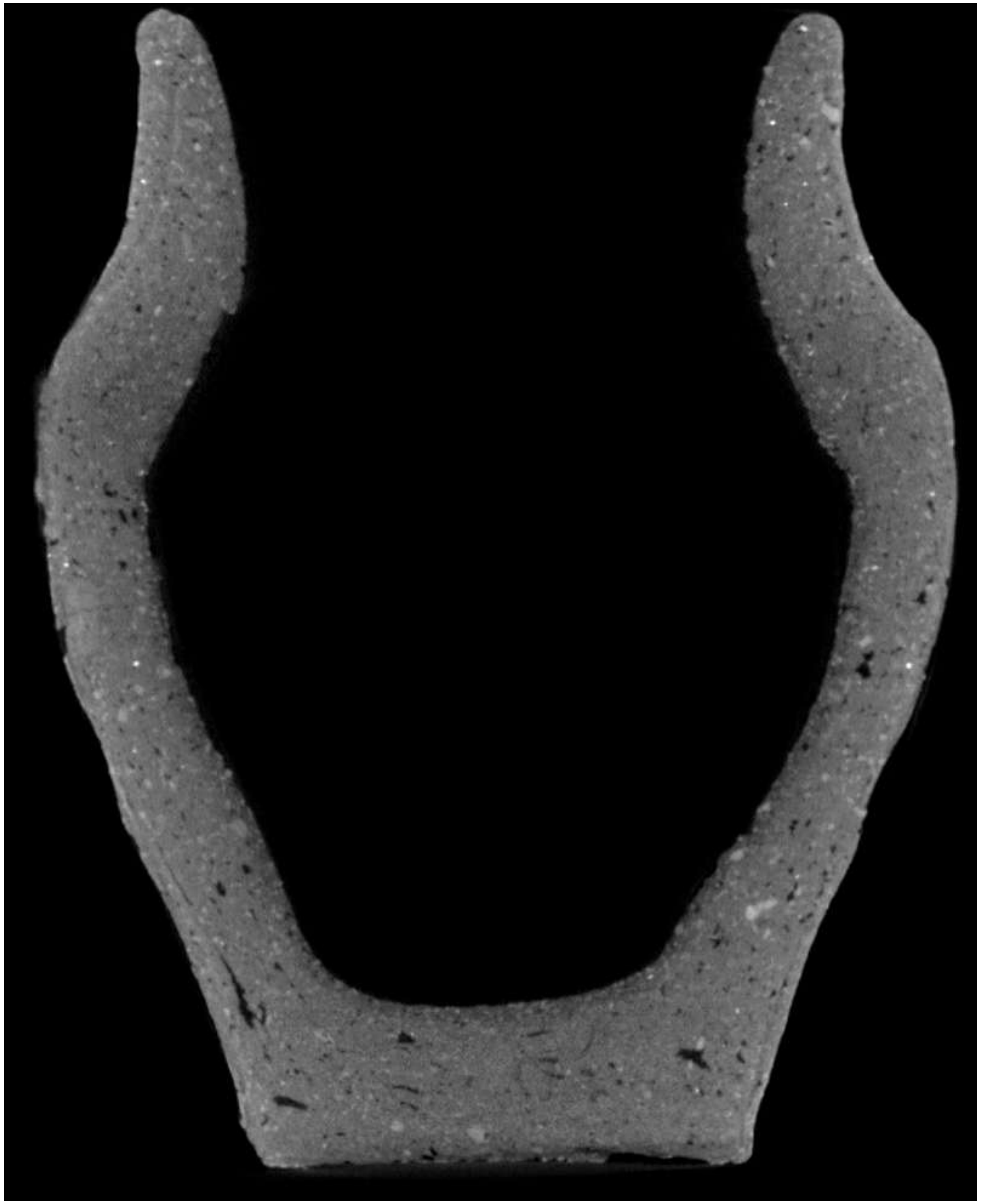

Non destructive paste characterization of pottery: a non destructive approach

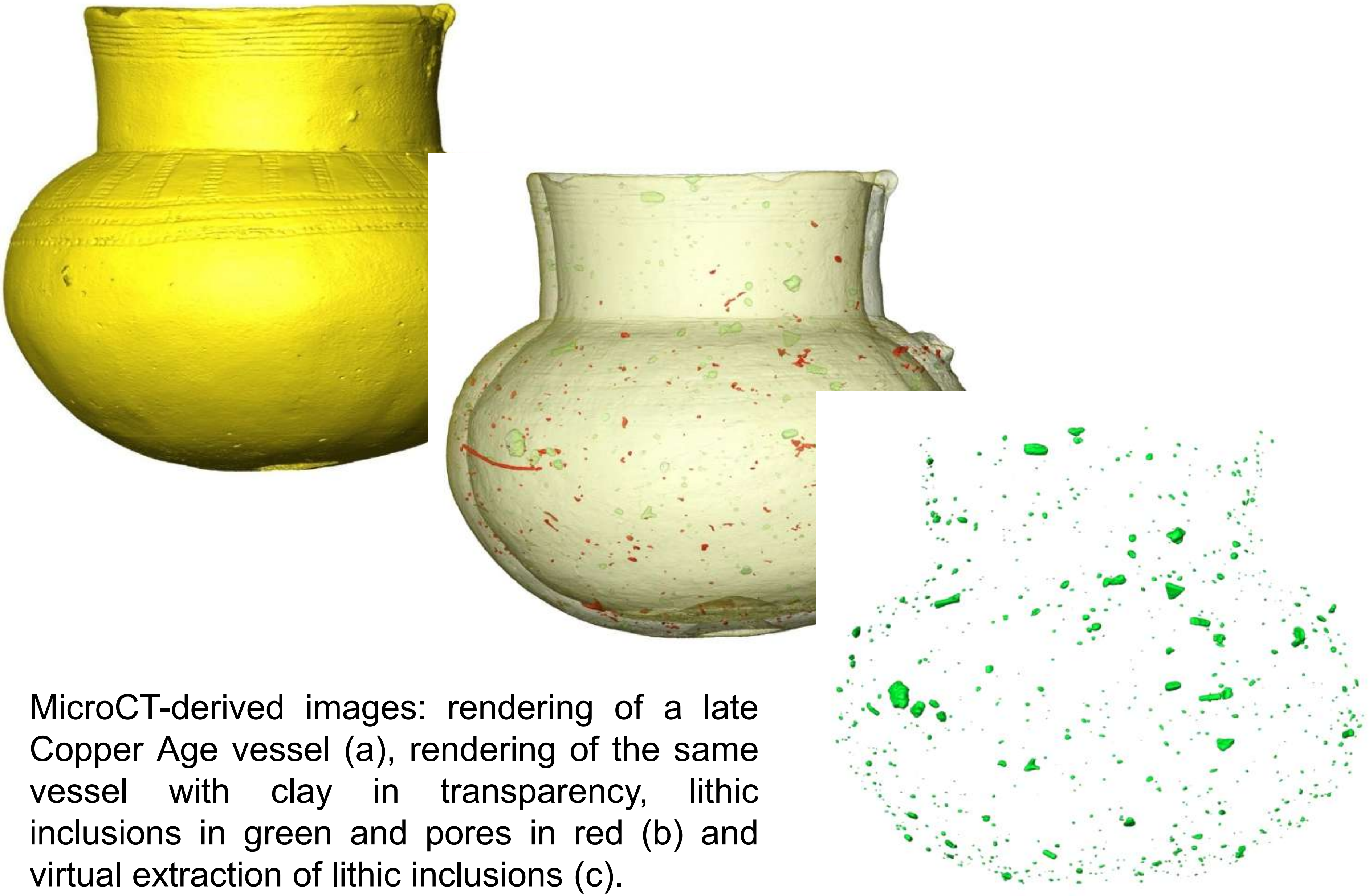

MicroCT-derived images: rendering of a late Copper Age vessel (a), rendering of the same vessel with clay in transparency, lithic inclusions in green and pores in red (b) and virtual extraction of lithic inclusions (c).

Paste characterization and analysis of microCT-derived data

1. segmentation of 3 slices for each vessel
2. quantification of total area of clay, lithic inclusions and pores
3. quantification of area, maximum width and length of each single inclusion

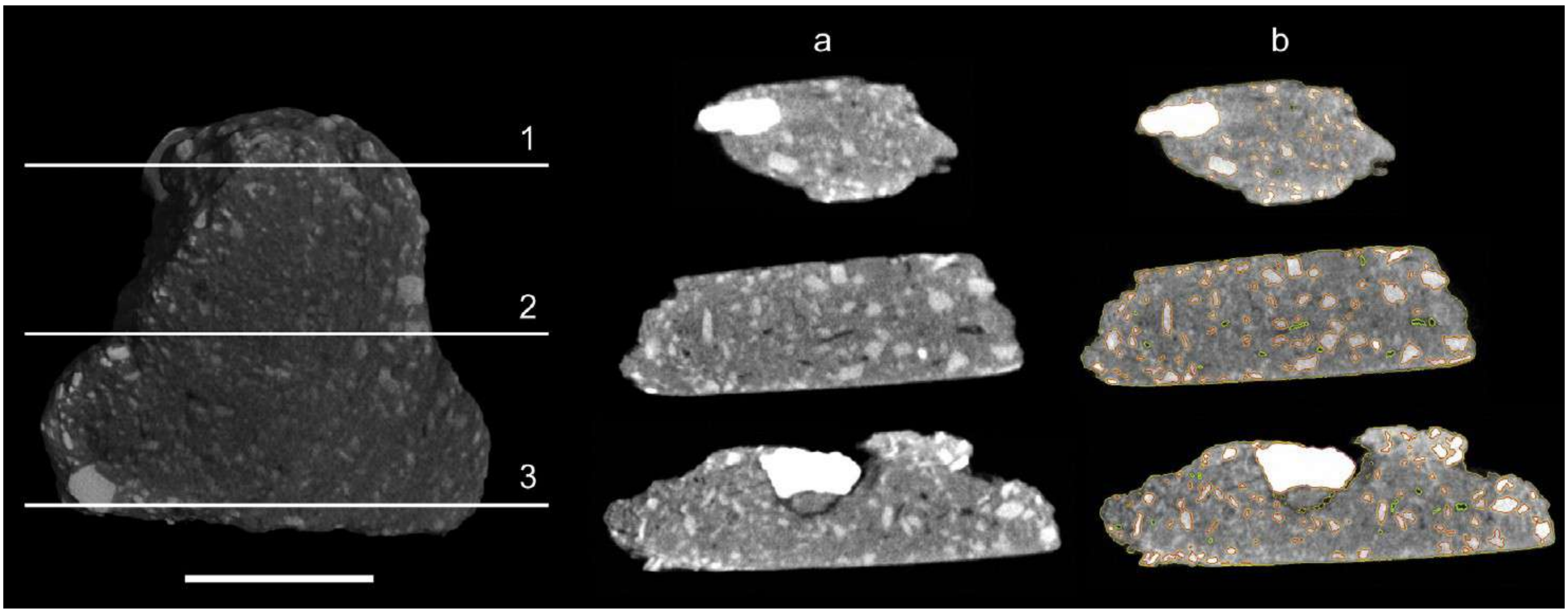

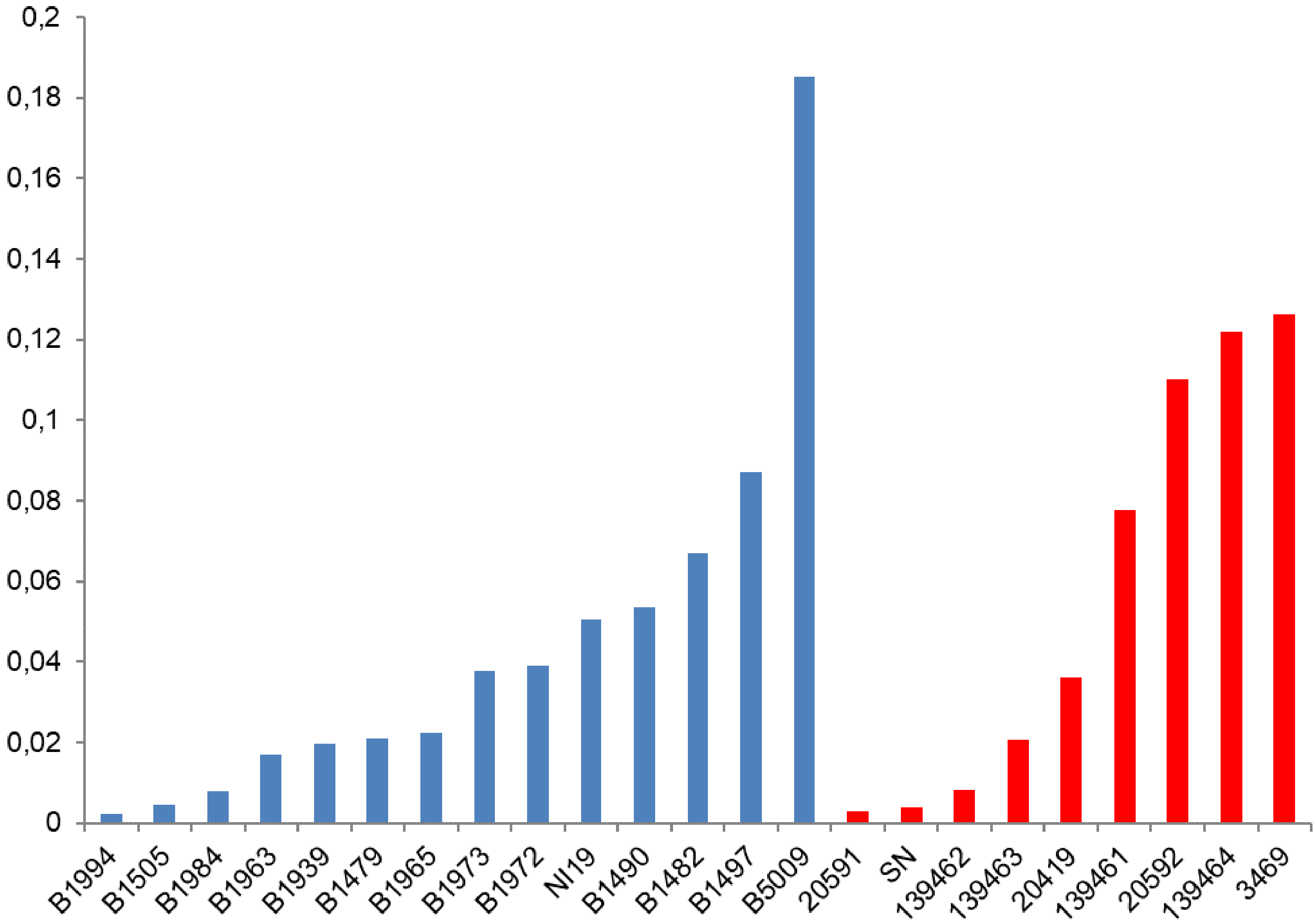

Lithic inclusion/clay ratio for the Slovenian (light blue) and Italian samples (red).

Number of lithic inclusions divided into four size intervals

	Area				Max. Length				Max. Width			
Name	**Very small** 0-50000 μm^2	**Small** 50000-100000 μm^2	**Medium** 100000-200000 μm^2	**Big** >200000 μm^2	**Very small** 0-500 μm	**Small** 500-1000 μm	**Medium** 1000-1500 μm	**Big** >1500 μm	**Very small** 0-200 μm	**Small** 200-300 μm	**Medium** 300-400 μm	**Big** > 400μm
B_1505	30	32	18	10	60	27	3	0	20	30	24	16
B_5009	220	155	180	206	345	288	86	42	136	184	150	291
B_1482	237	309	306	157	509	449	47	4	156	313	249	291
B_1490	73	66	75	70	134	113	25	12	49	69	53	113
B_1479	78	68	32	20	130	59	7	2	55	55	48	40
B_1939	126	99	46	20	218	70	2	1	82	96	73	40
B_1963	255	54	16	7	309	22	1	0	185	109	25	13
B_1965	24	17	4	7	40	9	2	1	13	21	7	11
B_1972	257	118	44	13	353	73	4	2	183	148	67	34
B_1973	101	87	58	30	198	68	4	6	80	89	62	45
B_1984	1	7	9	7	8	12	1	3	0	6	9	9
B_1994	3	5	1	2	7	3	1	0	2	6	0	3
B_1497	193	185	339	453	413	545	162	50	173	141	257	599
NI_19	66	94	106	116	145	165	52	20	34	83	84	181
3469	59	80	65	102	130	126	29	21	29	72	69	136
20591	86	9	0	0	89	6	0	0	77	14	3	1
20592	28	85	185	489	82	347	239	119	22	35	103	627
20419	10	30	46	109	33	92	45	25	3	27	32	133
139461	562	74	40	28	626	66	8	4	478	143	31	52
SN	33	4	6	1	38	6	0	0	25	11	5	3
139462	54	27	18	15	79	31	4	0	34	36	22	22
139463	116	47	16	10	153	31	4	1	95	60	19	15
139464	345	140	69	68	457	131	22	12	264	169	87	102

Statistical analysis of microCT-derived data

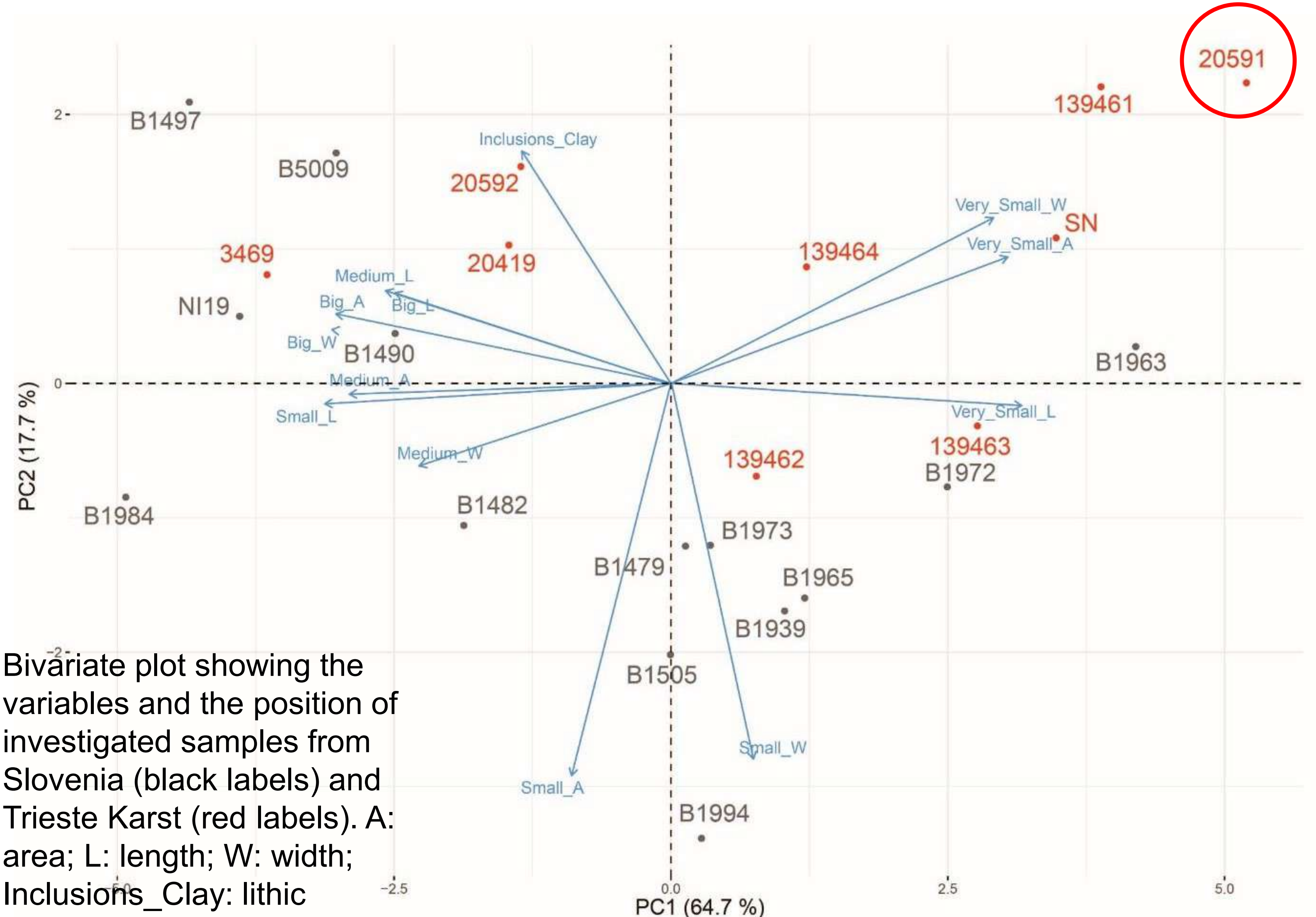

Bivariate plot showing the variables and the position of investigated samples from Slovenia (black labels) and Trieste Karst (red labels). A: area; L: length; W: width; Inclusions_Clay: lithic inclusion/clay ratio.

BNC
BUDAPEST NEUTRON CENTRE

Prompt Gamma Activation Analysis (PGAA)

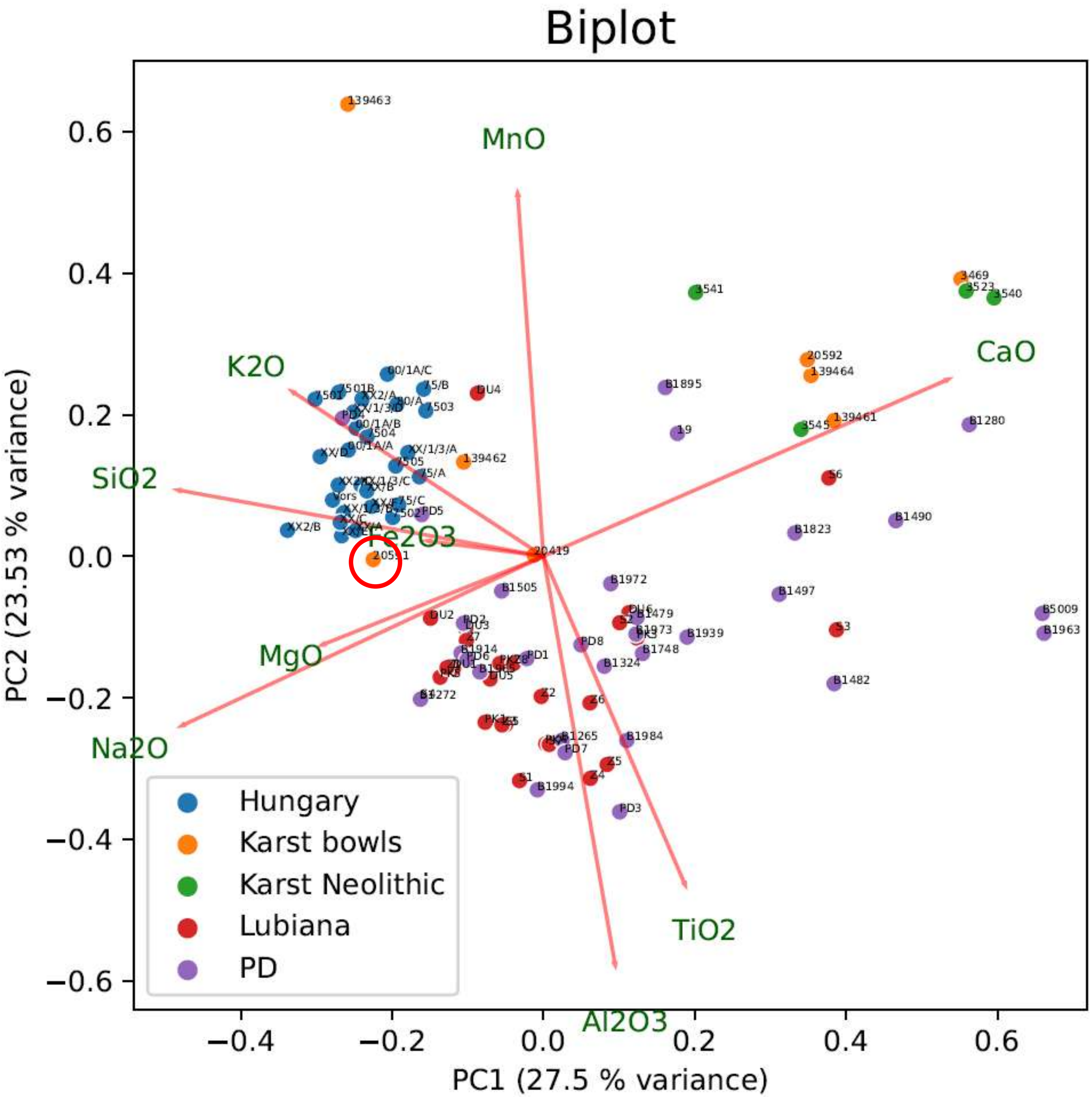

Biplot
PC1 (27.5 % variance)
PC2 (23.53 % variance)
MnO
K2O
SiO2
Fe2O3
MgO
Na2O
CaO
TiO2
Al2O3
Hungary
Karst bowls
Karst Neolithic
Lubiana
PD

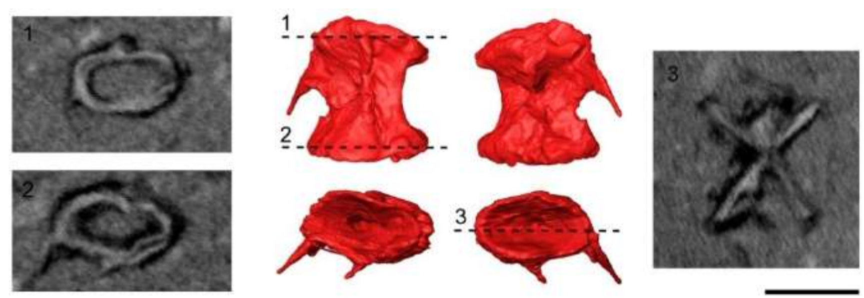

Virtual extraction of a fish vertebra from sample B1939

Projectile impact marks (PIM)

Projectile impact mark, found on a rib of Ursus arctos from the Late Epigravettian site of Cornafessa rock shelter.

Ursus arctos rib from Cornafessa rock shelter with taphonomic features highlighted. Green lines: roots marks; red lines: scraping marks; blue lines: trampling marks; black arrow: PIM. a: PIM and root etchings; b: scraping marks.

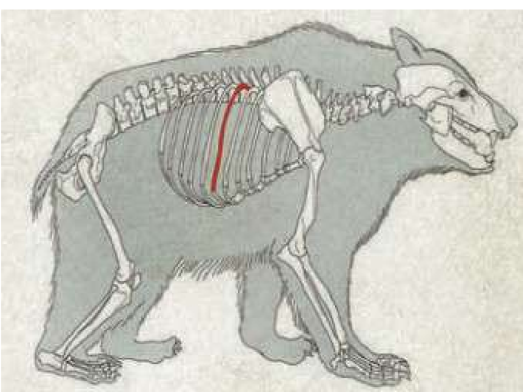

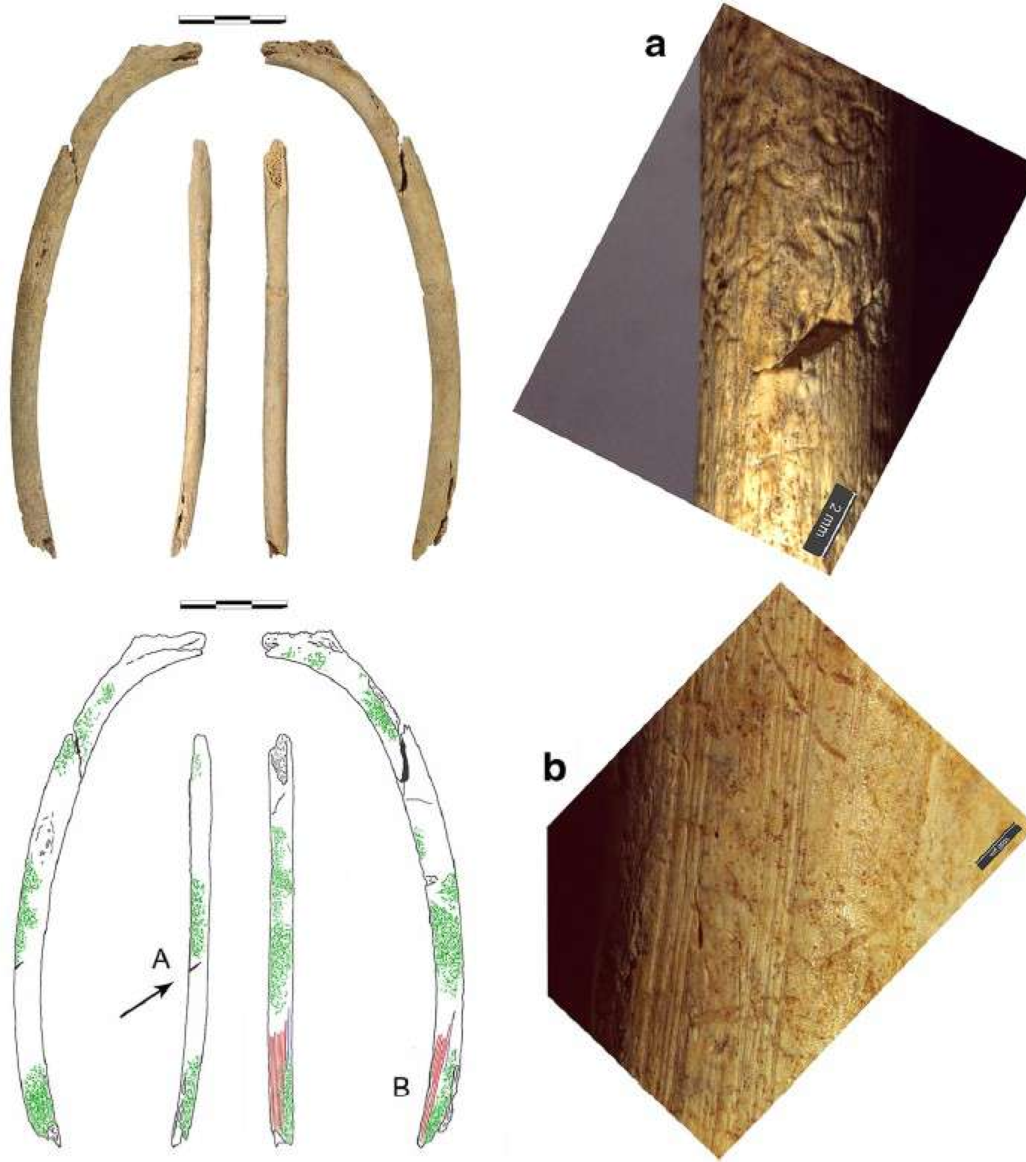

Duches R. et al 2018 Archeological bone injuries by lithic backed projectiles: new evidence on bear hunting from the Late Epigravettian site of Cornafessa rock shelter (Italy).*Archaeological and Anthropological Sciences*.

The drag's morphometric features are consistent with the experimental ones, connecting this mark to Late Epigravettian composite projectiles and declaring this evidence as the first direct proof of a bear hunted by using bow and arrow.

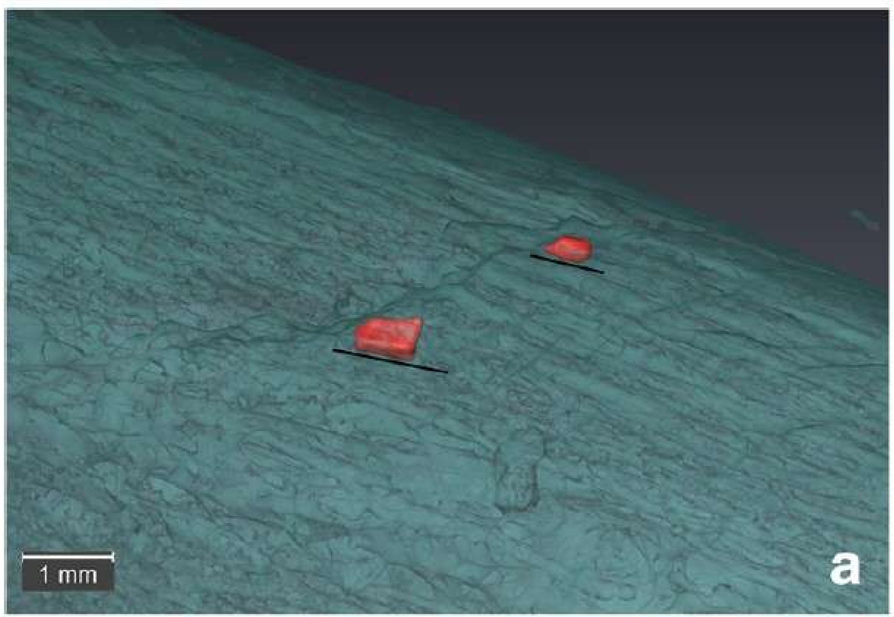

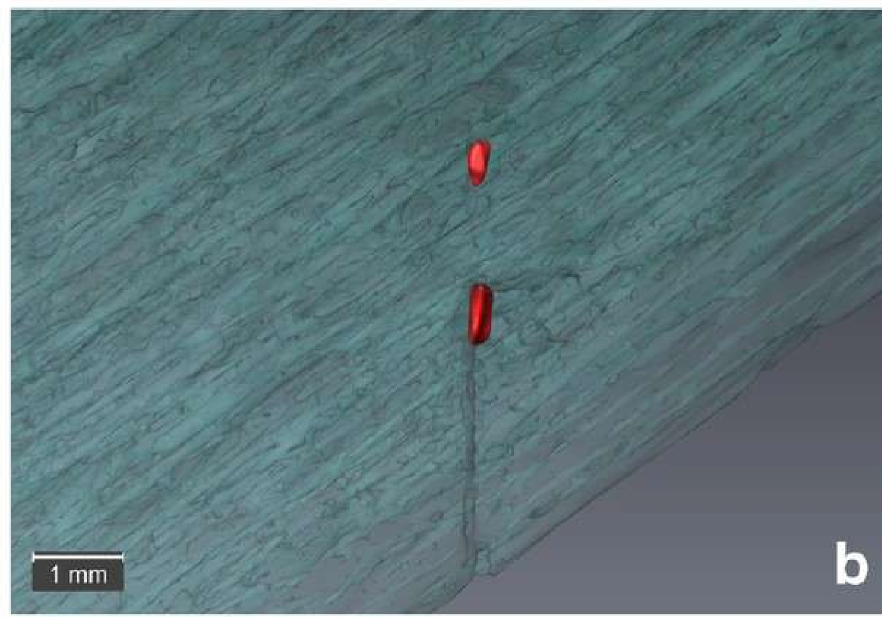

Projectile impact marks (PIM): part of a mesolithic bone point still embedded within a rib of a *Bos primigenius* (unpublished data)

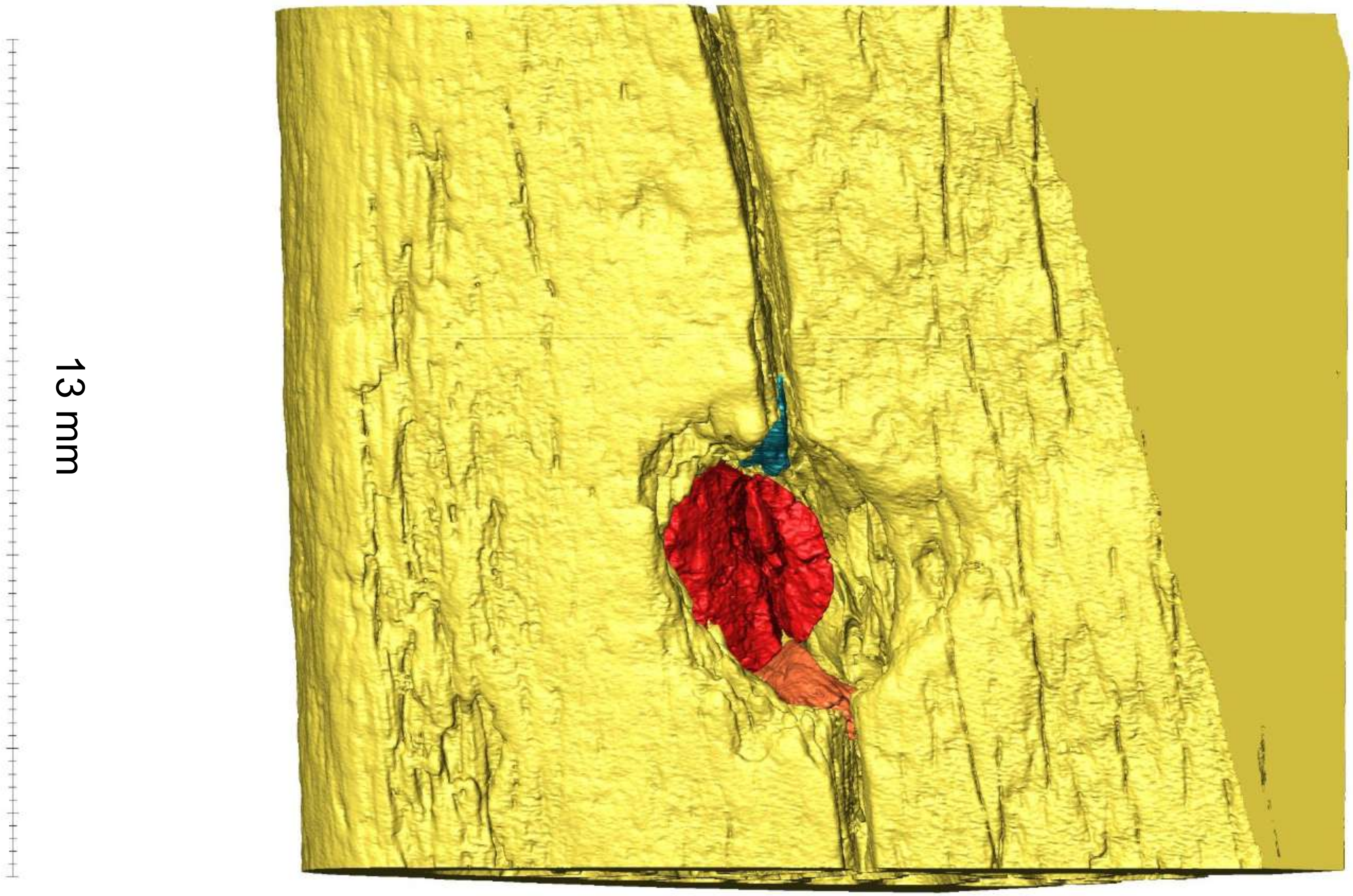

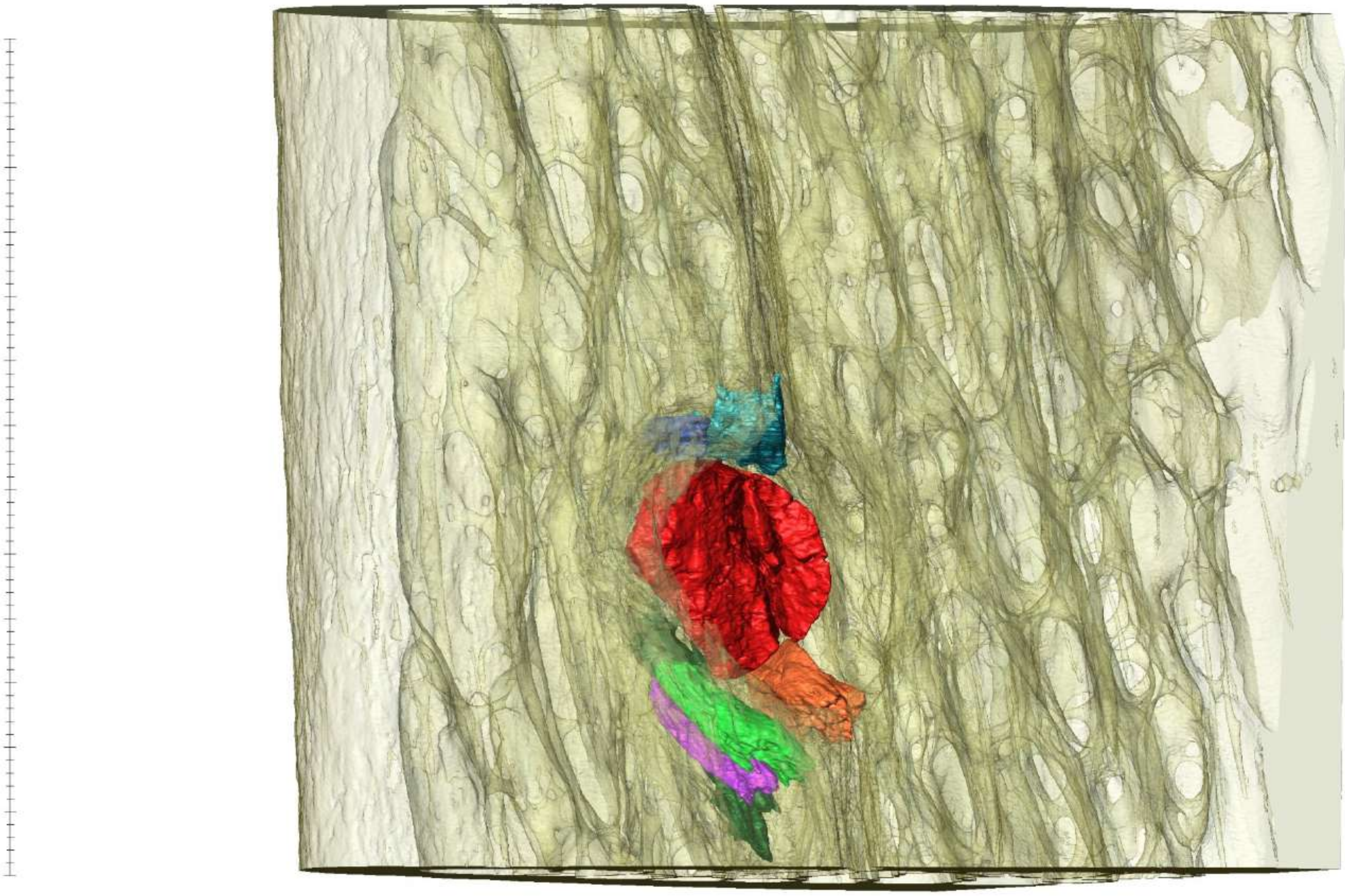

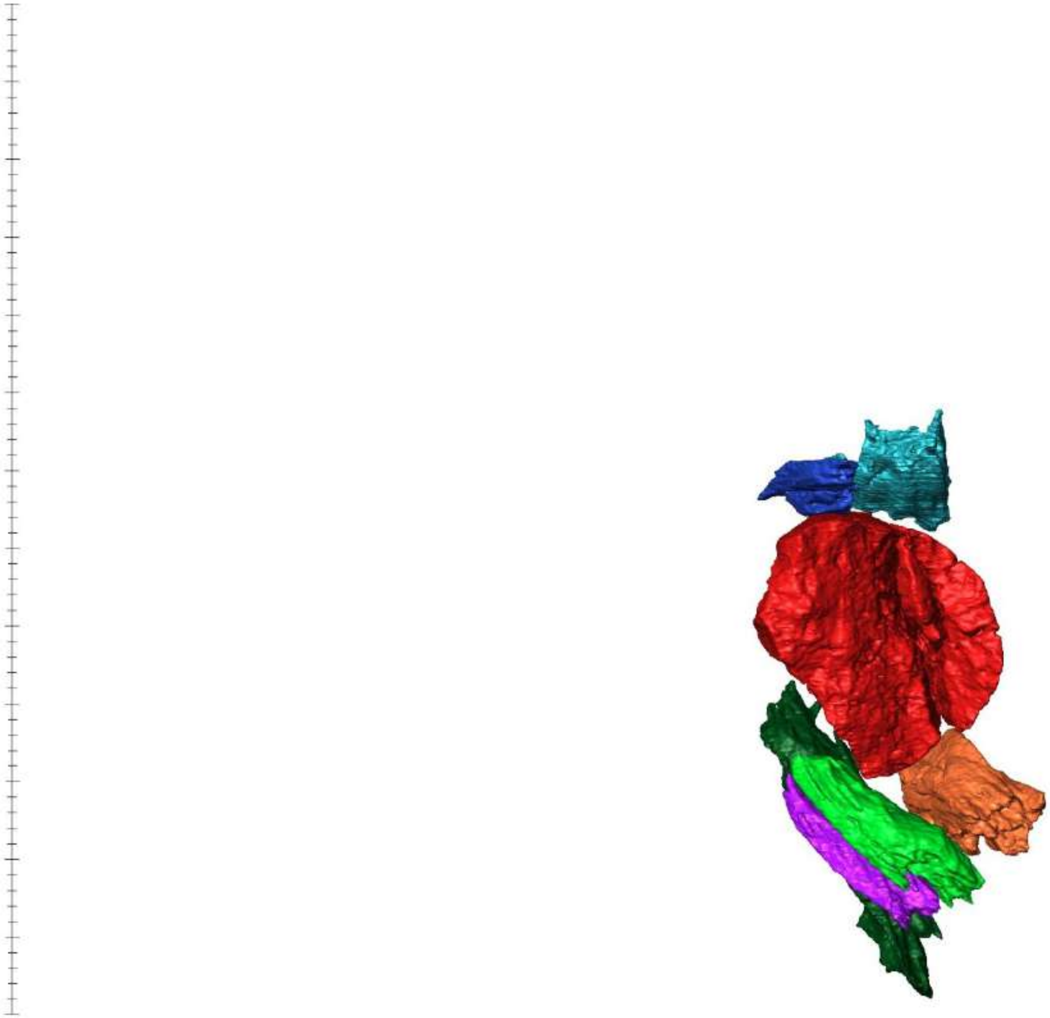

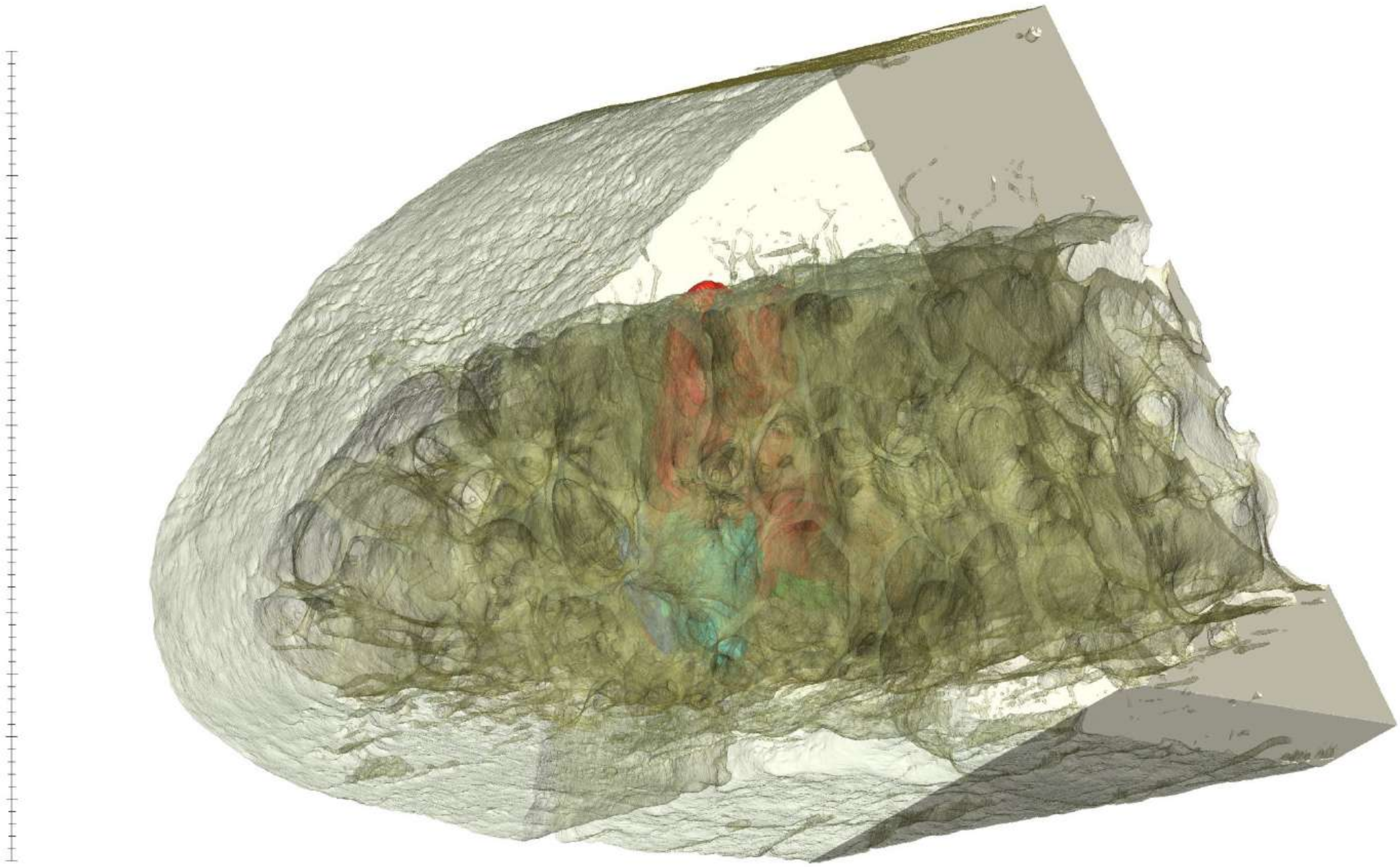

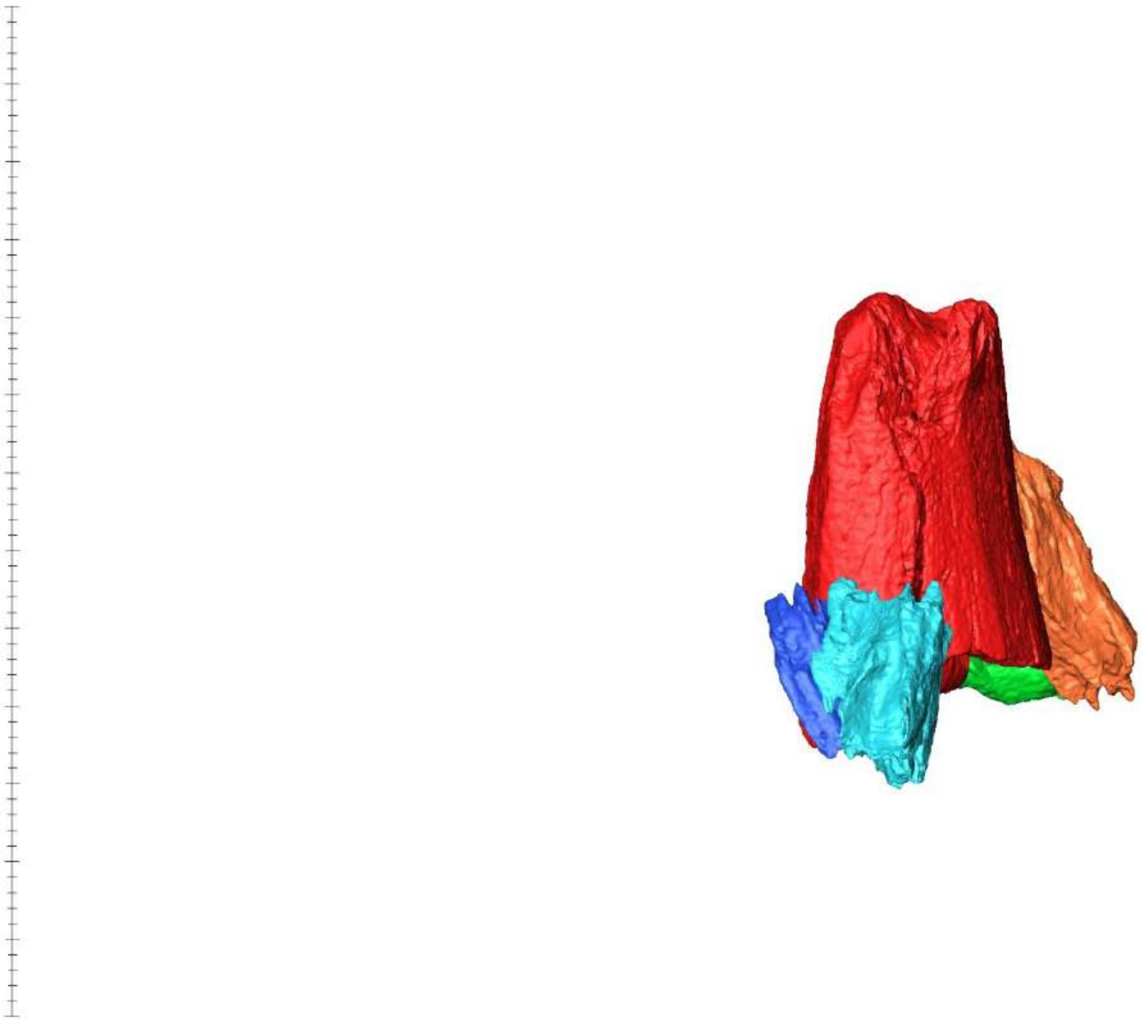

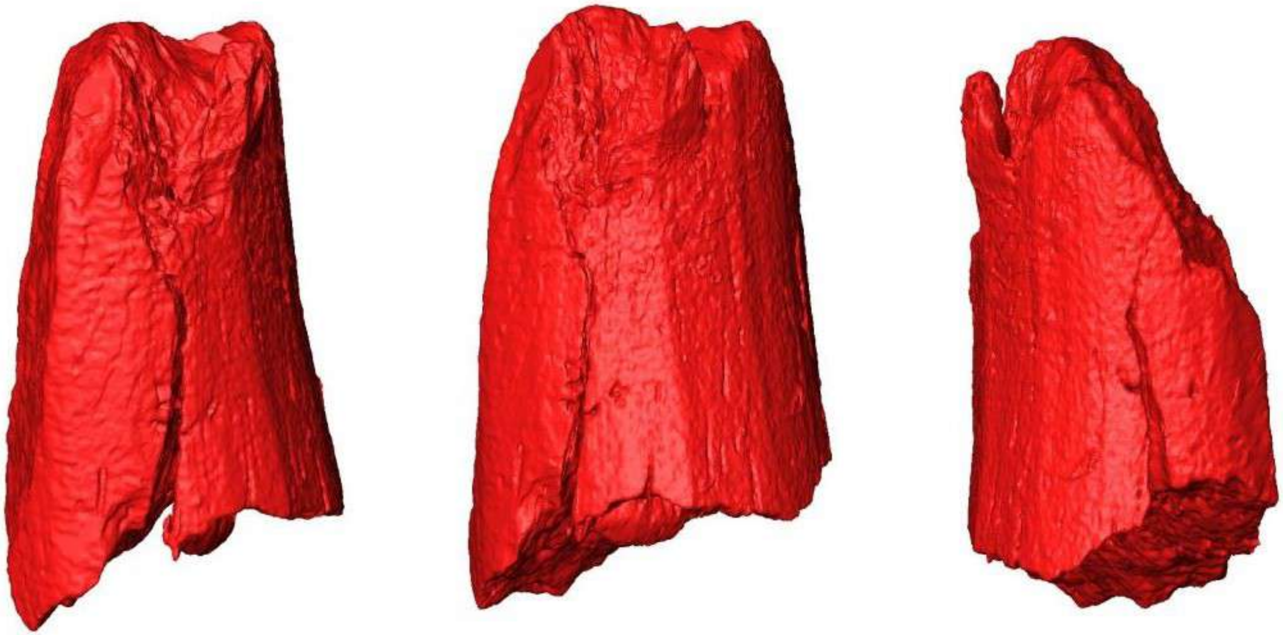

Prehistoric (shell) beads

Grotta di San Michele di Saracena

Early Impresso culture

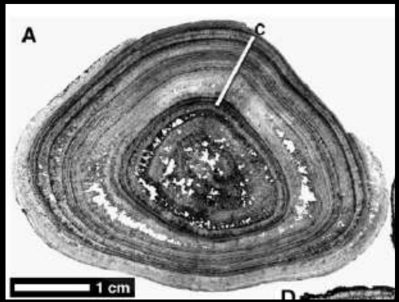

cave pearl

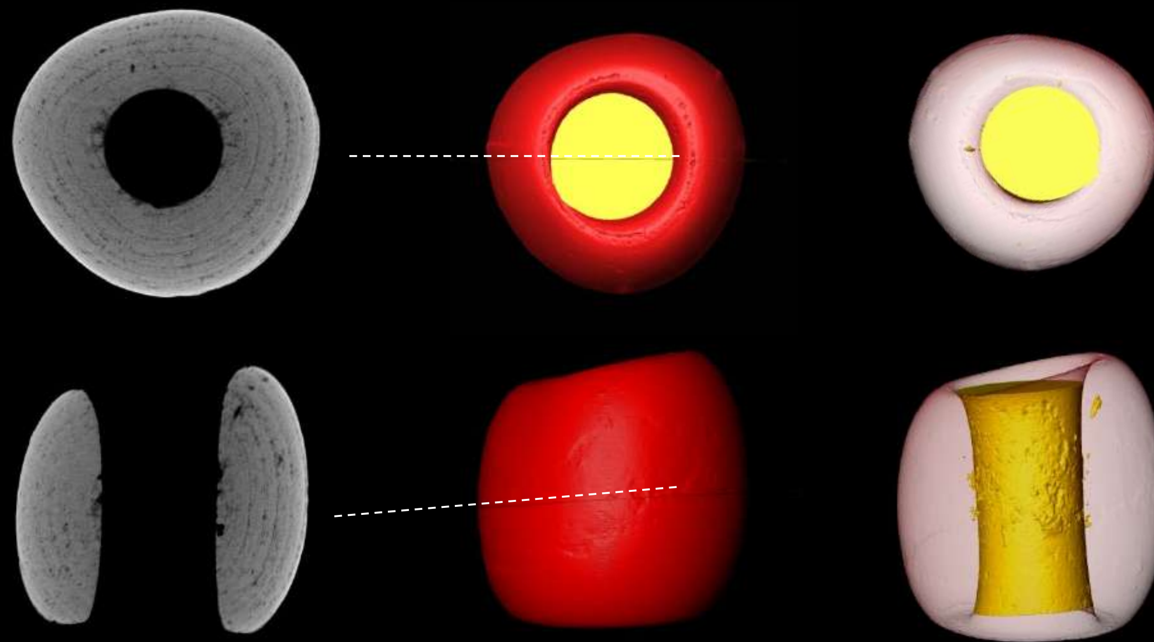

Riva del Garda (TN) – via Brione

Cultura dei Vasi a Bocca Quadrata 2/Square-Mouthed Pottery culture, phase 2

RR 61

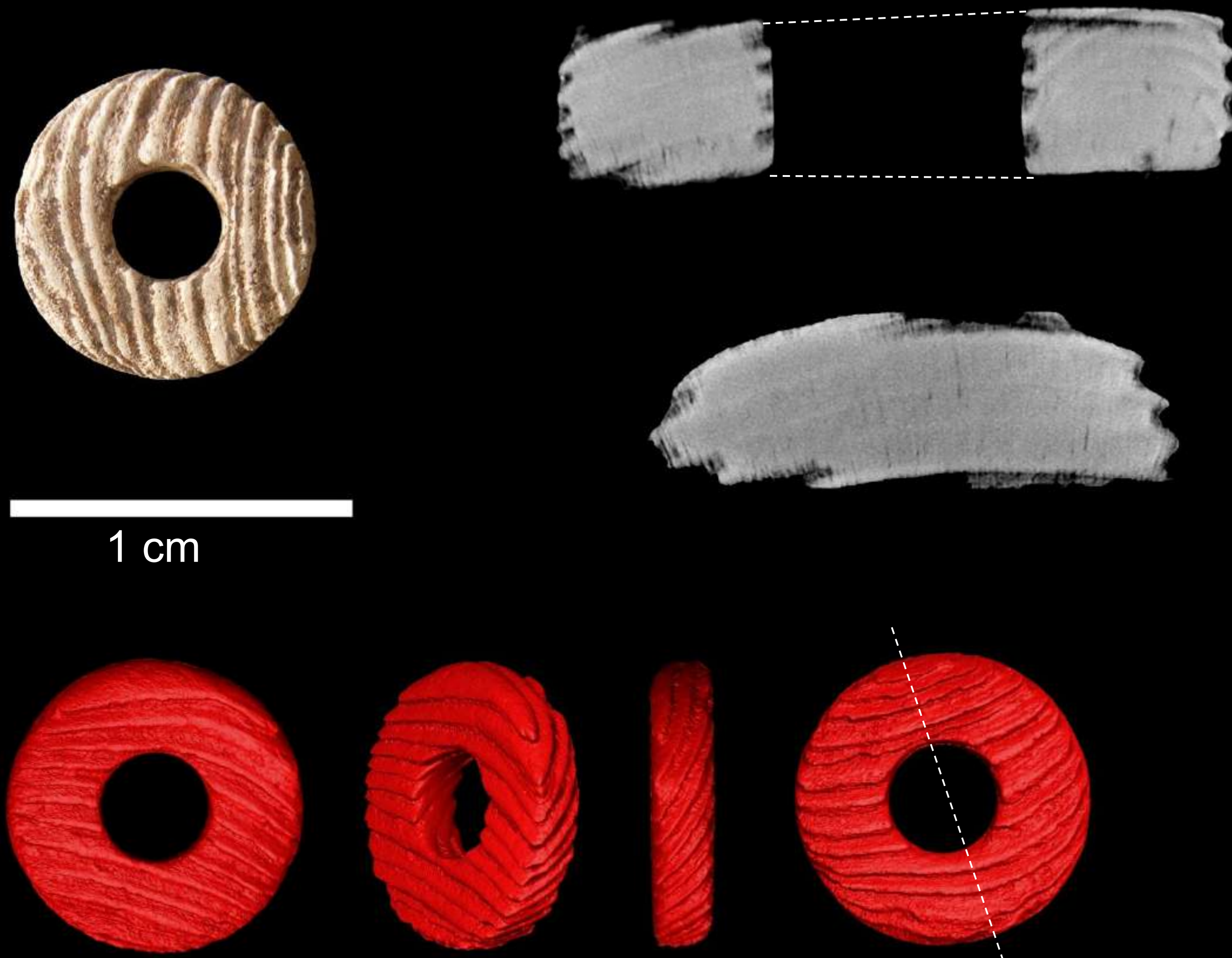

Riva del Garda (TN) – via Brione

Cultura dei Vasi a Bocca Quadrata 2/Square-Mouthed Pottery culture, phase 2

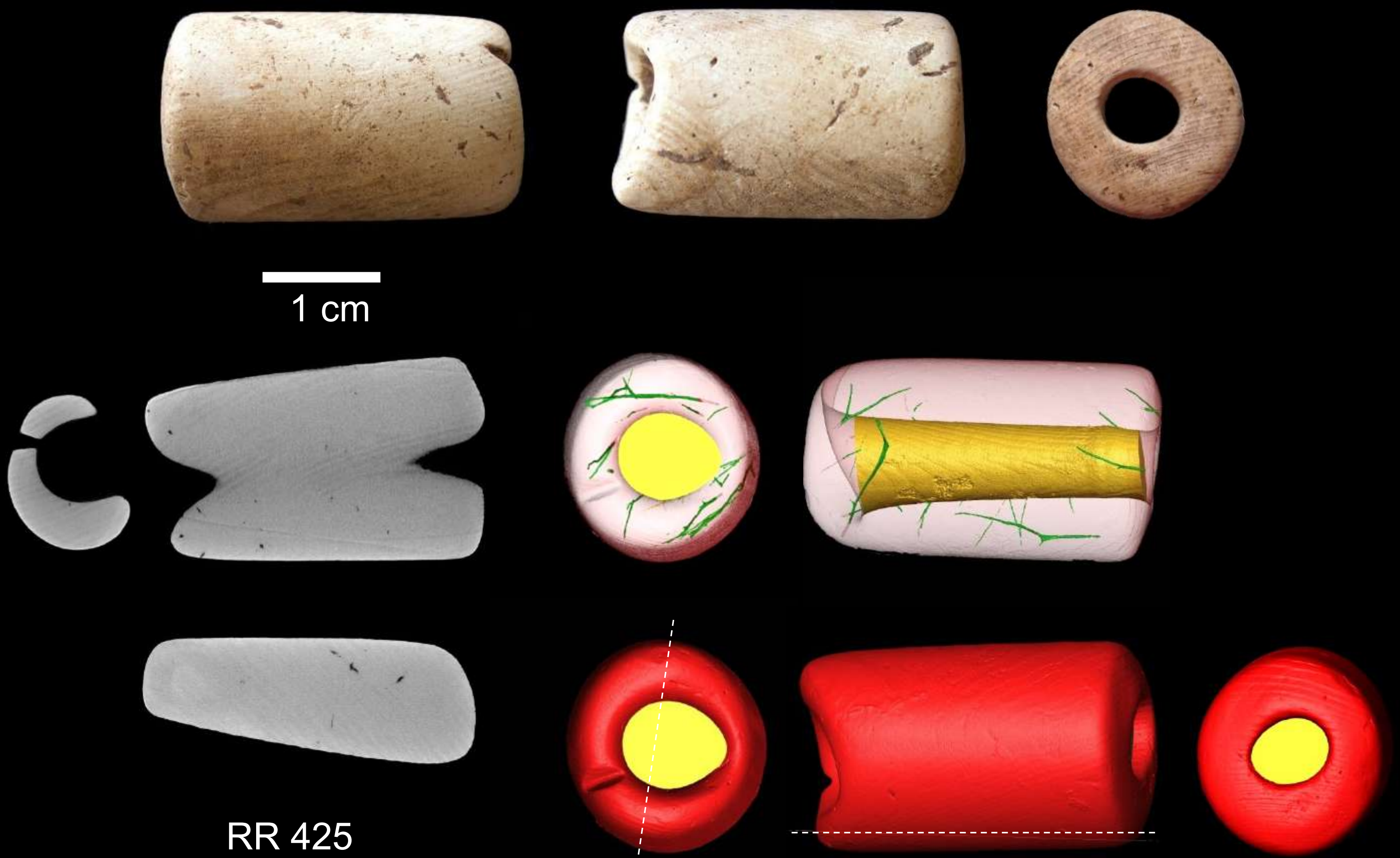

Production and use of birch bark tar at the Neolithic pile dwelling of Palù di Livenza (north-eastern Italy) revealed by X-ray computed micro-tomography and synchrotron Fourier-transform infrared spectroscopy

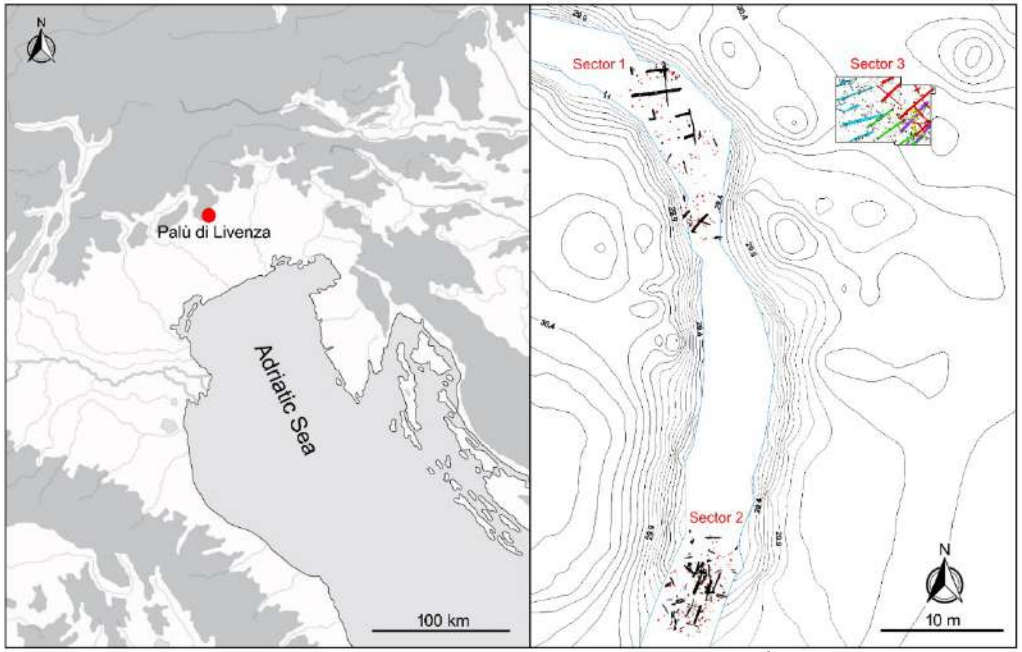

a b

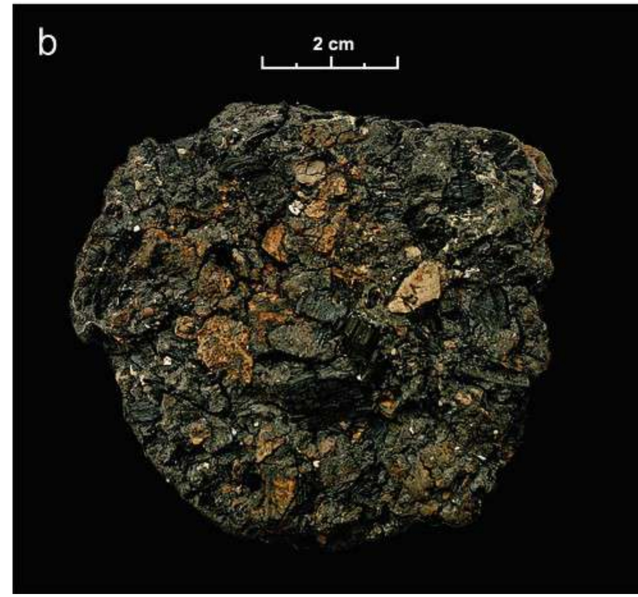

(from Bernardini et al 2022)

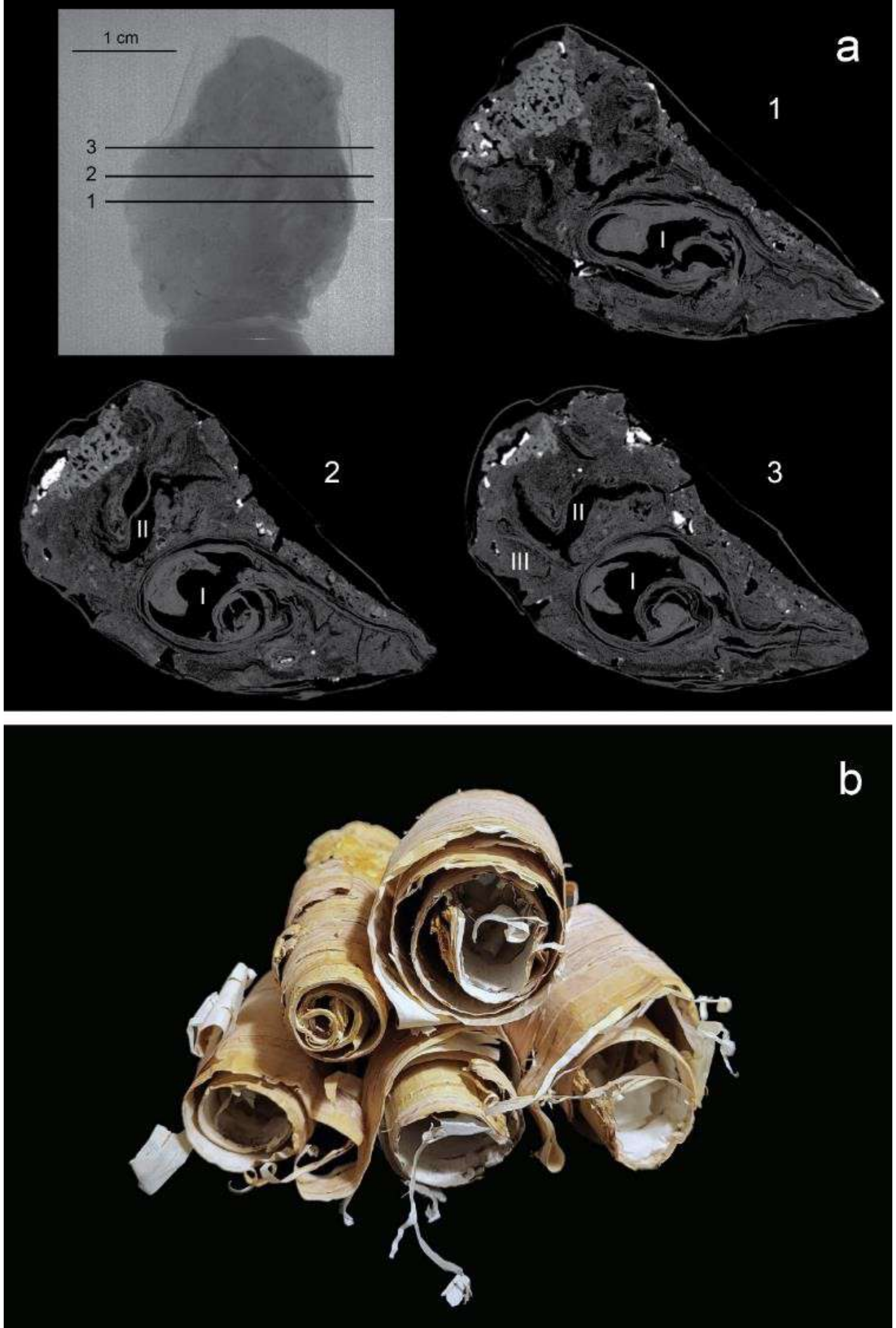

(a) MicroCT virtual sections of sample CORT, showing its scroll-up structure. (b) Birch bark rolls. The birch bark naturally curls into loose rolls when it is removed.

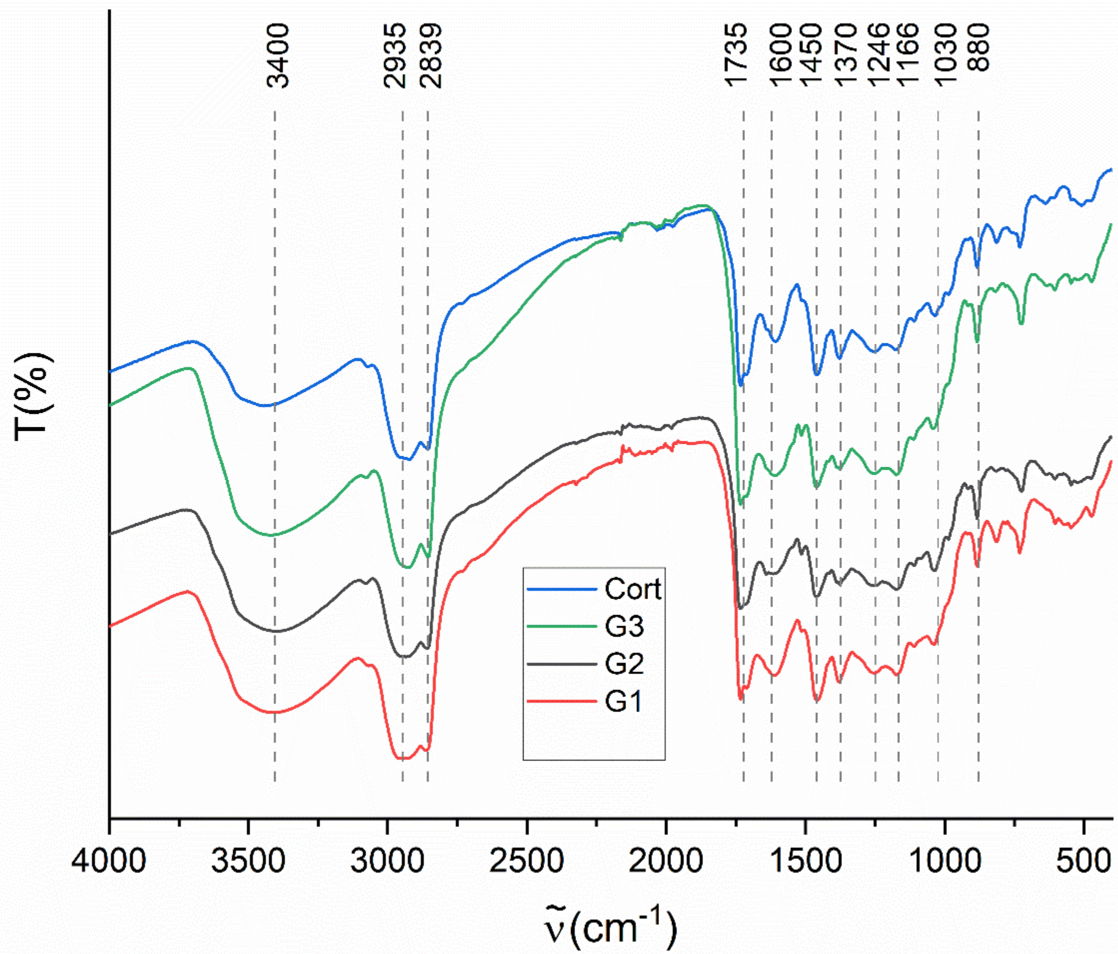

FTIR absorbance spectra of the investigated samples. The main spectral bands are indicated by dashed arrows and related peak positions. The spectra obtained from all four samples match quite well that of birch bark tar reported in literature.

Zooarchaeology 1: non-destructive evaluation of age at death

Talus of red foxes

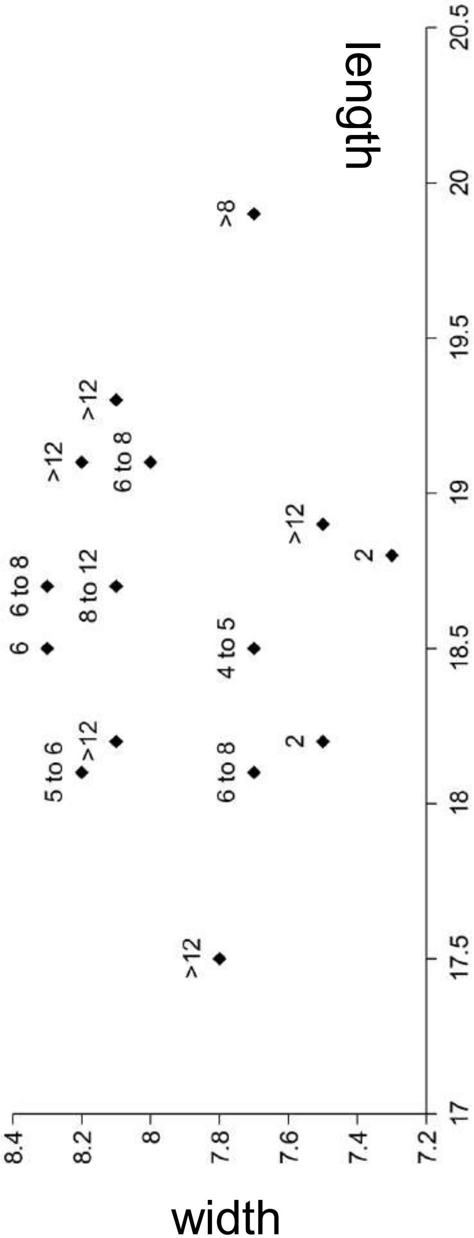

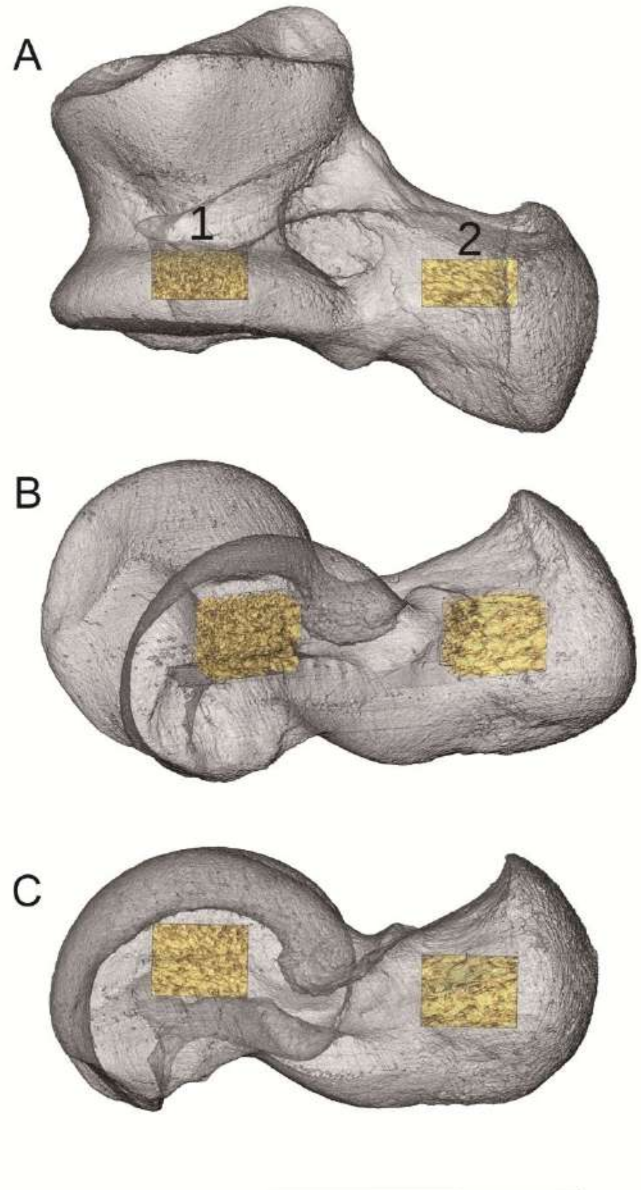

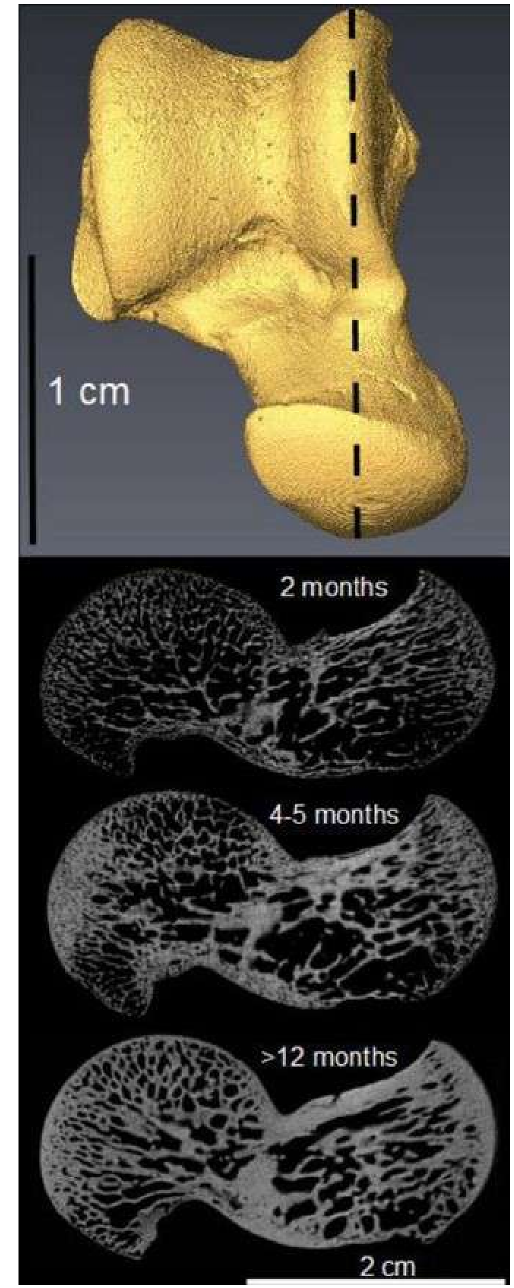

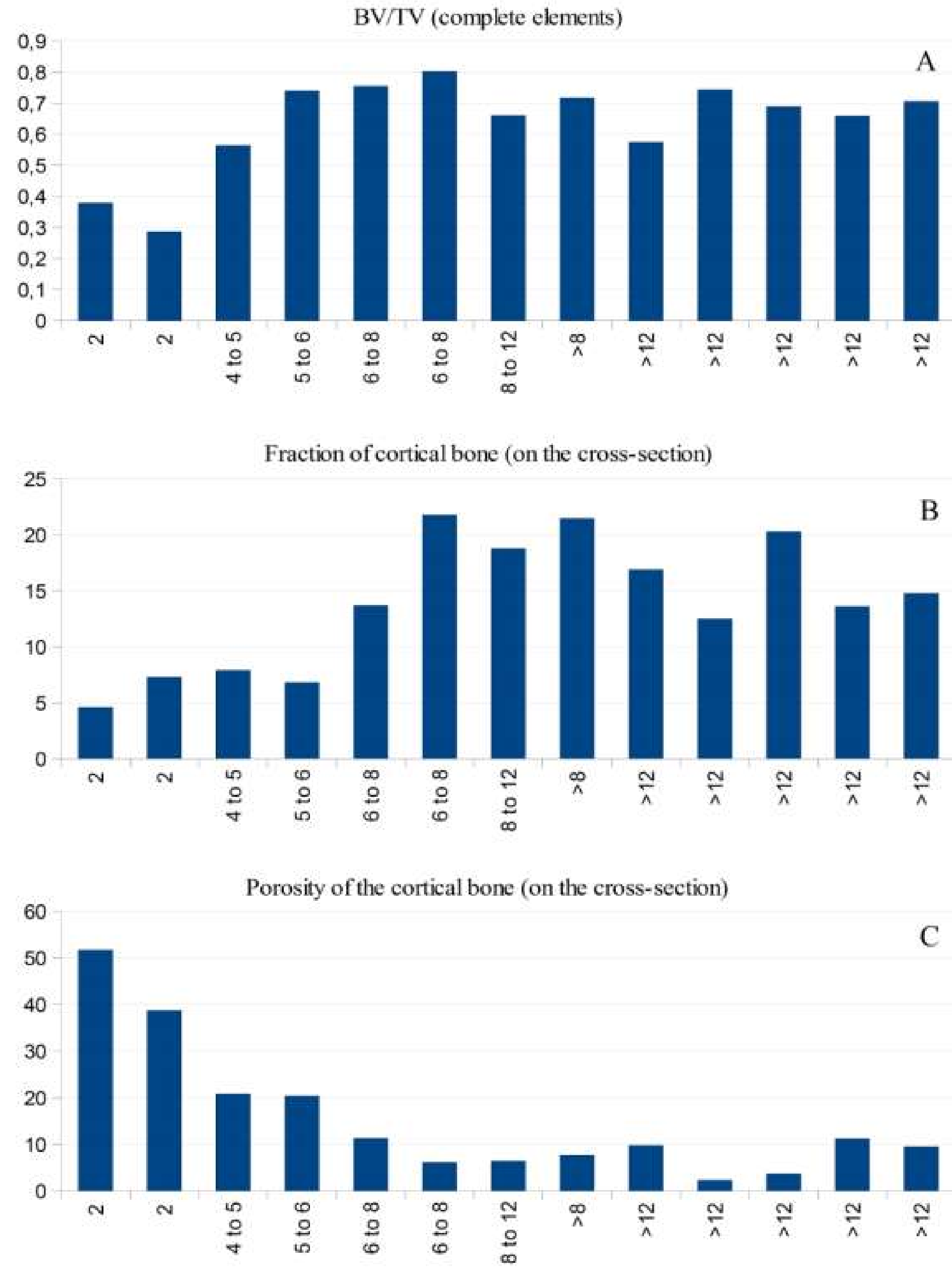

Boschin F., et al 2015 MicroCT imaging of Red Fox talus: a non-destructive approach to age at death estimation, *Archaeometry* 57(S1):194-211.

Boschin F. et al 2015, MicroCT analysis of archaeozoological remains: a non-destructive approach to the age estimation. *Annali dell'Università di Ferrara. sezione: museologia scientifica e naturalistica* 11: 1-6

Zooarchaeology 2: modifications of burned bones

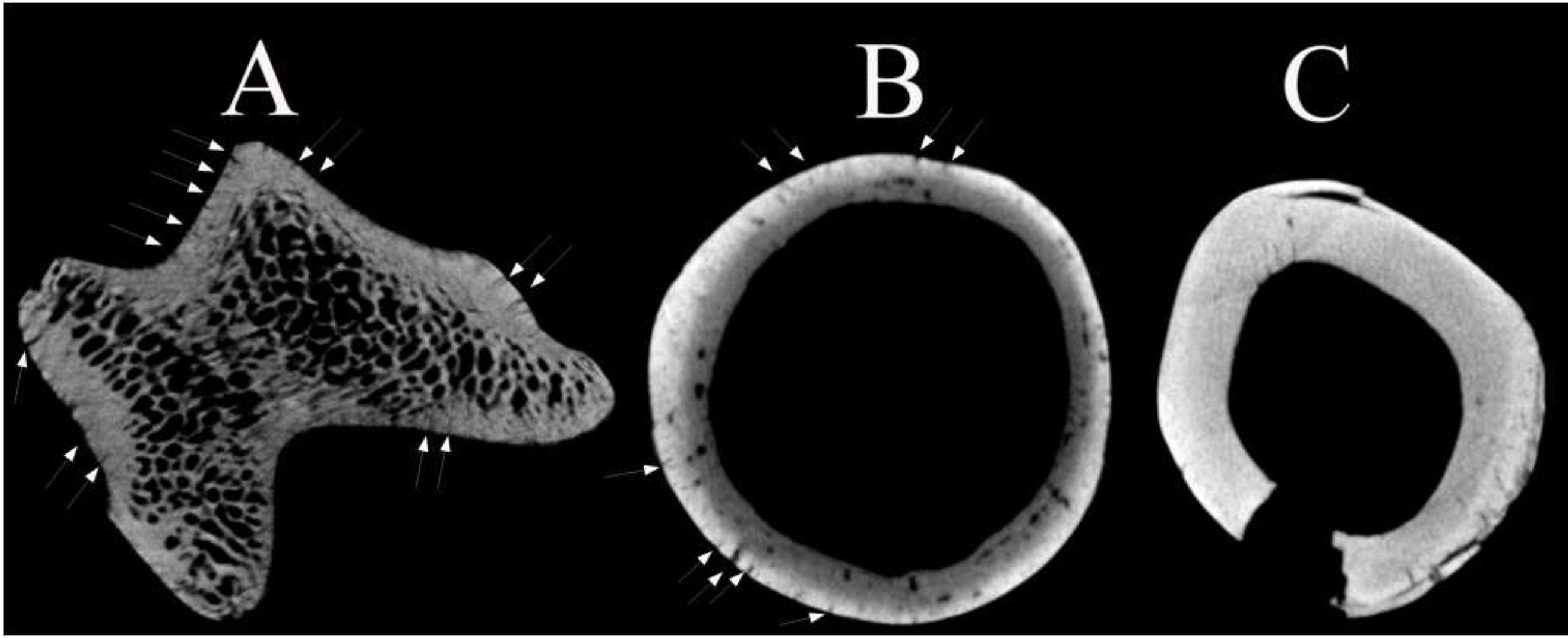

Figure 3. Cross-sections of burned specimens 1 (A), burned at 600°C, 4 (B), burned at 900°C, and 5 (C), burned at 900°C. Thin cracks perpendicular to the outer surface are visible in the cortical region of specimens A and B (white arrows). Cracks parallel to the outer surface, related to bone deformation, are visible in C. A change in greyscale values from the marrow cavity to the outer surface (indicating an increase in bone density) is visible in B.

Boschin F. et al 2015 A Look from the Inside: MicroCT Analysis of Burned Bones. *Ethnobiology Letters* 6(2): 41-49.

Zooarchaeology 3: discrimination between dogs' and wolves' lower carnassial tooth

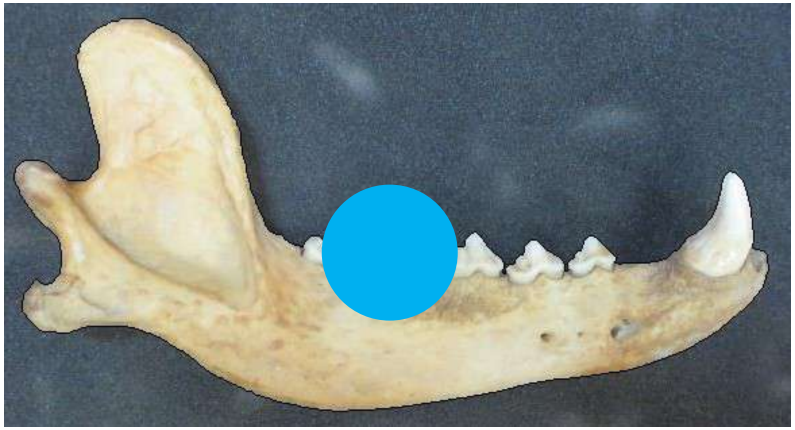

Relative reduction of carnassial teeth's size in dogs: is carnassial reduction followed by any modification of the tooth's internal structure?

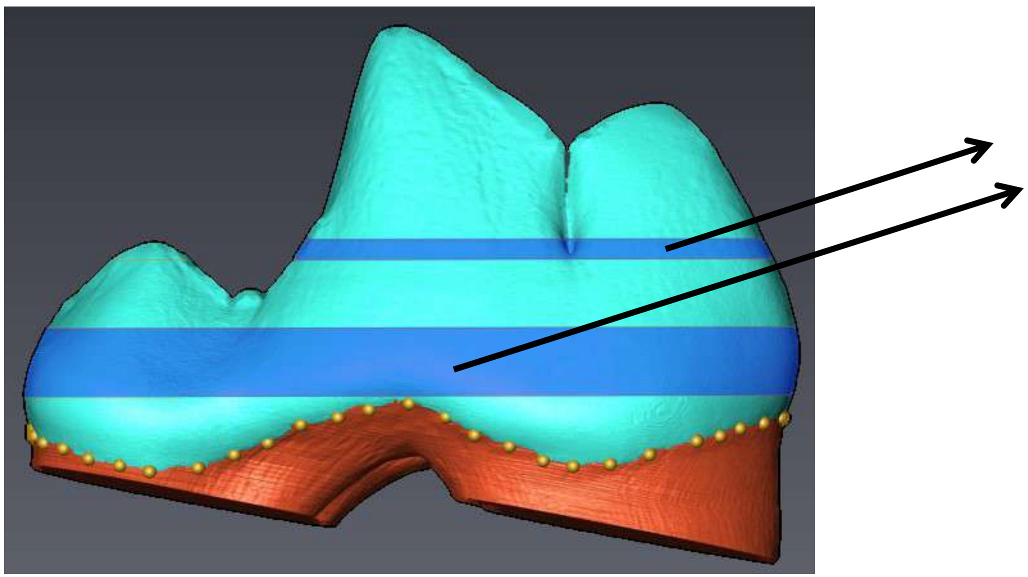

Virtual extraction of two Sub-volumes

Analysis of enamel thickness expressed in :

Dentine volume/
Total volume

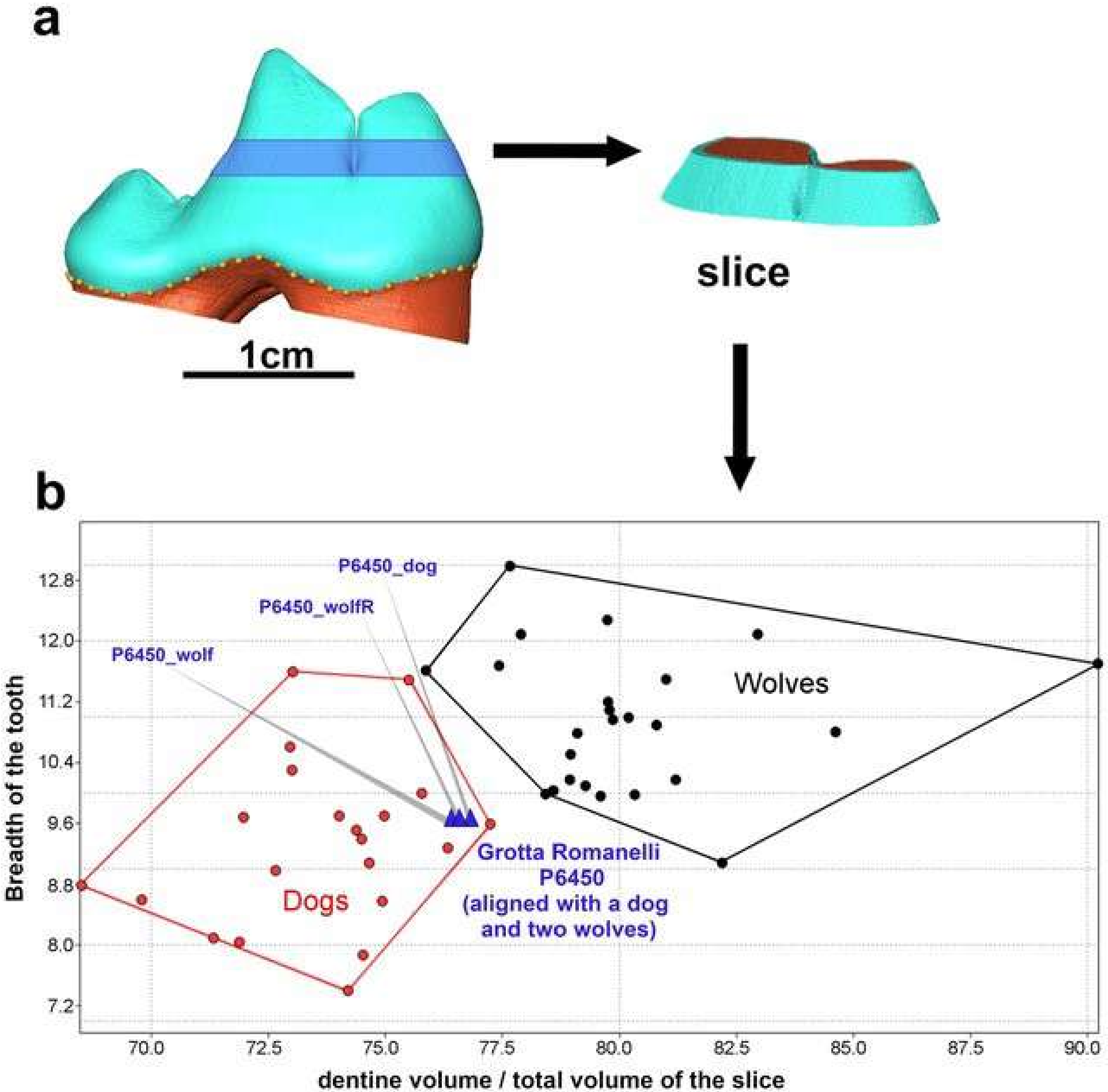

a
slice
1cm
b
P6450_dog
P6450_wolfR
P6450_wolf
Wolves
Dogs
Grotta Romanelli
P6450
(aligned with a dog
and two wolves)
Breadth of the tooth
dentine volume / total volume of the slice
12.8
12.0
11.2
10.4
9.6
8.8
8.0
7.2
70.0
72.5
75.0
77.5
80.0
82.5
85.0
87.5
90.0

Virtual dendrochronology on charcoals from excavations

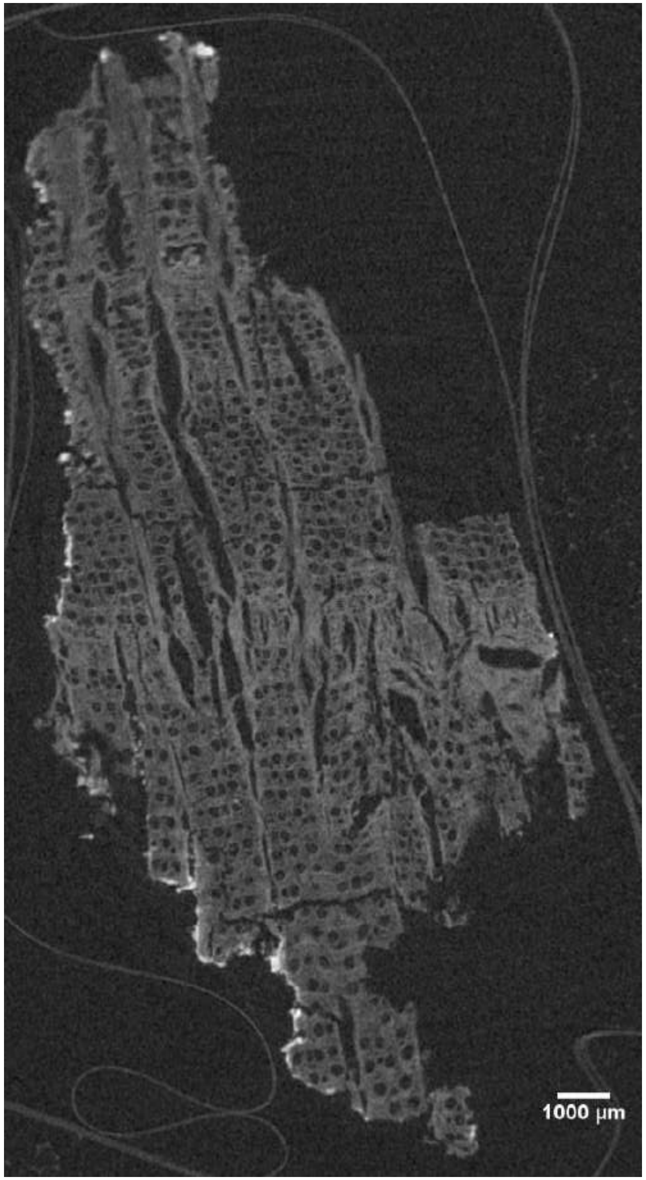
1000 µm

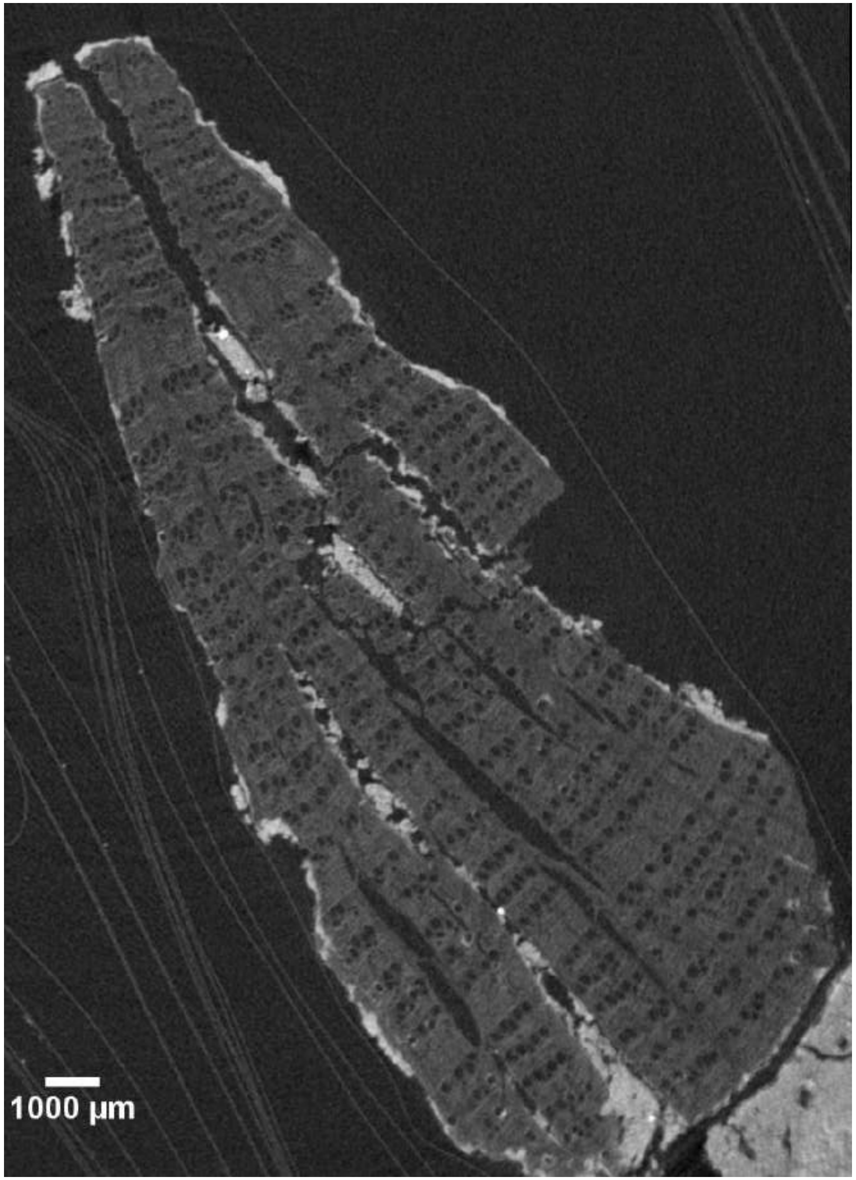
1000 µm

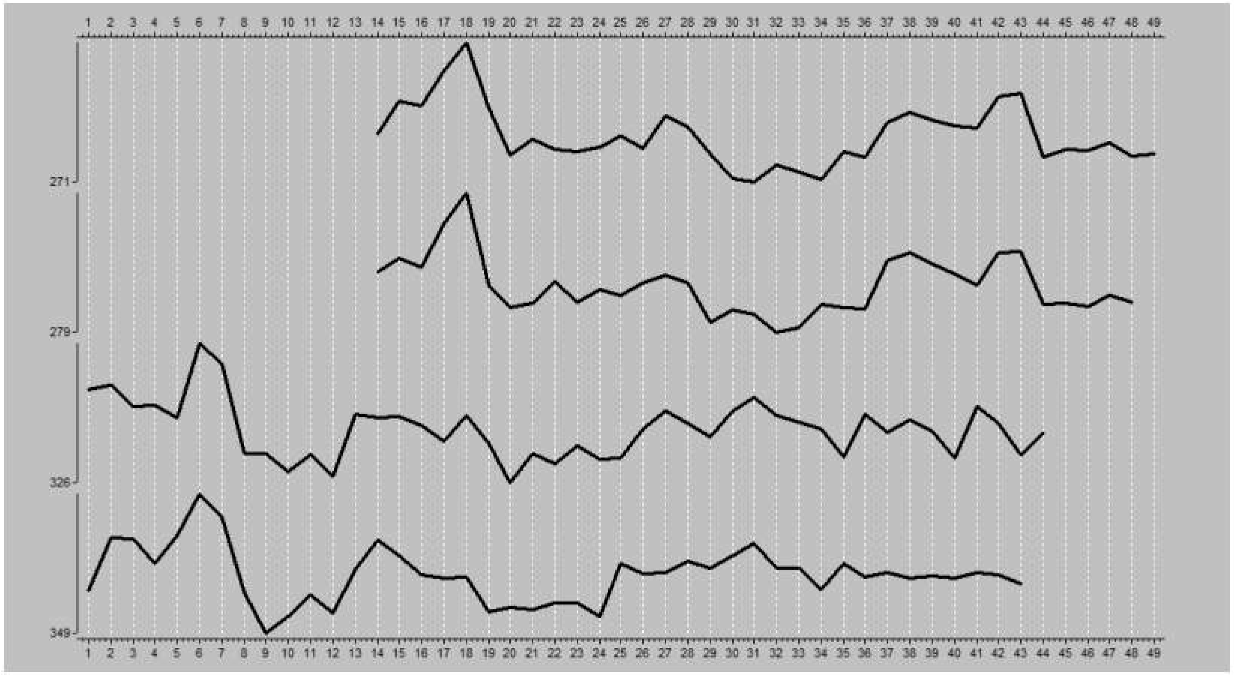

Fig. 1 – Sincronizzazione delle serie ottenute per il carbone 6 e il carbone 9 in cronologia relativa.

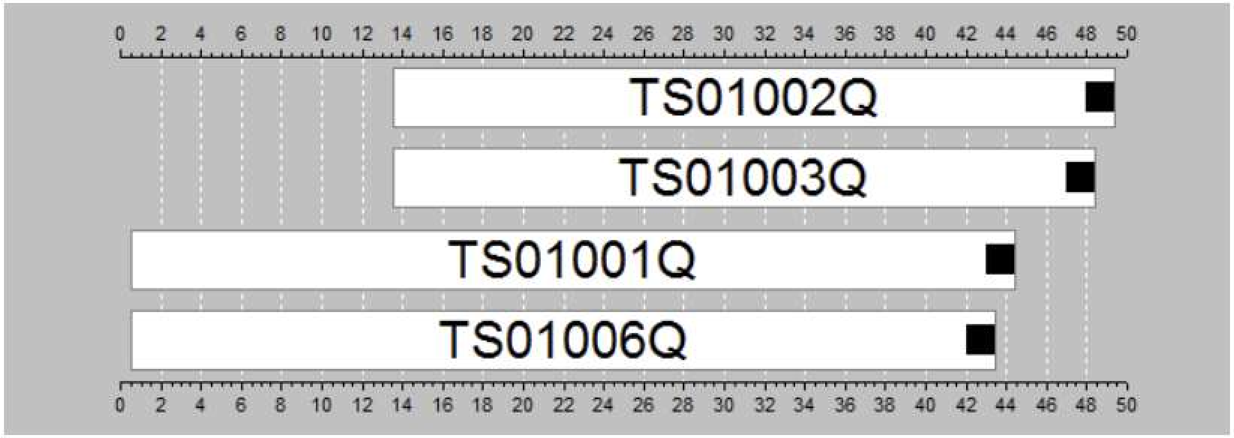

Fig. 2 – Schema della posizione reciproca (*bar diagram*) delle 4 sequenze dei 2 carboni sincronizzati.

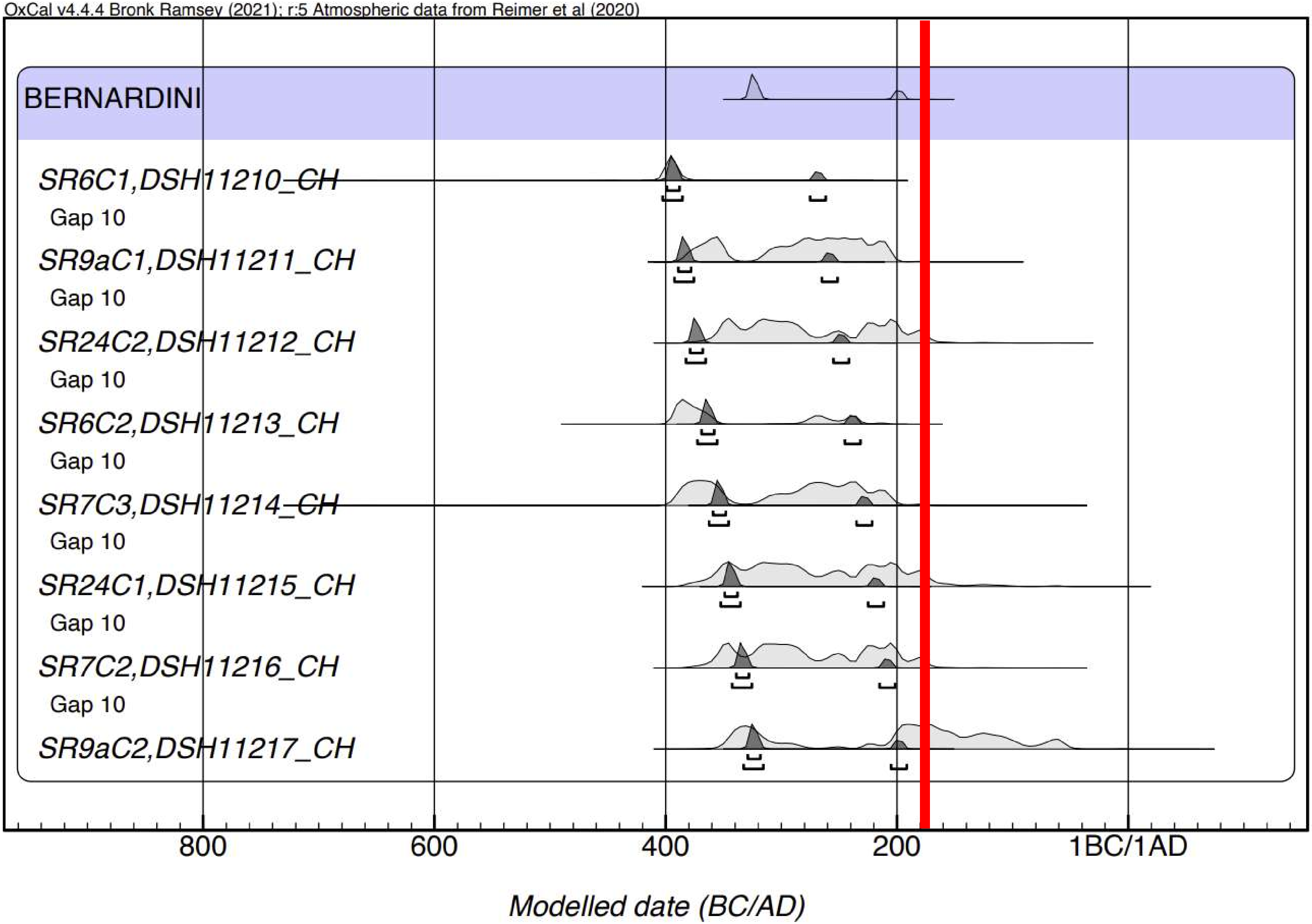
OxCal v4.4.4 Bronk Ramsey (2021); r:5 Atmospheric data from Reimer et al (2020)
BERNARDINI
SR6C1,DSH11210_CH
Gap 10
SR9aC1,DSH11211_CH
Gap 10
SR24C2,DSH11212_CH
Gap 10
SR6C2,DSH11213_CH
Gap 10
SR7C3,DSH11214_CH
Gap 10
SR24C1,DSH11215_CH
Gap 10
SR7C2,DSH11216_CH
Gap 10
SR9aC2,DSH11217_CH
800
600
400
200
1BC/1AD
Modelled date (BC/AD)

Prehistoric dentistry

OPEN ACCESS Freely available online

PLOS ONE

Beeswax as Dental Filling on a Neolithic Human Tooth

Federico Bernardini[1]*, Claudio Tuniz[1,2], Alfredo Coppa[3], Lucia Mancini[4], Diego Dreossi[4], Diane Eichert[4], Gianluca Turco[5], Matteo Biasotto[5], Filippo Terrasi[6], Nicola De Cesare[7], Quan Hua[8], Vladimir Levchenko[8]

1 Multidisciplinary Laboratory, ''Abdus Salam'' International Centre for Theoretical Physics, Trieste, Italy, **2** Centre for Archaeological Science, University of Wollongong, Wollongong, New South Wales, Australia, **3** Department of Environmental Biology, University ''La Sapienza'', Rome, Italy, **4** Sincrotrone Trieste S.C.p.A., AREA Science Park, Basovizza (Trieste), Italy, **5** Department of Medical Sciences, University of Trieste, Trieste, Italy, **6** CIRCE, INNOVA and Department of Environmental Sciences, 2nd University of Naples, Caserta, Italy, **7** CIRCE, INNOVA and Department of Life Sciences, 2nd University of Naples, Caserta, Italy, **8** Australian Nuclear Science and Technology Organisation, Lucas Heights, New South Wales, Australia

Abstract

Evidence of prehistoric dentistry has been limited to a few cases, the most ancient dating back to the Neolithic. Here we report a 6500-year-old human mandible from Slovenia whose left canine crown bears the traces of a filling with beeswax. The use of different analytical techniques, including synchrotron radiation computed micro-tomography (micro-CT), Accelerator Mass Spectrometry (AMS) radiocarbon dating, Infrared (IR) Spectroscopy and Scanning Electron Microscopy (SEM), has shown that the exposed area of dentine resulting from occlusal wear and the upper part of a vertical crack affecting enamel and dentin tissues were filled with beeswax shortly before or after the individual's death. If the filling was done when the person was still alive, the intervention was likely aimed to relieve tooth sensitivity derived from either exposed dentine and/or the pain resulting from chewing on a cracked tooth: this would provide the earliest known direct evidence of therapeutic-palliative dental filling.

Citation: Bernardini F, Tuniz C, Coppa A, Mancini L, Dreossi D, et al. (2012) Beeswax as Dental Filling on a Neolithic Human Tooth. PLoS ONE 7(9): e44904. doi:10.1371/journal.pone.0044904

Editor: Luca Bondioli, Museo Nazionale Preistorico Etnografico 'L. Pigorini', Italy

Received April 20, 2012; **Accepted** August 9, 2012; **Published** September 19, 2012

Funding: This work is part of the ICTP/Elettra EXACT Project (Elemental X-ray Analysis and computed Tomography) funded by Friuli Venezia Giulia (Italy). The funders had no role in study design, data collection and analysis, decision to publish, or preparation of the manuscript.

Competing Interests: The authors have declared that no competing interests exist.

* E-mail: fbernard@ictp.it

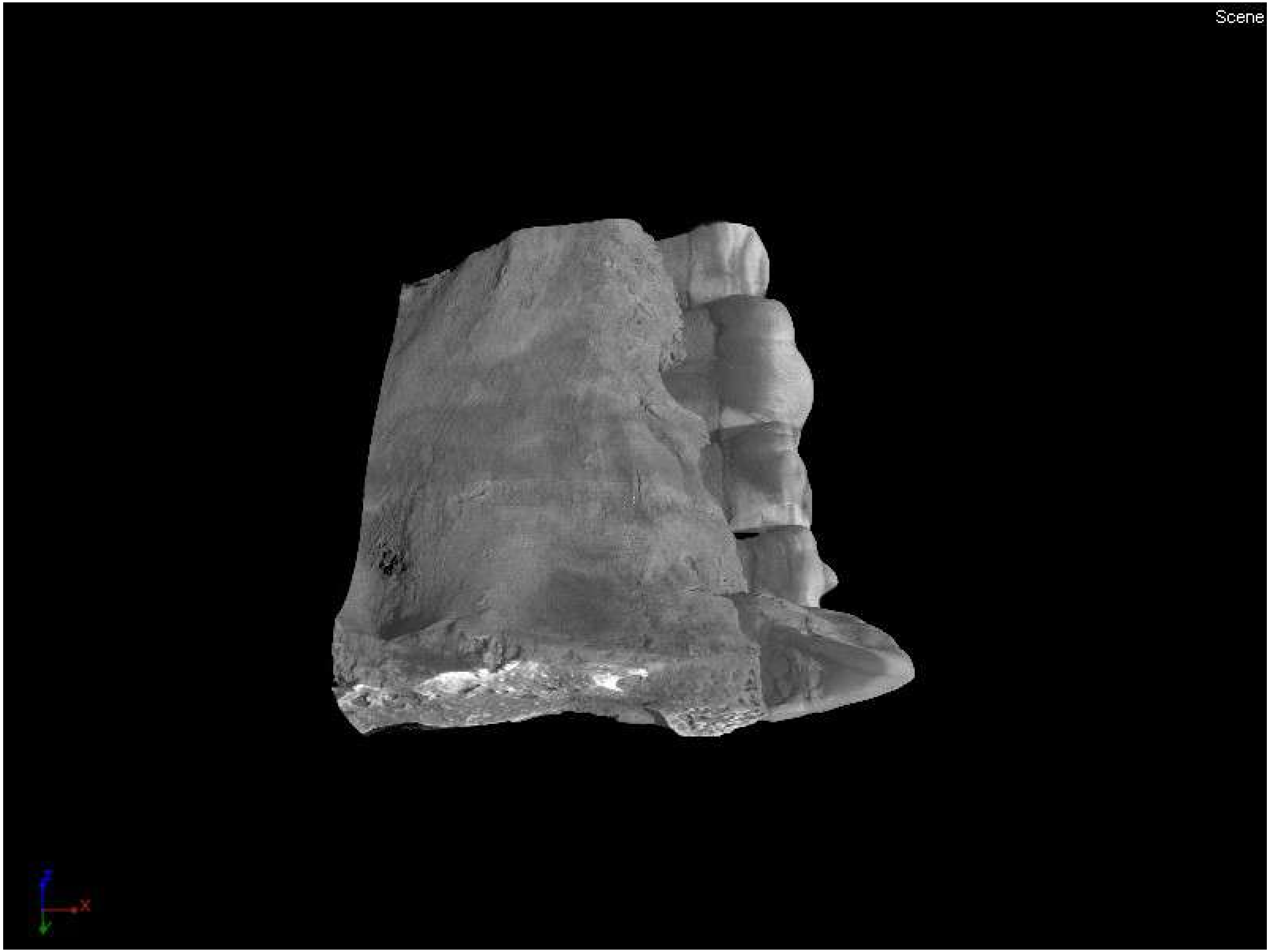
Scene
x
z

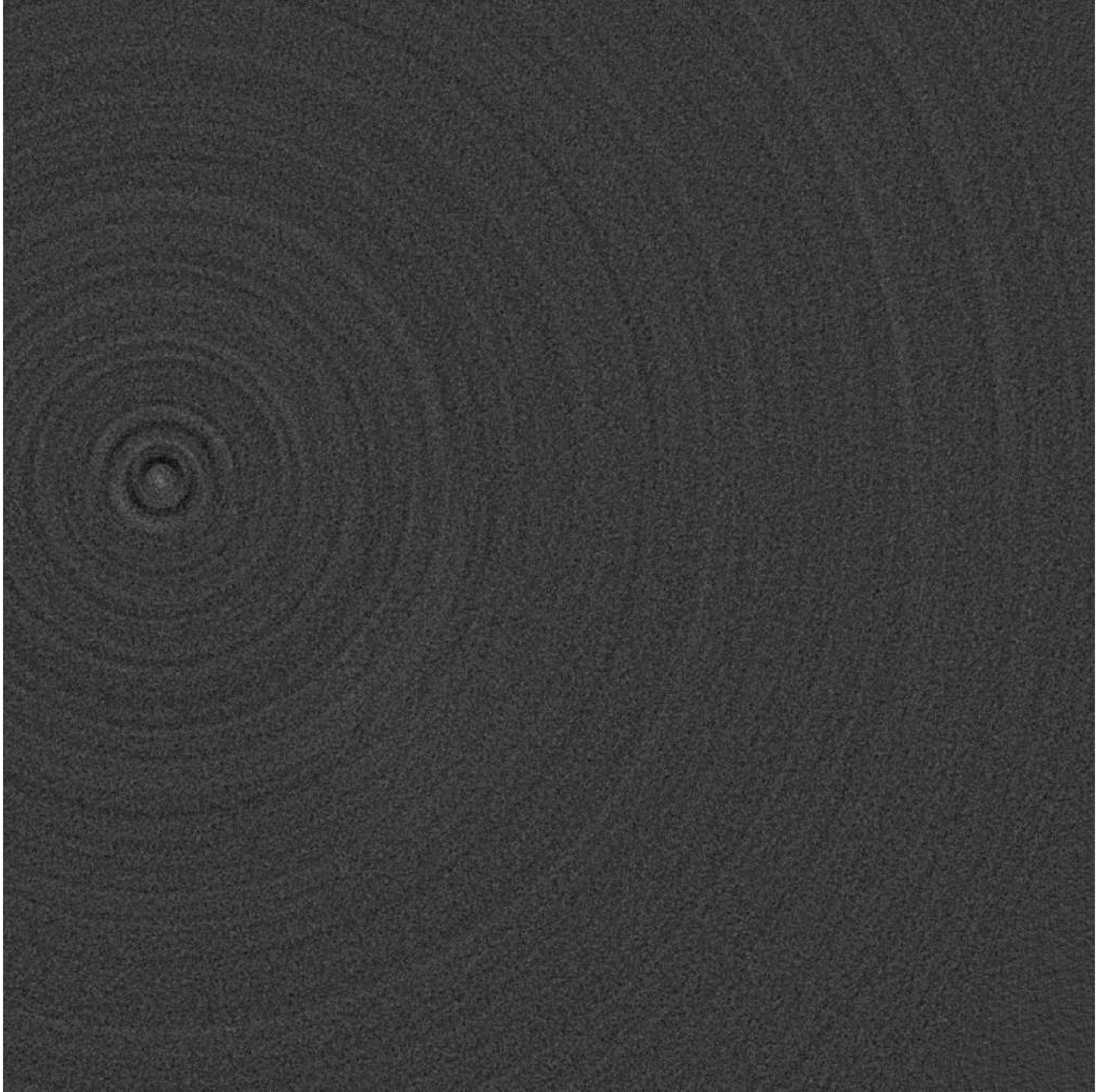

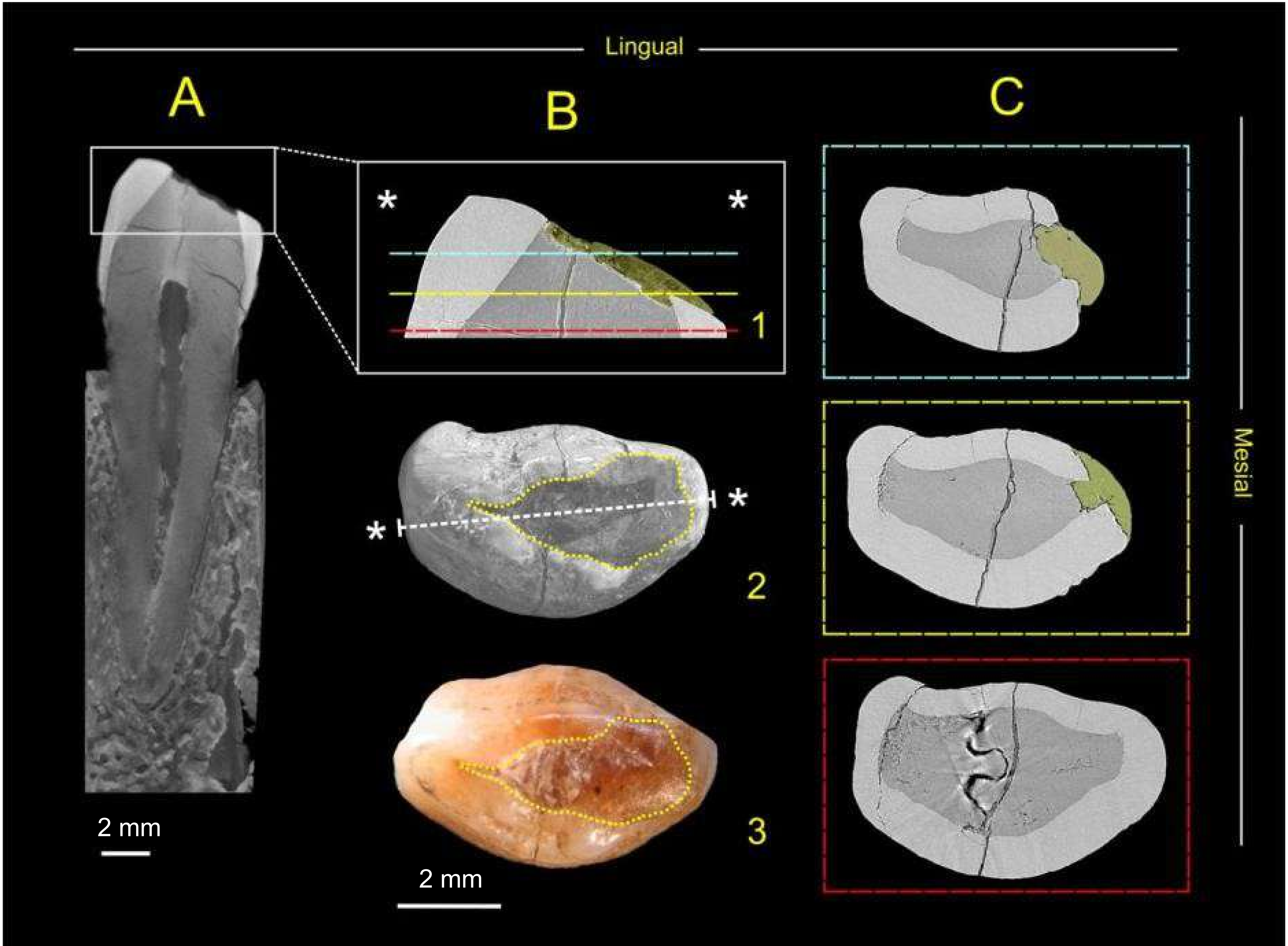

Lingual
A
B
C
1
2
3
Mesial
2 mm
2 mm

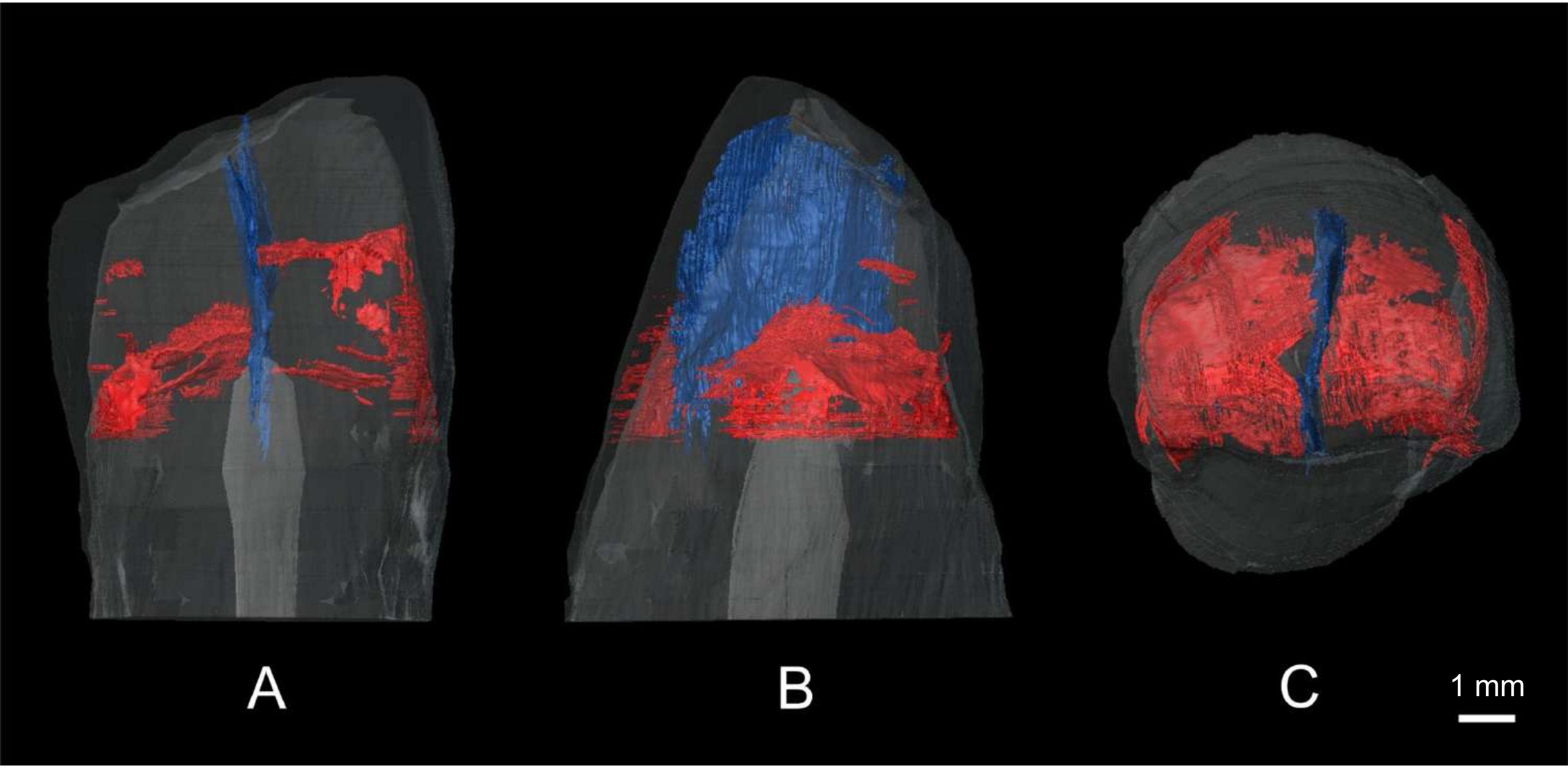

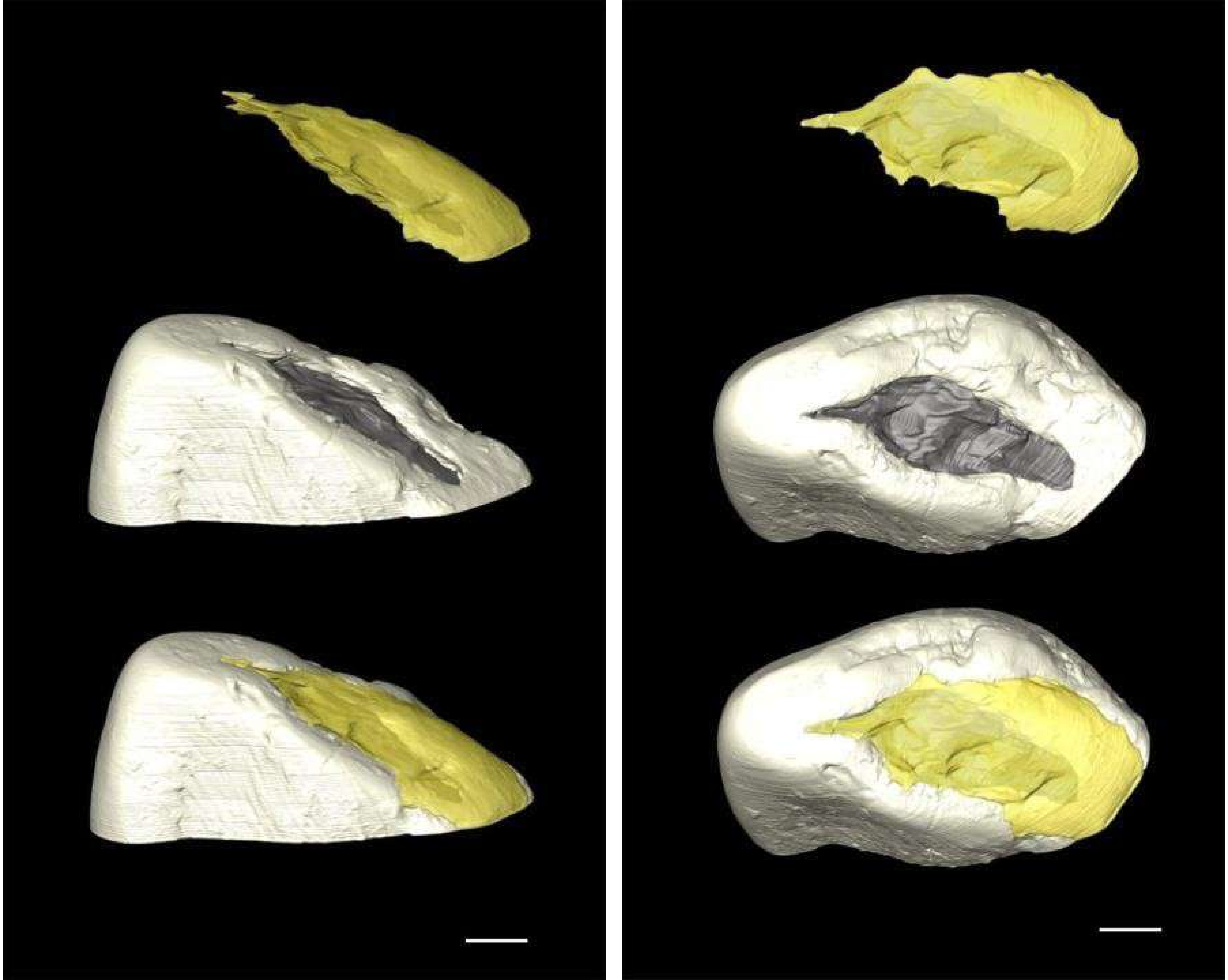

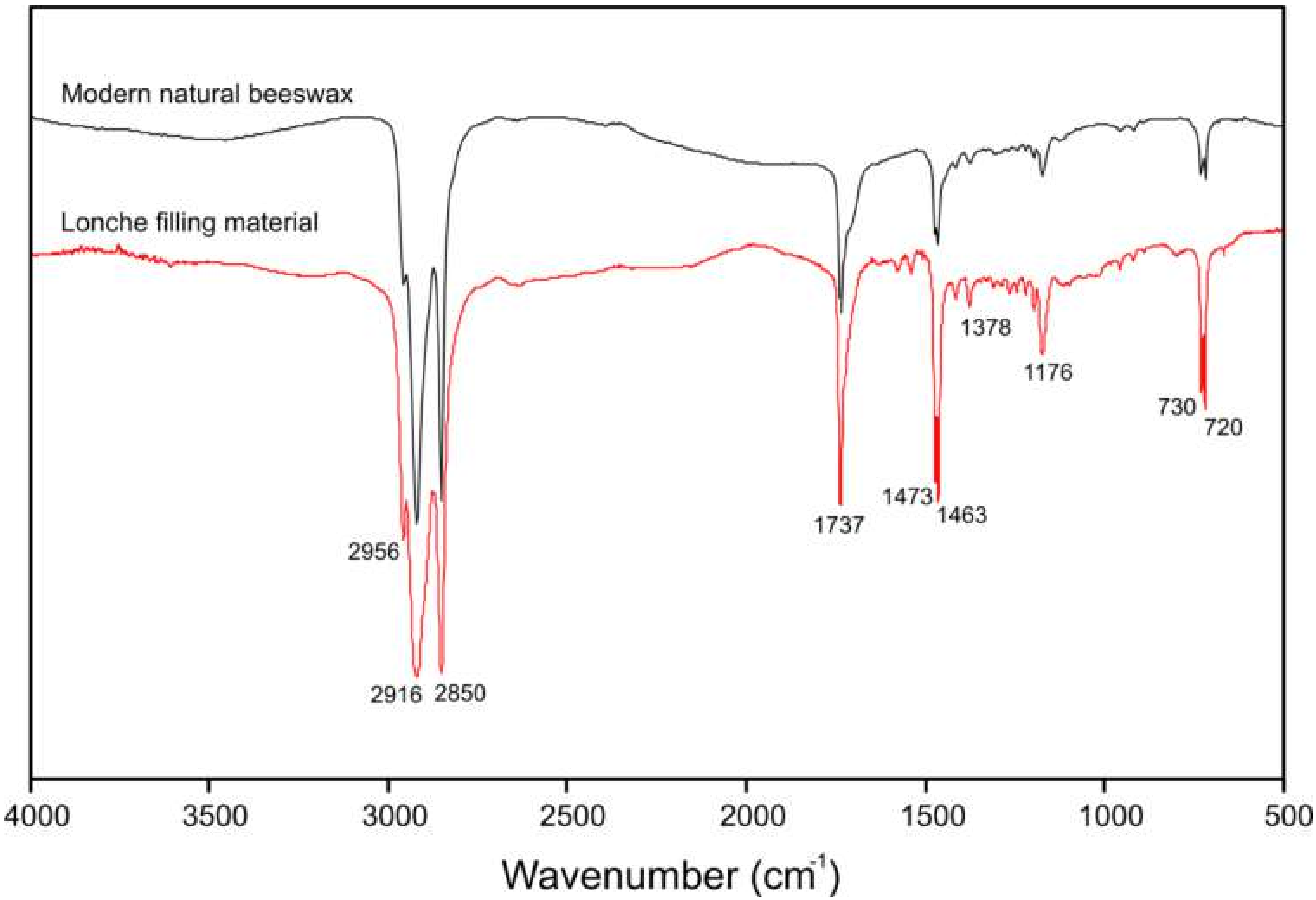

Infrared spectroscopy

Center for **I**sotopic **R**esearch on **C**ultural and **E**nvironmental heritage

a
s
e
r
t
a

INNOVA

CENTRO REGIONALE DI COMPETENZA
PER LO SVILUPPO ED IL TRASFERIMENTO
DELL'INNOVAZIONE APPLICATA AI
BENI CULTURALI E AMBIENTALI

DSA-SUN

Lucas Heights - Australia

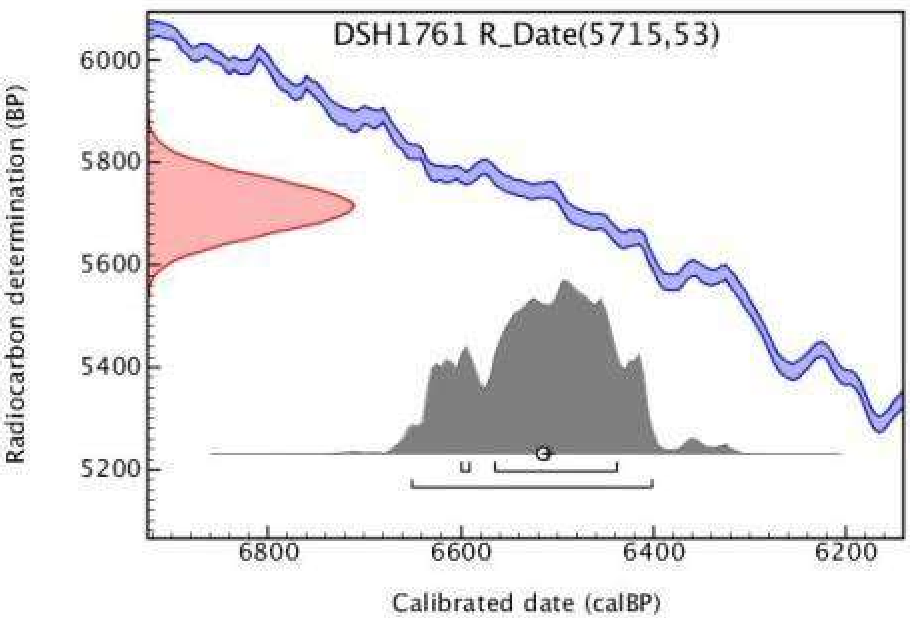

Beeswax:
4695-4453 BC (two sigma)

^{14}C measurements were performed using the STAR facility at ANSTO (Australia)

Mandible:
4688-4496 BC (two sigma)

^{14}C measurements were performed using the CIRCE AMS facility (Italy)

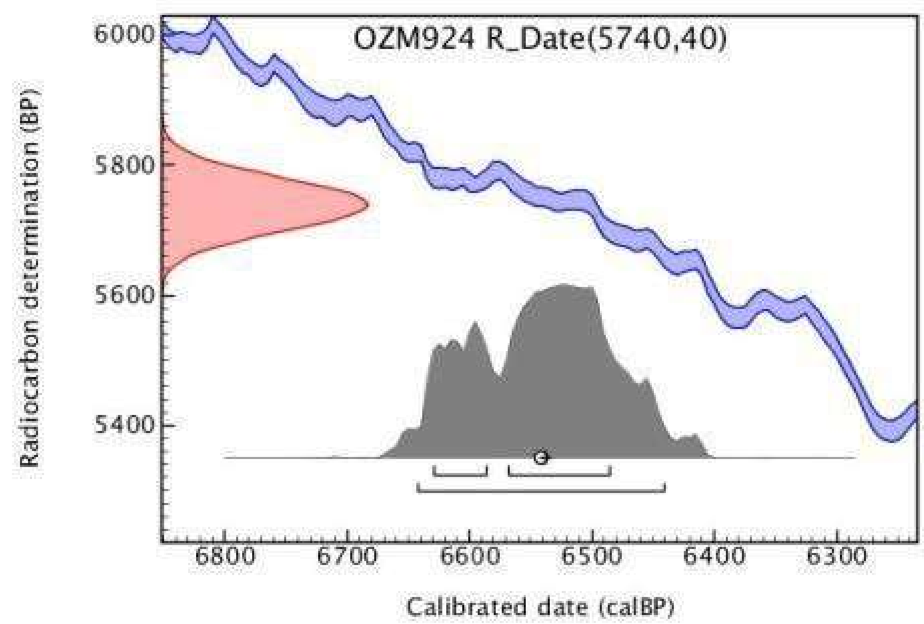

THANK YOU FOR YOUR ATTENTION!